ORNL/TM-2021/1961

Extended-Enrichment Accident-Tolerant LWR Fuel Isotopic and Lattice Parameter Trends

Robert Hall
Ryan Sweet
Randy Belles
William A. Wieselquist

March 2021

OAK RIDGE NATIONAL LABORATORY
MANAGED BY UT-BATTELLE FOR THE US DEPARTMENT OF ENERGY

ORNL/TM-2021/1961

Nuclear Energy and Fuel Cycle Division

EXTENDED ENRICHMENT ACCIDENT TOLERANT LWR FUEL ISOTOPIC AND LATTICE PARAMETER TRENDS

Robert Hall
Ryan Sweet
Randy Belles
William A. Wieselquist

Date Published: March 2021

Prepared by
OAK RIDGE NATIONAL LABORATORY
Oak Ridge, TN 37831-6283
managed by
UT-BATTELLE, LLC
for the
US DEPARTMENT OF ENERGY
under contract DE-AC05-00OR22725

CONTENTS

LIST OF FIGURES

LIST OF TABLES

SUMMARY

Commercial light water reactor (LWR) operators and fuel vendors in the United States (US) are pursuing changes to the reactor fuel that include increased enrichment and accident-tolerant fuel (ATF) designs. Enrichments under consideration are between 5 wt % and 10 wt % ^{235}U, which are a subset of high-assay low-enriched uranium fuels. ATF features are designed to improve fuel system performance under accident conditions. With increased enrichment, fuel cycle economics can be improved if fuel can be licensed for higher burnup (HBU) than typical current limits (e.g., 62 GWd/MTU maximum fuel pin).

To prepare for and support these potential changes, the effects of ATF and HBU are being assessed for selected representative LWR fuel designs. Lattice physics parameter and used fuel isotopic changes are investigated for a conventional 17×17 pressurized water reactor (PWR) design and a conventional 10×10 boiling water reactor (BWR) design. This study focuses on effects related to the introduction of ATF features including coated clad, doped UO_2, and FeCrAl clad. Calculations were performed using the pre-release SCALE 6.3 Polaris and ORIGEN computer codes. The SCALE/Polaris code using the 56-group ENDF/B-VII.1 neutron cross-section library is the primary investigation tool. Previous work has determined best acceptable ATF modeling practices and confirmed the fidelity of Polaris ATF calculations to higher-order calculations.

Near-term ATF concepts include doped pellets, chromium-coated cladding, and FeCrAl cladding (with FeCrAl channel boxes for BWR assemblies). Batch average enrichments of 6 wt % (PWR) and 5.4 wt % (BWR) are estimated to be adequate to support increased maximum pin burnup to the equivalent of 75 GWd/MTU. Additional enrichments needed to cover variations within a batch (split batch) and variations within an assembly (axial blankets and radial zoning) are estimated to be 0.6 wt % for PWRs and 1.0 wt % for BWRs. Enrichments required to offset the negative reactivity of PWR ATF materials range from 0.1 to 0.15 wt % for chromium-clad coating to 0.4 to 0.8 wt % for FeCrAl. Due to the complexity of BWR design, an equivalent enrichment penalty was not determined in this work.

A delta approach is used to evaluate the effects ATF concepts compared with non-ATF fuels. Key quantities of interest include reactivity effects, enrichment requirements, lattice physics parameters (reactivity coefficients and kinetics parameters), and isotopic inventories at various decay times. In general, doped pellets and chromium-coated clad have only minor effects on the reactivity, reactivity coefficients, and isotopic content of used fuel. Larger effects are seen for FeCrAl with a large reactivity penalty (~5000 pcm), minor MTC changes, and reduced control element worth (5–10%) due to the slightly harder spectrum. There is no significant impact of any ATF design on delayed neutron fraction, decay heat, or isotopics predictions.

1. INTRODUCTION

Commercial light water reactor (LWR) operators and fuel vendors in the United States (US) are pursuing changes to the reactor fuel that include increased enrichment and accident-tolerant fuel (ATF) designs. Enrichments under consideration are between 5 wt % and 10 wt % ^{235}U, which are a subset of high-assay low-enriched uranium (HALEU) fuels. ATF features are designed to improve fuel system performance under accident conditions. With increased enrichment, fuel cycle economics can be improved if fuel can be licensed for higher burnup (HBU) than typical current limits (e.g., 62 GWd/MTU [metric ton of uranium] maximum fuel pin). [Diaz 2019; Pimental 2019]

To prepare for and support these potential changes, the effects of ATF and HBU are being assessed for selected representative LWR fuel designs. The project is divided into phases. Phase 1 evaluates lattice physics parameter and used fuel isotopic changes for a conventional 17×17 pressurized water reactor (PWR) design [Hall et al. 2021] and a conventional 10×10 boiling water reactor (BWR) design. [Cumberland et al. 2021] This report focuses on effects related to the introduction of ATF features including coated cladding, doped UO_2, and iron-chromium-aluminum (FeCrAl) clad. The SCALE/Polaris code using SCALE 56-group ENDF/B-VII.1 neutron cross sections is the primary investigation tool. [Wieselquist et al. 2020] Previous work has determined best acceptable ATF modeling practices and confirmed the fidelity of Polaris ATF calculations to higher-order calculations. [Jessee et al. 2020]

The goals of the current work are to:

- Review industry work on near-term and longer-term ATF concepts to identify near-term concepts for evaluation and provide ATF modeling input
- Determine the expected range of enrichment and burnup of interest for the ATF evaluation under various fuel cycle scenarios
- Review prior ATF modeling and code validation work to determine the ATF assessment scope in this work
- Identify and explain important effects of ATF materials (reactivity, lattice physics, and isotopic) assuming fuel design and usage remain similar to current-enrichment non-ATF fuel
- Provide limited comparisons with results using higher-order cross-section libraries and/or codes
- Identify any apparent anomalous trends in the results for further investigation, in particular, in the following areas of interest:
  - the effects of ATF designs on the range of enrichment needed to support HBU limits
  - the effects of ATF designs and compensatory enrichment changes on lattice reactivity parameters
  - the effects of ATF on depleted fuel isotopic contents of interest for severe accidents, decay heat, and used fuel shielding
  - the effects of unirradiated ATF on transportation package criticality safety margins.

Calculations were performed using the pre-release SCALE 6.3 Polaris and ORIGEN computer codes. A delta approach was used to evaluate the effects of ATF concepts compared with non-ATF fuels. A representative commercial PWR fuel assembly (Westinghouse 17×17 with integral fuel burnable absorber, or IFBA, rods) was used for the PWR evaluation, which focused on differences between well-understood depletion of non-ATF fuel within current limits (5 wt % ^{235}U depleted to 60 GWd/MTU) and depletion with enrichments of up to 8 wt % and burnups of up to 80 GWd/MTU. To model the effects of

the ATF concepts on the neutronic performance of the BWR fuel assembly (GE14 10×10 with Gd_2O_3 rods), representative dominant and vanished region lattices were used. Because of the large differences in the enrichment zones for the BWR fuel lattices, depletions compared ATF and non-ATF fuel for both 5 wt % and 10 wt % ^{235}U enrichment limits up to a burnup limit of 80 GWd/MTU.

Commercial LWR operators and fuel vendors in the United States are pursuing changes to the fuel that include extended-enrichment (EE) and ATF designs. EE (8 wt % > ^{235}U > 5 wt %%) is used in this report to refer to a subset of HALEU fuel that is considered usable in commercial US LWRs in the near term. ATF features are designed to improve fuel system performance under accident conditions. [Diaz 2019; Pimental 2019] One goal of EE is to improve fuel cycle economy by enabling fuel to be depleted to HBU than typical current maximum pin burnup limits (62 GWd/MTU). Adoption of EE, ATF, and HBU in the US commercial fleet requires a clear understanding of the effects on core physics parameters and used fuel isotopic content, as well as confidence in the accuracy of computer code predictions over an expanded range of materials, enrichment, and burnup. Understanding the applicability and adequacy of benchmark data (e.g., criticality, decay heat, isotopic content) for computer code validation is needed to ensure appropriate safety margins are maintained.

2. ATF CONCEPTS AND MATERIALS

This section provides a review of ATF concepts associated with recent licensing activities. It includes value ranges and references to support modeling details and assumptions such as coating thickness, doping concentrations, and material specifications. Concepts are categorized as near term (dopants, CR-coated clad, and FeCrAl clad) and longer term (e.g., U_3Si_2 fuel pellets and SiC clad). Analyses in this report are focused on near-term ATF concepts.

Staff members of the US Nuclear Regulation Commission (NRC) have prepared an ATF project plan [NRC 2019] in anticipation of the receipt of license amendment requests by utilities to test and use ATF. The plan notes

> In coordination with DOE, several fuel vendors have announced plans to develop and seek approval for various fuel designs with enhanced accident tolerance (i.e., fuels with longer coping times during loss of cooling conditions). The designs considered in the development of this plan, both within and outside of the DOE program, include coated Zr claddings, doped uranium dioxide (UO_2) pellets, iron-chrome-aluminum-based (FeCrAl) cladding, SiC cladding, uranium silicide (U_3Si_2) pellets, and metallic fuels (e.g., Lightbridge). For the purpose of developing this plan, ATF concepts are broadly categorized as near term and longer term. The plan considers near-term ATF concepts as those for which the agency can largely rely on existing data, models, and methods for its safety evaluations (SEs). Coated Zr cladding, FeCrAl cladding, and doped UO_2 pellets are a few examples of near-term ATF concepts. In general, the industry is pursuing these near-term concepts for deployment by the early to mid-2020s. Longer term ATF concepts are those for which substantial new data, models, and methods need to be acquired or developed to support the agency's SEs. U_3Si_2 fuel, metallic fuel, and SiC-based cladding are a few examples of longer term ATF concepts. Note that "near term" and "longer term" are terms of convenience used to indicate the current expected deployment timeframe for the ATF concept. [NRC 2019]

In 2019, as part of its Enhanced Accident Tolerant Fuel (EATF) Program, the US Department of Energy (DOE) Office of Nuclear Energy (NE) awarded $111.2 million to three industry partners to develop ATF.[1] The awards went to Westinghouse Electric Company (Westinghouse), Framatome, and General Electric (Global Nuclear Fuels, or GNF). Specifically, their responsibilities are as follows:

- Westinghouse[2] will continue to develop ATF under its EnCore Fuel Program. It includes the development of uranium silicide (U_3Si_2) and Doped UO_2 Advanced Doped Pellet Technology (ADOPT) in Cr-coated zirconium (Zr) alloy cladding. Westinghouse will also continue its silicon carbide (SiC) cladding concepts and uranium nitride fuel pellet development. [WEC 2020]

- Framatome[3] will continue the development and deployment of Cr-coated M5 cladding with chromia-enhanced uranium oxide (UO_2) pellets (Cr-Cr_2O_3). Additionally, Framatome will continue and expand development efforts on its SiC/SiC composite cladding concepts with Cr_2O_3-doped pellets. [Cole et al. 2012]

[1] https://www.energy.gov/ne/articles/doe-awards-111-million-us-vendors-develop-accident-tolerant-nuclear-fuels
[2] https://www.westinghousenuclear.com/operating-plants/fuel/fuel-innovation
[3] https://nextevolutionfuel.com/framatome-eatf-program/

- GNF will continue the development of FeCrAl alloy cladding, known as IronClad. GNF will also continue to develop its Abrasion Resistant, More Oxidation Resistant (ARMOR) coating program for Zr alloys and the study of UO_2-based ceramic metal fuels. [Lin et al. 2018]

2.1 CLADDING

Past severe accidents in LWRs have shown that nuclear fuel will fail under extreme conditions; and high-temperature reactions between Zr alloys and water will lead to the generation of hydrogen, creating the potential for beyond-design-basis accident hydrogen ignition. As a result, there is continued interest in alternative fuel designs that will be more resistant to fuel failure and hydrogen production in these extreme conditions.

Near-term approaches involve gradual design iterations to reduce the high-temperature oxidation of the fuel cladding. These include coating the outer cladding surfaces of materials that present more favorable oxidation kinetics, such as Cr, or using alternative cladding materials entirely, such as FeCrAl or SiC/SiC. Unfortunately, adding Fe- and Cr-containing materials to the reactor presents fairly large reactivity penalties compared with traditional Zr-based claddings, requiring an increase of the ^{235}U enrichment and/or a decrease in the cycle length. [NEA 2018]

2.1.1 Chromium-Coated Cladding

Chromium is a leading choice for coated cladding to inhibit the Zr-steam reaction because it meets the requirements of improved corrosion resistance over a wide range of temperatures without any significant neutron absorption penalty. [Shah et al. 2018; Bischoff, Delafoy, and Chaari 2018] Westinghouse and Framatome are currently working on fuel with a Cr coating over Zr-Nb alloy cladding. [WEC 2020; Cole et al. 2012] GNF is working on fuel with a proprietary coating over Zircaloy-2–based cladding. [Lin et al. 2018] Nominal compositions (where available) and nominal chemistry ranges for selected LWR clads currently in use across the industry are shown in Table 1. Following the table is a synopsis of the Cr coating ATF efforts by each US fuel vendor.

Table 1. Chemical composition of various LWR fuel claddings by wt %. [Bischoff, Delafoy, and Chaari 2018; Shah 2006; Pint et al. 2015; ATI 2015; IAEA 2014; Motta, Couet, and Comstock, 2015]

Alloy	Zr	Fe	Nb	Cr	Si	C	O	Sn	Ni
Zircaloy-2		0.15		0.1			0.1	1.5	0.05
Range	Balance	0.07–0.2	–	0.05–0.15				1.2–1.7	0.03–0.08
Zircaloy-4	98.2	0.22		0.11	0.01	0.016	0.118	1.27	
Range	Balance	0.18–0.24	–	0.07–0.13			0.09–0.16	1.2–1.7	–
M5™	98.8	0.038	1.0				0.135		
Range	Balance	0.015–0.038	–	–			0.118–0.148	–	
ZIRLO™		0.1	1.0				0.1	1.0	
Range	Balance	0.09–0.13	0.8–1.2	–			0.09–0.16	0.8–1.2	–
Optimized ZIRLO									
Range	Balance	0.09–0.13	0.8–1.2	–			0.09–0.16	0.6–0.79	–

Westinghouse

Westinghouse is currently working toward commercializing Cr-coated ZIRLO and Optimized ZIRLO PWR fuel cladding using a cold spray process as part of its EnCore fuel program. Cold spray coating can be applied on variety of substrates, including Zr alloys. The deposition process disrupts the inherent oxide formation on the surfaces of Zr alloys, improving the adherence of the coating to the substrate. Polishing processes have been developed to achieve the thickness and surface finish required for in-reactor performance and seamless integration into current fuel designs, without a need for fuel assembly structure modifications. [Bischoff, Delafoy, and Chaari 2018; Geelhood and Luscher 2019] The final coating thickness is between 20 and 30 μm. [Bischoff, Delafoy, and Chaari 2018] Lead test assemblies (LTAs) have been inserted in the Byron Generating Station reactor in Illinois. ZIRLO is a modification of Zircaloy-4 that includes a reduction in the tin, Fe, and Cr content and the addition of nominally 1% niobium. The proposed optimization of ZIRLO still meets the original definition, reducing the tin and Fe content, eliminating the Cr content, and adding 1% niobium. [Shah 2006]

Framatome

Like Westinghouse, Framatome is currently working toward commercializing a Cr coating for its Zr alloy PWR fuel cladding (M5). The Cr coating is deposited using a physical vapor deposition technique that does not modify the microstructure of the underlying Zr substrate and forms a dense layer with no porosity at the Cr-Zr interface. [Bischoff, Delafoy, and Vauglin 2018]

The final coating thickness is between 8 and 22 μm, [Geelhood and Luscher 2019] although a Framatome paper proposes a nominal value of 15 μm. [Bischoff, Delafoy, and Vauglin 2018] LTAs have been inserted in the Vogtle and ANO-1 reactors.

GNF

GNF supplies BWR fuel using Zircaloy-2 clad and is developing a coating, called ARMOR (Abrasion Resistant, More Oxidation Resistant), to be applied to Zircaloy-2 cladding. [Lin et al. 2018] The ARMOR coating is proprietary; therefore, the chemical composition of the coating, its application process, and its thickness have not been presented in a public forum. [Geelhood and Luscher 2019] However, as discussed at the Top Fuel conference in 2018, [Lin et al. 2018] ARMOR is applied to the outer surface of normal production Zircaloy-2 fuel rods. It is designed to improve the abrasion and fretting resistance of the cladding and to improve the oxidation performance of the Zircaloy-clad fuel rod. Laboratory tests show that coated Zircaloy-2 has improved wear resistance at room temperature and improved corrosion/oxidation resistance compared with uncoated Zircaloy-2 under operational corrosion environments and in high-temperature steam. When examined following laboratory testing, the coating appears fully dense without microcracks or pores. [Lin et al. 2018] LTAs have been inserted in the Hatch and Clinton reactors.

A summary of the LWR Cr-coated fuel concepts for each vendor is shown in Table 2. [Geelhood and Luscher 2019] A summary of typical LWR clad thicknesses is shown in Table 3.

Table 2. Summary of LWR Cr-coated fuel concepts. [Geelhood and Luscher 2019]

Vendor	Coating	Coating thickness (μm)
Westinghouse	Cr-coated ZIRLO	20–30
Framatome	Cr-coated M5	8–22
GNF	ARMOR-coated Zircaloy-2	Proprietary

Table 3. Summary of typical LWR clad thickness. [IAEA 2014; Kim et al. 2017; Parisi et al. 2020; NRC 2020b]

Cladding	Cladding thickness (µm)
Zircaloy (range)	570–725 [Kim et al. 2017] 500–700 [NRC 2020b]
PWR (17×17)	572 [IAEA 2014] 617 Parisi et al. 2020] 550 [IAEA 2014]
BWR (10×10)	660 [IAEA 2014]
FeCrAl	309 [Parisi et al. 2020]

Regulatory Implications

LTA testing is under way to supply the necessary experimental material data required for batch use of the coatings. Since the parent cladding material is not expected to change, no additional experimental data seem to be warranted. [EPRI 2018] For coatings of less than 20 µm, the neutronic impact on the fuel cycle cost or cycle length of all investigated coating types is small and can be easily compensated by very slight design modifications. [NEA 2018] Since coating materials usually have a higher thermal neutron absorption cross section than Zr, a thick coating will negatively impact the fuel cycle cost; therefore, the coating thickness must be taken into account in the normal operational assessment. [NEA 2018] Additionally, the coating will likely need to remain bonded to the Zr-based alloy substrate throughout the entire irradiation process and during any potential design-basis-accidents to provide beneficial oxidation resistance. In the event that the coating spalls off, the remaining cladding has already been approved by the regulator; therefore, no major negative effects are expected to occur, provided the coating does not impact the underlying material. [EPRI 2018]

2.1.2 FeCrAl Cladding

GNF

In addition to the ARMOR coating, GNF is developing an FeCrAl clad with UO_2 fuel known as IronClad. [Lin et al. 2018] The ferritic alloy concept is a robust replacement for Zircaloy-2 BWR cladding. These alloys contain sufficient Cr to remain passive under normal operation conditions and sufficient Al to develop a protective alumina external layer under severe accident conditions of high-temperature steam. [Lin et al. 2018] Interest in ferritic alloys also stems from several technical reasons, including their resistance to stress corrosion cracking, high thermal conductivity, low coefficient of thermal expansion, and dimensional stability under irradiation. Ferritic alloys also exhibit higher strength than current Zr alloys at reactor temperatures, allowing for a thinner tube wall to diminish the neutron penalty. These alloys also exhibit higher thermal creep resistance than Zr alloys which, given the anticipated thinner wall, is expected to allow them to perform similarly under high-pressure, high-temperature conditions.

In general, the FeCrAl alloys under consideration have low corrosion in environments typical of LWRs. [Rebak 2018] FeCrAl cladding also offers resistance to debris fretting and eliminates the occurrence of shadow corrosion. However, FeCrAl claddings exhibit higher thermal neutron absorption and hydrogen/tritium permeability than traditional Zr-based cladding. [Rebak 2018]

GNF has tested several different FeCrAl alloys, including C26M, Kanthal APMT, and MA956. GNF has not publicly stated which FeCrAl alloy will be used for batch production of IronClad; however, 2 unfueled IronClad rods irradiated at Hatch were C26M; 8 fueled IronClad rods inserted in Clinton were

C26M; and 16 unfueled rods inserted in Clinton were C26M, APMT, and MA956. [Goodson and Geelhood 2020] The compositions of C26M, Kanthal APMT, and MA956 are shown in Table 4.

Table 4. Chemical composition of various FeCrAl fuel claddings by wt %. [Goodson and Geelhood 2020]

Alloy	Fe	Cr	Al	Mo	Si	Y	Other
C26M	Balance	12	6	2	0.2	0.03	
Kanthal APMT	Balance	20.5–23.5	5	3	0.7 max	–	0.08 C+ 0.4 Mn (max) + (max)
MA956	Balance	18.5–21.5	3.75–5.75	–	–	0.3–0.7	0.1 C + 0.3 Mn + 0.5 Ni all max*

*MA956: + 0.3 Co (max) + 0.15 Cu (max) + 0.02 P (max) + [0.2–0.6] titanium

GNF has not shared the FeCrAl cladding thickness for the above LTAs in a public forum. A paper from the Korea Atomic Energy Research Institute (KAERI) [Kim et al. 2017] discusses the calculated minimum thickness for an FeCrAl clad based on elastic buckling and ovality. The paper notes the neutronic penalty of using FeCrAl and the resulting need to minimize the FeCrAl clad thickness. It concludes that the FeCrAl clad thickness needs to be at least 0.45 mm in fuel rods, with an overall fuel rod diameter of 9.5 mm, to provide a safety factor of 2.0 against buckling failure and provide 1% ovality. The paper also concluded that the FeCrAl thickness should be between 0.38 mm and 0.45 mm for a safety factor of 2.0 against buckling failure and varying values of ovality from 0 to 1%. An additional study targeting necessary modifications to FeCrAl-clad fuel rods to achieve an equivalent cycle length in BWRs suggests the cladding will need to be ~300–350 µm to offset the neutronic penalty. However, modifications to fuel enrichment and fuel pellet diameter can assist in offsetting the neutronic penalty. [George et al. 2019]

An Idaho National Laboratory study [Pastore, Gamble, and Hales 2017] made a comparison of PWR fuel using FeCrAl cladding (UO_2/Zircaloy-4 and UO_2/FeCrAl) with traditional Zircaloy. The thermal neutron absorption cross section of FeCrAl is about ten times that of Zircaloy. The higher strength of the FeCrAl alloys compared with Zircaloy allowed the neutronic penalty to be offset somewhat by using thinner cladding. This approach allowed for slightly larger fuel pellets to give the same cold gap size in the rod. However, the slight increase in pellet diameter was not sufficient to compensate for the neutronic penalty; therefore, enriching the fuel beyond the current 5% limit may be necessary. Dimensional values used in the PWR fuel study are shown in Table 5. These values are consistent with the KAERI results. [Kim et al. 2017]

Table 5. Specifications for comparison of Zircaloy-4 and FeCrAl clad on PWR fuel. [Pastore, Gamble, and Hales 2017]

Parameter	UO_2/Zircaloy-4 rodlet	UO_2/FeCrAl rodlet
Number of pellets	10	10
Pellet length (mm)	11.86	11.86
Pellet outer diameter (mm)	8.19	8.57
Radial gap width (µm)	80	80
Cladding inner diameter (mm)	8.35	8.73
Cladding thickness (mm)	0.575	0.385
Cladding outer diameter (mm)	9.5	9.5

The BWR channel box is currently constructed from a 2 mm thick Zircaloy-4 sheath. [GE 2011] The use of FeCrAl alloys for this part of the assembly would introduce a significant reactivity penalty for the BWR fuel assembly. The EATF program is investigating alternatives for the BWR channel box material, such as SiC. This issue is discussed further in Section 2.3.

2.2 FUEL DOPING

An advantage of doping UO_2 fuel with small amounts of metal oxides is that it facilitates densification and diffusion during sintering, which results in a higher density and an enlarged grain size. Increasing the fuel density provides more ^{235}U per fuel assembly. It extends the available fuel burnup and leads to less fuel densification during irradiation. This can reduce the potential for fuel-clad interaction and ultimate clad failure. Enlarging the fuel grain size extends the diffusion path for fission product gases to the grain boundary [Massih 2014]. However, recent investigations have shown that the fission gas diffusivities may be higher in chromia (Cr_2O_3)-doped fuels as a result of changes to the fuel oxygen potential. [Cooper et al. 2021] Despite these counteracting effects, chromia-doped fuel is still expected to have a delay and/or reduction in the gas release compared to UO_2 with a standard grain size.

Westinghouse

Westinghouse is currently pairing its studies of Cr-coated Zr alloy cladding with doped fuel pellets. ADOPT fuel pellets consist of a modified UO_2 pellet doped with small amounts of chromia and alumina (Al_2O_3). Westinghouse has obtained extensive operating experience with ADOPT fuel through its commercial use in European reactors. Through May 2020, Westinghouse has delivered more than 600 metric tons of ADOPT pellets. [Hallman et al. 2020] LTAs are currently being irradiated at the Byron reactor.

Westinghouse has not released the fuel doping specifications for its ADOPT fuel. However, a 2006 journal article discusses some irradiation results performed at the Studsvik R2 test reactor for various ADOPT experimental rods doped with metal oxides. While Cr_2O_3 promotes the formation of larger grain sizes in UO_2 fuel, it also tends to increase parasitic neutron absorption. Therefore, the ADOPT experiment includes Al oxide and manganese oxide to offset some of the Cr oxide. [Arborelius et al. 2006]

A subsequent experiment with ADOPT fuel was documented in 2008. [Che, Pastore, and Hales 2018] The samples were irradiated in the Halden reactor. The properties of the experimental variations are shown in Table 6.

Table 6. Properties of experimental ADOPT fuel pellets. [Arborelius et al. 2006; Che, Pastore, and Hales 2018]

Option	Pellet composition	Grain size (µm)
Standard pellet	UO_2	10–12
Studsvik Option 1	UO_2 + 1,000 ppm Cr_2O_3	44
Studsvik Option 2	UO_2 + 1,000 ppm Cr_2O_3 + 100 ppm MgO	42
Studsvik Option 3	UO_2 + 500 ppm Cr_2O_3 + 200 ppm Al_2O_3	52
Halden Option 1	UO_2 + 900 ppm Cr_2O_3 + 200 ppm Al_2O_3	56
Halden Option 2	UO_2 + 500 ppm Cr_2O_3 + 200 ppm Al_2O_3	45

The 2006 journal article concluded that the experimental ADOPT pellets demonstrated a stable microstructure, a higher as-fabricated density, and a higher dimensional stability than conventional UO_2 pellets. At moderate burnup, the ADOPT pellets revealed improved properties such as reduced fission gas

release, increased pellet-cladding interaction margins, and improved corrosion resistance. [Arborelius et al. 2006]

Framatome

Framatome is pairing its studies of Cr-coated M5 fuel with studies of chromia-doped fuel pellets. LTAs are planned for Brunswick and Calvert Cliffs.

As with Westinghouse, Framatome has not commented publicly on the characteristics of its chromia-doped fuel. A 2008 Idaho National Laboratory report [Che, Pastore, and Hales 2018] discusses Framatome's plans for this fuel variant, but it references the Westinghouse fuel experiments in the Halden reactor. Framatome has noted that Cr_2O_3-doped fuel is standard UO_2 with Cr_2O_3 added at a level that is above the ASTM impurity level allowed for Cr (~250 ppm). The assumption in this report is that that the Framatome Cr_2O_3-doped fuel will have similar Cr content to the Westinghouse experiments in Halden.

GNF

In 2015, GNF submitted the licensing technical report NEDO-33406, Revision 3, *Additive Fuel Pellets for GNF Fuel Designs*, to the NRC regarding the incorporation of aluminosilicate (SiO_2:Al_2O_3) additive fuel pellets into GNF fuel products to increase the fuel reliability and operational flexibility of nuclear fuel bundles and cores. However, since 2015, no subsequent public information on doped fuel has been made available by GNF. The LTA press releases for the Hatch and Clinton reactors referenced only the ATF fuel cladding.

2.3 LONGER-TERM PROPOSALS

The DOE EATF program is also supporting longer-term ATF research focusing on fundamentally different nuclear fuel and cladding materials to improve reactor safety and costs.

Westinghouse

Westinghouse is evaluating a Cr-coated Zr alloy cladding with uranium silicide (U_3Si_2) fuel. This ATF proposal is expected to deliver improved fuel cycle economics because of the higher density and thermal conductivity of the U_3Si_2 fuel pellets. The U_3Si_2 fuel provides a 17% increase in ^{235}U density while remaining below the 5% ^{235}U design-basis enrichment limit for many operating plants. This enables longer fuel cycles. [Shah et al. 2018]

One of the weaknesses of U_3Si_2 fuel is its poor water/steam corrosion resistance. When U_3Si_2 fuel is exposed to water and/or steam, the exothermic oxidation reaction introduces additional heat and drives thermal expansion, which if unaccounted for, may cause cladding breach or exacerbate an existing cladding breach. [Sweet et al. 2020] Because of the pulverization, the fuel is available to washout faster than UO_2. To mitigate the fuel washout issue in a leaking rod, Westinghouse is studying placing the U_3Si_2 fuel pellets in short, cladded segments within the outer fuel rod cladding, so that the total amount of fuel subject to washout will be significantly reduced. For the segmented rod design, the U_3Si_2 pellet outer diameter is reduced to mitigate the pellet volumetric expansion due to the oxidation that could occur in a leaking rod. [Shah et al. 2018] As this fuel option is matured, further modeling evaluation and performance confirmation will be required.

Lead test assemblies of Westinghouse EnCore fuel rods containing uranium silicide fuel pellets were loaded into Exelon's Byron unit 2 in September 2019. The two assemblies contain Cr-coated Zr cladding for enhanced oxidation and corrosion resistance, segmented higher-density ADOPT Cr_2O_3 and Al_2O_3 pellets for improved fuel economics, and U_3Si_2 pellets. The silicide pellets in the lead test assemblies are

enclosed in a Zr alloy cladding and were manufactured at the Idaho National Laboratory [Richardson et al. 2019].

The superior fissile density of U_3Si_2 fuel compared with UO_2 fuel provides additional design flexibility such as offsetting neutronic penalties of advanced cladding with other operational and safety benefits. [NEA 2018]

Framatome

Framatome is developing SiC/SiC composite cladding and the associated manufacturing process. SiC ceramics, especially in their composite form, have superior high-temperature properties. Many attractive features make SiC composite material a next-generation candidate for LWR ATF cladding and core structures to replace coated Zircaloy. Fabrication of thin-walled long tubes, the hermetic joining of end-cap seals, and corrosion (the inability to form a protective silica layer under normal operating conditions) are key issues for research. [Kim et al. 2016] A study has shown that because of the irradiation swelling behavior of SIC/SiC composites, the cladding may exhibit significant lateral bowing under typical neutron flux and temperature gradients. [Singh et al. 2018] As this structural technology matures, further modeling evaluation and performance confirmation will be required.

BWR Channel Box Material

SiC/SiC composite material is also under investigation for BWR channel box applications. Most of the focus on the use of SiC composites has been on its possible application as LWR fuel cladding in place of Zircaloy. The channel box is a major BWR fuel component making up approximately 40% of the Zircaloy in a typical BWR core. Evaluation results indicate SiC composite could meet BWR channel mechanical design requirements. [NEA 2018] In addition, work has been performed demonstrating that SiC/SiC materials may exhibit bowing under irradiation and temperature gradients in BWRs. [Singh et al. 2019] Again, further modeling evaluation and performance confirmation will be required.

Lined Molybdenum Cladding

This clad concept uses molybdenum's high strength at elevated temperatures to maintain fuel rod integrity and core cooling during accident conditions. The outer surface is lined with a metallurgically bonded Zircaloy or FeCrAl layer to provide corrosion resistance in LWR coolants for operational states and enhance steam oxidation resistance. [NEA 2018] Further modeling evaluation and performance confirmation will be required.

High-Density Fuels

One option for compensating for the reactivity penalties imposed by the use of metallic coating and cladding is to use higher-density fuel. In addition to the silicide fuel under consideration by Westinghouse, other high-density fuel forms are under consideration, including uranium nitride (UN), uranium carbide (UC), and metallic fuel. [NEA 2018; Khatib-Rahbar et al. 2020]. As these options progress, further modeling evaluation and performance confirmation will be required.

3. EXPECTED RANGE OF BURNUP AND ENRICHMENT

ATF concepts and materials are linked to increased burnup and enrichment because of the potential benefit of improved ATF cladding performance at HBU, and reduced HBU ATF fuel pellet fragmentation during design-basis-accident conditions. [Khatib-Rahbar et al. 2020] Fuel fragmentation, relocation, and dispersal is considered an obstacle to increasing the fuel rod burnup limit above current levels (~ 62 GWd/MTU). [NEA 2018]

Improved safety performance of ATF concepts at increased burnup would enable improvements in fuel cycle economics via increased LWR enrichment and burnup. [Pimental 2019] Improved fuel economy can be realized by reducing the number of feed assemblies (batch size) in a cycle, through power uprating or through longer cycles (e.g., transitioning from 18-month cycles to 24-month cycles). Evaluation of the effects of EE, HBU, and ATF concepts and materials is performed over expected ranges of LWR burnup and enrichment. Estimates of the expected ranges of enrichment and burnup relevant to ATF fuel use were determined using a combination of industry historical data from the GC-859 fuel assembly database [ORNL 2016] and a simple Excel spreadsheet PWR fuel management estimator.

3.1 PWR CYCLE ESTIMATOR VALIDATION WITH GC-859 DATA

The cycle estimator is used to quickly explore the relationships between equilibrium cycle batch average enrichment and batch or sub-batch average discharge burnup, with numerous variables to describe the core operation. Cycle estimator input variables are shown in Table 7; additional details are available in Appendix A.

Table 7. Cycle estimator input variable description.

Parameter	Description
Fuel assemblies in core	Number of fuel assemblies in the core
Rated power	Core thermal power at 100% (MWth)
MTU/assembly	Fuel assembly uranium loading
Batch size	Number of fuel assemblies per reload batch
Enrichment	Assembly average enrichment in the reload batch
Cycle length	Cycle length in days including outages
Outage + maintenance	Number of days per cycle shutdown for refueling
Cycle load factor	Fraction of maximum energy produced between refueling outages
Last cycle power penalty (20% of fuel assemblies in core)	Power of a fuel assembly on the core periphery relative to the same assembly in the core interior. Assumes low leakage loading strategy.

The cycle estimator uses Polaris k_{inf} predictions for a Westinghouse 17×17 fuel assembly and estimates end-of-cycle (EOC) batch burnups and weighted core average k_{inf}. EOC is assumed to occur when the weighted core average k_{inf} reaches a target value. Benchmarking of the estimator with 26 cycles of GC-859 enrichment and discharge burnup (DBU) data from six PWR plants indicated a best-estimate core average EOC k_{inf} target of 1.044. Data for the benchmark cycles are provided in Table 8.

Table 8. Cycle estimator benchmark data.

Parameter / plant	Plant A	Plant B	Plant C	Plant D	Plant E	Plant F	Average
Plant design	Westinghouse 4 Loop	Westinghouse 2 Loop	Combustion Engineering	Westinghouse 3 Loop	Westinghouse 3 Loop	Combustion Engineering	
Fuel design for benchmark batches	Westinghouse 17 × 17 LOPAR	Westinghouse 14 × 14 OFA	CE 14 × 14 Areva	Westinghouse 17 × 17 OFA	Westinghouse 17 × 17 OFA	CE 14 × 14 Westinghouse	
Cycle length (months)	18	18	18	18	18	24	–
Core power (MWth)	3413	1677	2700	2900	2775	2737	–
Fuel assemblies	193	121	217	157	157	217	–
MTU/assembly	0.456	0.350	0.399	0.418	0.423	0.408	–
Power (MW/MTU)	38.8	39.6	31.2	44.2	41.8	30.9	–
Benchmark batches	K-M	V-CC	V-X	T-V	3A-3D	1T-1X	–
Batch avg. enrichment (wt % ^{235}U)	4.52	4.83	4.02	4.69	4.36	4.24	4.44
Assemblies / batch	76.3	48.4	68.0	70.0	66.5	89.0	–
GC-859 DBU (MWd/MTU)	51,059	51,898	48,109	49,980	48,900	46,307	49,376
Load factor to match GC-859 DBU	100.0%	100.0%	95.4%	100.0%	96.5%	87.8%	96.6%
Cycle estimator k-inf	1.040	1.052	1.042	1.048	1.038	1.045	1.044
Maximum batch split (wt % ^{235}U)	0.25	0.13	0.09	0.09	0.22	0.03	0.14
Maximum assembly avg. enrich. (wt % ^{235}U)	4.81	4.97	4.53	4.81	4.61	4.67	4.73
Batch fraction	40%	40%	31%	45%	42%	41%	40%
Max. assembly DBU/ batch DBU	1.11	1.13	1.12	1.13	1.15	1.13	1.13
Pin BU limit / max assembly average BU	1.10	1.06	1.14	1.07	1.07	1.06	1.08

Two calculation benchmarks are available for an increased-enrichment, 24-month cycle PWR. [Zhang et al. 2019; Capps et al. 2020]. Both studies establish an equilibrium 24-month cycle for a four-loop Westinghouse 17×17 fuel design PWR and assume a maximum fuel rod burnup of 75 GWd/MTU. Using the available information, the cycle estimator was used to determine the batch average enrichment for each equilibrium cycle for comparison. A target k_{inf} of 1.044 was assumed. Table 9 shows the results of the comparison. The cycle estimator calculated the enrichment required within 0.2 wt % for these cases.

Table 9. Cycle estimator comparison with 24-month cycle calculations.

	Zhang et al. 2019	Capps et al. 2020
Cycle length (months)	24	24
Assemblies in core	193	193
Core thermal power (MWt)	3853	3622
MTU per assembly	0.543	0.463
Batch size	80/81	84/85
Effective full power days	690	693.5
Sub-batches	2	3
Maximum enrichment (wt % ^{235}U)	6.0	6.6
Benchmark batch average enrichment	***5.3***	***6.0***
Cycle estimator batch average enrichment	**5.5**	**5.9**

The purpose of the cycle estimator is to provide a reasonable estimate of the relationship between increased enrichment and increased DBU under a variety of cycle transition scenarios. Increased enrichment can be used to reduce batch size, to support higher load factors, to support power uprates, or to increase cycle length. There are numerous other factors that can influence the relationship between enrichment and DBU, including changes to burnable absorber design, lattice changes (particularly for BWRs), HBU fuel use restrictions (e.g., rod burnup limits, peaking factor limits, and fuel placement restrictions), power coastdown practices, and fuel failures. GC-859 historical data reflect all of these influences in varying proportions.

For all currently operating LWR plants in the GC-859 database, the range of DBU/wt % within an enrichment range of ~2.9 to <5.0 wt % is 5.0 to 20.0 GWd/MTU/wt %. These values were calculated using a linear least squares fit over a range of enrichments that avoids most first cycle batches. Figure 1 shows data from a typical plant with a slope of 10.6 GWd/MTU/wt %. Figure 2 shows the distribution of slopes for operating US LWRs, and Table 10 provides summary statistics. Because the PWRs and BWRs have very similar historical relationships between assembly average enrichment and DBU, conclusions developed for PWRs can be reasonably extended to BWRs without the need to develop more complex BWR models.

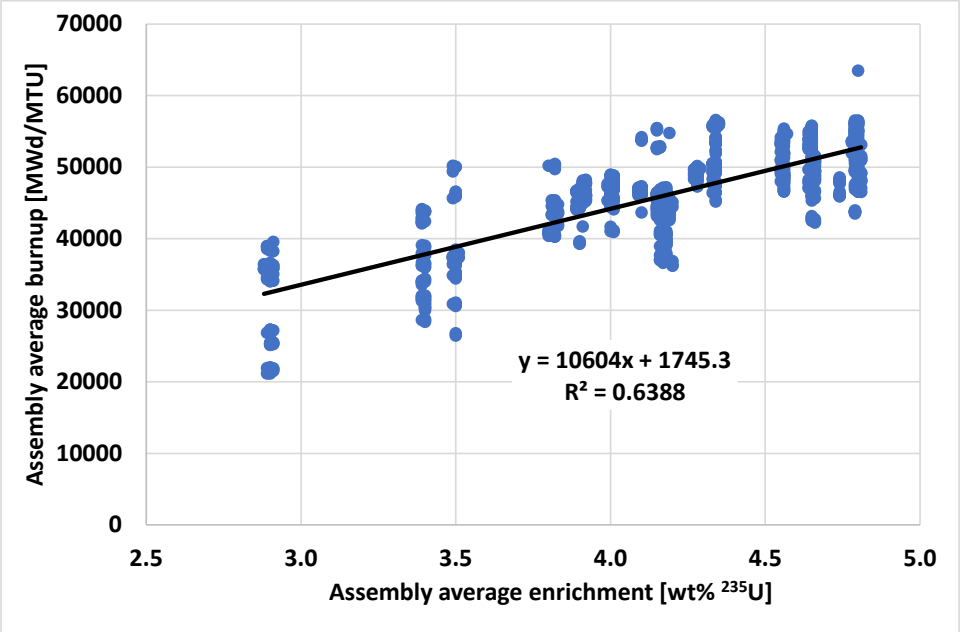

Figure 1. Three-loop PWR DBU versus enrichment.

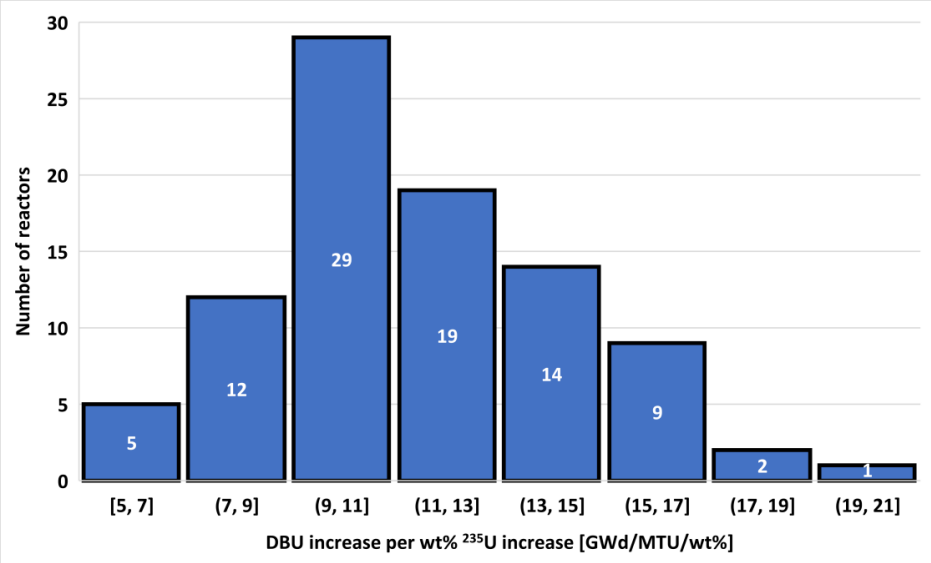

Figure 2. Operating US LWR DBU increase per wt % ^{235}U.

Table 10. Operating US LWR DBU/wt % statistics.

	BWR		PWR		Combined	
	Slope (GWd/MTU per 1 wt %)	DBU at 4 wt % (GWd/MTU)	Slope (GWd/MTU per 1 wt %)	DBU at 4 wt % (GWd/MTU)	Slope (GWd/T per 1 wt %)	DBU at 4 wt % (GWd/MTU)
Average	12.2	44.8	11.2	44.1	11.5	44.3
Median	11.5	45.1	10.7	43.8	10.9	43.9
Std. deviation	25%	6%	25%	4%	25%	5%
Max	20.0	51.0	18.3	49.2	20.0	51.0
Min	5.5	37.9	5.0	41.2	5.0	37.9

The cycle estimator cannot anticipate fuel design changes or the effects of fuel failures. It can model transitions involving reduced batch size, higher load factors, power uprates, and increased cycle length, assuming a consistent fuel design and normal cycle operation. Table 11 shows the DBU/wt % results predicted for each type of transition. Each model starts from a base case with 40 MW/MTU power, 48% batch fraction, a 45-day outage length (OL), 90% load factor (LF), and 4 wt % batch average enrichment. Results show that using enrichment increase to reduce batch size results in nearly twice the DBU increase of transitioning from 18- to 24-month cycles. Uprating, reducing outage length, or increasing load factor produces a DBU/wt % slope very similar to the GC-859 historical results. The range of results produced is supported by the range of GC-859 data.

Table 11. Cycle estimator results for various cycle transitions.

Case	Power (MW/MTU)	Batch fraction	LF (%)	OL (days)	Cycle (months)	Enrichment (wt %)	DBU (GWd/MTU)	Slope (DBU/wt %)
Base	40	42%	90	45	18	4.00	43.6	–
Batch	40	34%	90	45	18	4.50	52.6	18.0
Cycle	40	48%	90	45	24	4.80	51.0	9.2
LF/OL	40	42%	98	25	18	4.50	49.4	11.6
Uprate	45	42%	90	45	18	4.46	49.0	11.7

3.2 PWR AND BWR ENRICHMENT AND BURNUP ESTIMATES

Estimation of the maximum expected PWR and BWR fuel enrichment required to support an increase in maximum pin burnup to 75 GWd/MTU is needed to inform an evaluation of HALEU, HBU, and ATF effects over realistic ranges. The evaluation of enrichment and burnup relationships involves values related to overall core reactivity (batch average), values related to core power distributions (intra-batch or split batch), and values related to limits (maximum assembly, pin, or pellet). Maximum required enrichment can be characterized as follows.

Maximum enrichment = Batch average + batch split + blanket offset + assembly zoning offset

- Batch average enrichment is primarily a function of cycle energy requirements and for this work can be estimated from historical data and/or the cycle estimator.

- An allowance of 0.25 wt % for batch split (maximum assembly average enrichment in a batch minus batch average enrichment) bounds the GC-859 data from benchmark cycles in Table 8.

- Blanket offset (central zone enrichment minus pin average enrichment) is a function of blanket enrichment and blanket length. Typical blanket length is approximately 8% of the fuel stack (6 inches on each end). Blanket enrichment has historically varied from natural enrichment to ~2.6 wt %. [Wagner and DeHart 1999] Assuming 6-inch blankets enriched 2.5 wt % less than the central zone on all fuel pins, the blanket offset is ~0.2 wt %.

- Enrichment loading patterns for pin power control are less common in PWR fuel than in BWR fuel but does occur, particularly when gadolinia neutron poisons are used. A reasonable approximation for PWR radial zoning is to assume 0.5 wt % enrichment reduction in 30% of fuel rods (rods with gadolinia or in high peaking locations) resulting in an allowance of 0.15 wt %.

Therefore, maximum required enrichment would be ~0.6 wt % greater than batch average enrichment, adding considerations for batch split (~0.25 wt %), blanket offset (~0.2 wt %), and assembly zoning offset (0.15 wt %).

Batch average enrichment can be estimated using the cycle estimator, if the maximum allowable batch DBU is known, using the following formula:

Maximum batch DBU = Pin burnup limit – Intra-batch allowance – Intra-assembly allowance

The pin burnup limit is currently ~62 GWd/MTU but is anticipated to increase to as much as 75 GWd/MTU. A low estimate of intra-batch allowance from Table 8 is 11% of the batch burnup. A practical estimate of the intra-assembly burnup allowance (maximum pin burnup minus assembly average DBU) is the minimum assembly burnup margin to the limit from Table 9 (6% of batch burnup). Other than test assemblies, no other assembly in 26 batches of fuel has less than 6% margin between the pin burnup limit and the assembly average DBU. Using these values, the maximum batch DBU is the pin burnup limit divided by 1.17. Assuming 75 GWd/MTU as the pin burnup limit, the estimated maximum practical batch DBU is 64 GWd/MTU.

The cycle estimator was used to estimate batch average enrichment assuming maximum batch burnup of 64 GWd/MTU for 18- and 24-month cycles. All cases use optimistic values of outage length (20 days) and cycle load factor (98%) to maximize projected enrichment. Batch fractions greater than 50% are not considered, because they would result in some high-enrichment fuel assemblies being discharged after only one cycle. Results are presented in Table 12 and Figure 3.

Table 12. Cycle estimator results with 64 GWd/MTU DBU.

Cycle length (months)	Batch fraction	MW/MTU	Batch average enrichment (wt % ^{235}U)	Batch average DBU (GWd/MTU)	Sub-batch DBU (GWd/MTU)
18	36.4%	45	5.54	64.0	67.5
18	32.3%	40	5.32	64.0	72.6
18	28.3%	35	5.18	64.0	67.9
18	24.2%	30	5.00	64.0	70.3
24	49.0%	45	6.02	64.0	77.7
24	43.5%	40	5.85	64.0	73.1
24	38.1%	35	5.62	64.0	67.9
24	32.6%	30	5.34	64.0	73.0

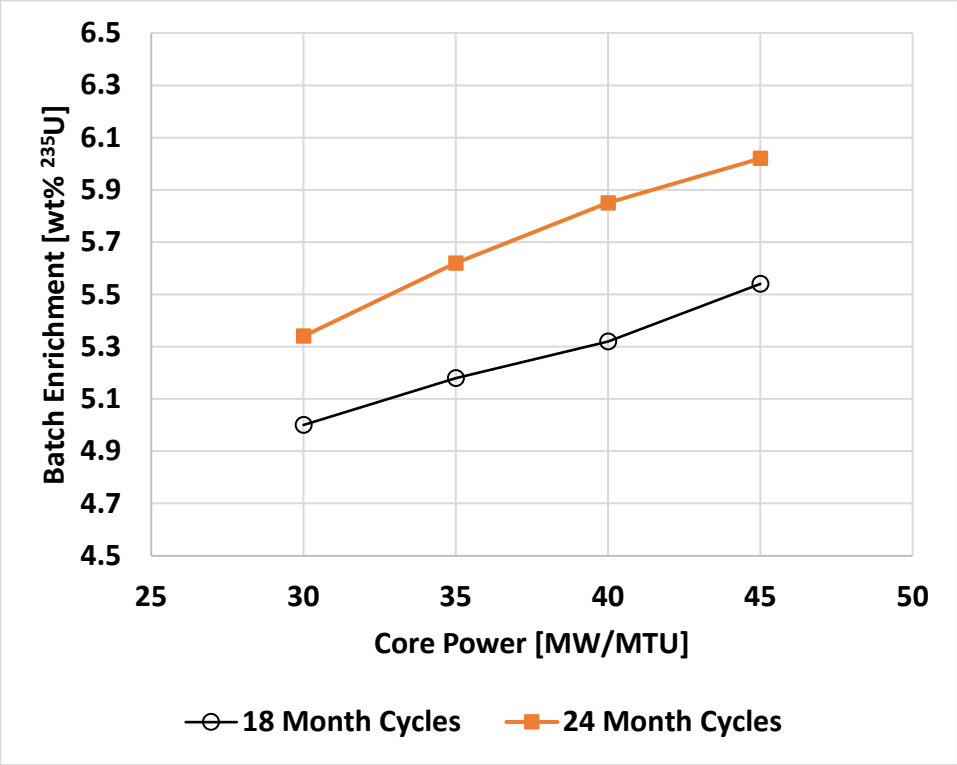

Figure 3. PWR batch average enrichment estimate.

When 0.6 wt % is added to batch-average values in Table 12, the maximum estimated PWR pellet enrichment to support a pin burnup limit of 75 GWd/MTU is 6.6 wt %. This value assumes a high specific power (45 MW/MTU), axial blankets, radial enrichment zoning, efficient refueling outages (20 days) and excellent operations (98% load factor). This suggests that for PWRs, evaluating ATF effects between 5 wt % and 6.6 wt % at up to 80 GWd/MTU provides good coverage of the application range, given a pin burnup limit of 75 GWd/MTU.

For BWRs, the relationship between DBU and average assembly enrichment is similar to that for PWRs, based on GC-859 data in Table 10. The PWR and BWR average slopes (DBU increase per wt %

enrichment increase) are similar, as are the average DBUs evaluated at 4 wt % enrichment. Given this historical similarity, it is reasonable to assume that the PWR and BWR maximum enrichments for a given pin burnup limit are also similar, provided margin is added for greater BWR intra-assembly enrichment variation. The maximum specific power is much lower for BWRs than PWRs. The maximum specific power of 31 BWRs surveyed using GC-859 data is 31.1 MW/MTU compared with 44.2 for the maximum PWR value in Table 9.

Relying on the historical similarity in enrichment and burnup trends between BWRs and PWRs, the PWR cycle estimator was used to simulate a 31.1 MW/MTU BWR with 624 assemblies, 24-month cycles, a 98% load factor, 20 day refueling outages, and 64 GWd/MTU batch average DBU. The model estimated batch average enrichment of 5.35 wt %. Using a BWR intra-assembly enrichment allowance estimate of 0.6–0.7 wt % for 5 wt % maximum pin enrichment, [Cumberland et al. 2021; ORNL 2015] and scaling up by a factor of 1.5 for increased enrichment, gives an ~1.0 wt % allowance for more highly enriched BWR assemblies. The upper enrichment limit estimate for BWRs is 6.4 wt %, very similar to the PWR estimate.

The upper limit enrichments derived are based on non-ATF fuel designs with increased DBU. ATF materials may exhibit more parasitic neutron absorption or displace water from the lattice, adversely affecting assembly reactivity. An enrichment penalty to offset adverse ATF reactivity effects can be added to the non-ATF upper enrichment estimate if needed.

4. REVIEW OF PREVIOUS ATF EVALUATIONS

Some aspects of the lattice physics effects and code performance related to ATF designs have been assessed in prior work [Jessee et al. 2020], where the primary purpose was to assess the ATF design-predictive capabilities of the SCALE/Polaris code with a focus on nuclear data uncertainties and the impact of modeling approximations. The ATF concepts evaluated include Cr_2O_3- and Al_2O_3-Cr_2O_3-doped UO_2 fuel, U_3Si_2 fuel, FeCrAl cladding, SiC cladding, and Cr-coated cladding. The following sections provide a brief summary of the previous work.

4.1 NUCLEAR DATA UNCERTAINTY

Sensitivity and uncertainty techniques using the SCALE/TSUNAMI sequence were used to evaluate nuclear data uncertainty associated with ATF designs and materials for unirradiated PWR and BWR fuel assemblies. The following PWR variants were investigated assuming fresh fuel in a 17×17 4.0 wt % ^{235}U lattice.

- UO_2 / Zircaloy-4 clad
- Al_2O_3-Cr_2O_3-doped UO_2 / Cr-coated Zircaloy-4 clad
- Cr_2O_3-doped UO_2 / Cr-coated M5 clad
- Cr_2O_3-doped UO_2 / SiC clad
- U_3Si_2 / SiC clad
- U_3Si_2 / Cr-coated Zircaloy-4 clad

Data-induced uncertainty in k_{eff} was nearly the same for all PWR variants. The uncertainty range (maximum – minimum) was only 27 pcm.

The following BWR variants were investigated assuming fresh fuel in a GE14 10×10 average ~4.3 wt % ^{235}U lattice (minimum pin 1.6 wt %, maximum pin 4.9 wt %).

- UO_2 / Zircaloy-2 clad
- UO_2 / Cr-coated Zircaloy-2 clad
- UO_2 / FeCrAl clad
- UO_2 / FeCrAl clad (optimized)

Data-induced uncertainty in k_{eff} was nearly the same for all fuel types. The uncertainty range (maximum – minimum) was 47 pcm. Uncertainty was highest for the nominal FeCrAl clad assembly.

4.2 BENCHMARK EXPERIMENT SIMILARITY ANALYSIS

Sensitivity and uncertainty techniques using the SCALE/TSUNAMI sequences were used to evaluate the similarity of unirradiated ATF fuel designs to 1643 critical experiments. The evaluation was performed for fuel assemblies at in-reactor hot full power (HFP) conditions. The primary concern in this study was how the introduction of ATF fuel concepts might change the set of applicable experiments used to perform computer code/model validation.

The same PWR variants were investigated as listed earlier. Doped UO_2, coated clad, and SiC clad caused only small similarity reductions compared with the reference non-ATF design. Introducing U_3Si_2 caused a larger similarity reduction (a few percentage points), but the introduction of ATF concepts did not significantly reduce the applicability of critical experiments for validation.

The same BWR variants were investigated as listed earlier. A coated clad had no significant effect on similarity. FeCrAl caused a significant but not large (a few percentage points) reduction in similarity.

4.3 POLARIS MODELING

A study of coated clad modeling options using fresh PWR fuel recommended modeling the Cr coating with the outer half of the clad, preserving the physical inner and outer clad diameter. Homogenizing the coating with all of the clad produced very similar results.

A study of FeCrAl cladding indicated fuel assembly k_{inf} was reduced between 4% and 8% in a burnup range of 0 to 80 GWd/MTU. The use of FeCrAl may require significant design changes because of the large magnitude of the reactivity penalty.

A comparison of Polaris, NEWT, and continuous energy KENO and Shift k_{inf} calculations for a U_3Si_2 pin cell identified a Polaris bias of ~300 pcm. The source of the bias was determined to be related to self-shielding factors tabulated in Polaris assuming UO_2. Improvement and generalization of these shielding factors is planned as a part of future SCALE enhancements.

Depletion of the cladding for Cr-coated or FeCrAl-clad fuel was performed from 0 to 80 GWd/MTU. Depletion reactivity effects were found to be negligible (33 pcm or less) compared with the standard approach of only depleting fuel.

4.4 ATF LATTICE PARAMETER AND CODE ASSESSMENTS

Code-to-code comparisons between Polaris and continuous energy Shift are presented for a 4 wt % PWR assembly for numerous quantities of interest, including k_{inf}, control rod worth, MTC, DTC, and soluble boron worth. Comparisons cover a burnup range of from 0 to 80 GWd/MTU. For the Shift and Polaris quantities of interest comparisons, the following acceptance criteria were used:

- 200 pcm difference in k_{inf}
- 400 pcm difference in four factors
- 0.25 difference in fast to thermal energy group flux ratio
- 5% difference in control rod worth (CRW)
- 4 pcm/k difference in moderator temperature coefficient (MTC)
- 0.5 pcm/k difference in doppler temperature coefficient (DTC)
- 1 pcm/ppm difference in differential boron worth (DBW)

Table 13 summarizes the effects of ATF on quantities of interest at the lattice level. The PWR ATF concepts listed in Section 4.2 were evaluated. For this summary, selected results (difference between non-ATF and ATF fuel) are grouped into three bins: doped pellets and coated clad, doped pellets and SiC clad, and U_3Si_2. Tabulated values are approximated from plots. The effects of U_3Si_3 are substantially larger (by an order of magnitude in some cases) than those of other ATF concepts. Table 14 summarizes the level of difference between Shift and Polaris.

Table 13. 4 wt % 17×17 PWR ATF effects. [Jessee et al. 2020]

Parameter	Doped pellets and coated clad	Doped pellets and SiC clad	U_3Si_2 effect
k_{inf}	–800 to –200 pcm	500 to 700 pcm	–750 to 2100 pcm
Fast/thermal flux ratio	0.0 to 0.2	~0.0	1.1 to 2.0
Moderator temperature coefficient (0 ppm boron)	–2.0 to –0.5 pcm/K	2.0 to 5.0 pcm/K	–11.0 to 0 pcm/K
Moderator temperature coefficient (1200 ppm boron)	–3.5 to –0.5 pcm/K	2.0 to 5.0 pcm/K	–24.0 to –4.0 pcm/K
Control rod worth (0 ppm boron)	0.0 to 0.5%	–1.5 to –1.0%	–12.3 to –6.3%
Doppler temperature coefficient	–0.02 to –0.03 pcm/K	0.0 to 0.02 pcm/K	–0.18 to 0.1 pcm/K
Boron worth (pcm/ppm)	0.0 to 0.3	0.0 to 0.1	0.9 to 2.4
Effective delayed neutron fraction	~0.0%	~0 to 0.5%	~0.4 to 1.3%
Delayed neutron decay constant	~0.0%	~0.1 to 0.2%	~1.0 to 1.4%

Table 14. Polaris – Shift PWR lattice parameter differences. Jessee et al. 2020

Parameter	Doped pellets and coated clad	Doped pellets and SiC clad	U_3Si_2	Non-ATF
k_{inf}	–230 to –10 pcm	–250 to –100 pcm	–350 to –150 pcm	–210 to 0 pcm
Fast/thermal flux ratio	~0.15	~0.15	~0.15 to 0.2	~0.15
Moderator temperature coefficient (0 ppm boron)	–3.0 to 0.0 pcm/K	–3.0 to 0.0 pcm/K	–3.0 to 0.0 pcm/K	–3.0 to 0.0 pcm/K
Moderator temperature coefficient (1200 ppm boron)	–4.0 to 0.0 pcm/K	–4.0 to 0.0 pcm/K	–4.0 to 0.0 pcm/K	–4.0 to 0.0 pcm/K
Control rod worth (0 ppm boron)	~0.0%	~0.0%	~0.0%	~0.0%
Doppler temperature coefficient	–0.25 to –0.0 pcm/K	–0.25 to –0.0 pcm/K	–0.25 to–0.0 pcm/K	–0.25 to –0.0 pcm/K
Boron worth (pcm/ppm)	~0.0	~0.0	~0.0	~0.0

Continuous-energy KENO and Polaris unirradiated BWR fuel k_{inf} comparisons were also performed for a GE14 10×10 assembly and an ATRIUM 11×11 assembly with no gadolinia. The following cases were modeled:

- GE14 10×10 UO_2 (baseline) Zircaloy-2
- GE14 10×10 UO_2 Cr-coated Zircaloy-2
- GE14 10×10 UO_2 FeCrAl
- GE14 10×10 UO_2 (optimized) FeCrAl
- ATRIUM 11×11 UO_2 (baseline) Zircaloy-2
- ATRIUM 11×11 Cr_2O_3 doped UO_2 Zircaloy-2

Differences (KENO kinf – Polaris kinf) were between –204 and 28 pcm, indicating no significant discrepancies related to modeling of ATF materials.

Polaris depletions were performed using the SCALE/Sampler sequence to calculate burnup-dependent cross section uncertainty in k_{inf} for multiple GE14 BWR and Westinghouse PWR lattices. Table 15 (reproduced from Table 19 of Reference 39) shows the ATF and non-ATF cases evaluated. Compared with the non-ATF PWR depletion uncertainty, doped fuel and Cr-coated clad make no significant difference. A SiC clad increases uncertainty (one sigma) slightly (<10 pcm), and U_3Si_2 increases uncertainty by approximately 50 pcm. In the BWR lattices, FeCrAl increases uncertainty by between 20 and 60 pcm. The largest increases are about 10% of the non-ATF uncertainty, indicating the effect of these ATF materials on k_{inf} uncertainty is modest.

Table 15. Polaris–Lattice types included in depletion uncertainty analysis. [Jessee et al. 2020]

Case	Lattice type	Fuel	Clad
Chromium-coated Zirc	GE14	UO_2	Cr-coated Zircaloy-2
FeCrAl		UO_2	FeCrAl
FeCrAl-optimized dimensions		UO_2	FeCrAl
UO_2-Zirc clad		UO_2	Zircaloy-2
Cr_2O_3–M5	W 17×17	Cr_2O_3-doped UO_2	Cr-coated M5
UO_2-SiC		UO_2	SiC
Cr_2O_3–Al_2O_3–Zirc		Cr_2O_3–Al_2O_3-doped UO_2	Zircaloy-4
Cr_2O_3–UO_2–SiC		Cr_2O_3-doped UO_2	SiC
U_3Si_2–Cr-coated		U_3Si_2	Cr-coated Zircaloy-4
U_3Si_2–SiC		U_3Si_2	SiC

4.5 SUMMARY OF PRIOR ATF LATTICE AND CODE ASSESSMENTS

The assessments performed in [Jessee et al. 2020] led to the general conclusion that ATF materials can be ranked in terms of the degree of perturbation to non-ATF lattice reactivity, code uncertainty, and physics parameters. Dopants and Cr coating have the smallest effect, followed by SiC clad, with FeCrAl and U_3Si_2 showing the largest effects. These effects were well predicted by Polaris, as determined by comparison with CE Shift and CE KENO. Only U_3Si_2 indicated a need for code improvements. Adjustments to the procedure used to generate self-shielding factors will be implemented to support higher-density fuels (U_3Si_2 and UN). Cross-section uncertainty associated with ATF lattices was only modestly larger than that associated with non-ATF lattices.

5. ATF EVALUATION SCOPE

To supplement the prior ATF lattice code assessment work, new work in this report focuses on four areas of interest for the near-term ATF concepts most likely to be deployed:

1. The effect of ATF on enrichments needed to support HBU limits
2. The effect of ATF and compensatory enrichment changes on lattice reactivity parameters
3. The effect of ATF on depleted fuel isotopic content of interest for severe accidents, decay heat, and fuel storage shielding
4. The effect of unirradiated ATF on transportation package subcriticality

Lattice combinations for Polaris k_{inf} calculations are shown in Table 16.

Table 16. Scope of LWR ATF combinations considered.

Lattice type	Enrichment (wt % ^{235}U)	Dopants	Clad	Notes
PWR 17×17	5.0, 8.0	None	ZIRLO	Base case ZIRLO
		None	M5	Base case M5
		None	FeCrAl	FeCrAl with increased fuel pellet outer diameter (OD) or reduced clad OD
		Cr_2O_3 (800 ppm) + Al_2O_3 (200 ppm)	ZIRLO	Doped vs. ZIRLO base
		Cr_2O_3 (800 ppm) + Al_2O_3 (200 ppm)	ZIRLO + Cr coating	Doped and coated vs. ZIRLO base
		Cr_2O_3 (1000 ppm)	M5	Doped vs. M5 base
		Cr_2O_3 (1000 ppm)	M5 + Cr coating	Doped and coated vs. M5 base
BWR 10×10	5 wt % limit, 10 wt % limit	None	Zirc-2	Base case Zirc-2
		None	FeCrAl	Base case FeCrAl
		None	Zirc-2 + Cr coating	Coated Zirc-2 vs. Zirc-2 base
		Cr_2O_3 (1000 ppm)	Zirc-2	Doped vs. Zirc-2 base
		Cr_2O_3 (1000 ppm)	Zirc-2 + Cr coating	Doped and coated vs. Zirc-2 base

The Cr coating thickness was assumed to be 20 μm, which was the approximate midpoint of the range proposed by different vendors. Two types of FeCrAl were considered (C26M and AMPT) for BWR assemblies. Based on the literature review, the FeCrAl clad thickness was assumed to be 0.385 mm (385 μm), or ~60% of the nominal Zirc-2 thickness

With a reduced clad thickness, there are two ways to offset FeCrAl parasitic neutron absorption: increase the UO_2 content (larger-diameter fuel pellets) or increase the enrichment (clad with a smaller OD). If the clad outer diameter, cycle length, and core rated power are not changed, an FeCrAl clad core will have more UO_2, lower specific power, lower burnup, and the same fuel pin heat flux. If the fuel pellet

diameter, cycle length and core rated power are not changed, an FeCrAl clad core will have the same UO_2 mass, the same specific power, the same burnup, and higher fuel pin heat flux. Regardless of the option used, FeCrAl can be expected to introduce significant fuel management challenges, as well as lattice physics effects. FeCrAl channel boxes were not considered in this BWR analysis, as additional engineering considerations must be made. Although no near-term proposals for using FeCrAl cladding in a PWR were found, calculations using FeCrAl cladding with undoped fuel are provided for reference in Section 7.3.

6. POLARIS MODELS

A 17×17 PWR fuel assembly with IFBA was used as a representative design for the dopant and clad coating evaluation. The assembly specifications and depletion conditions for the 5 wt % ^{235}U assembly were the same as in Reference 3. The 8 wt % assembly IFBA was increased from 104 rods to 156 rods [Sanders and Wagner 2001] and the depletion soluble boron was set to 1300 ppm to offset increased assembly reactivity and better simulate the expected change in depletion conditions. The soluble boron increase nearly preserved the mid-depletion boron worth and was estimated using previous lattice analysis results, [Hall et al. 2021] assuming a transition from 18- to 24-month cycles. With increased IFBA and boron, HFP depletion k_{inf} for the 8 wt % assembly remained higher than the 5 wt % assembly throughout the depletion, as shown in Figure 4. The doped pellet density was increased by 0.5%, reflecting the density effect of the larger grain size of doped UO_2. [Aborelius et al. 2006]

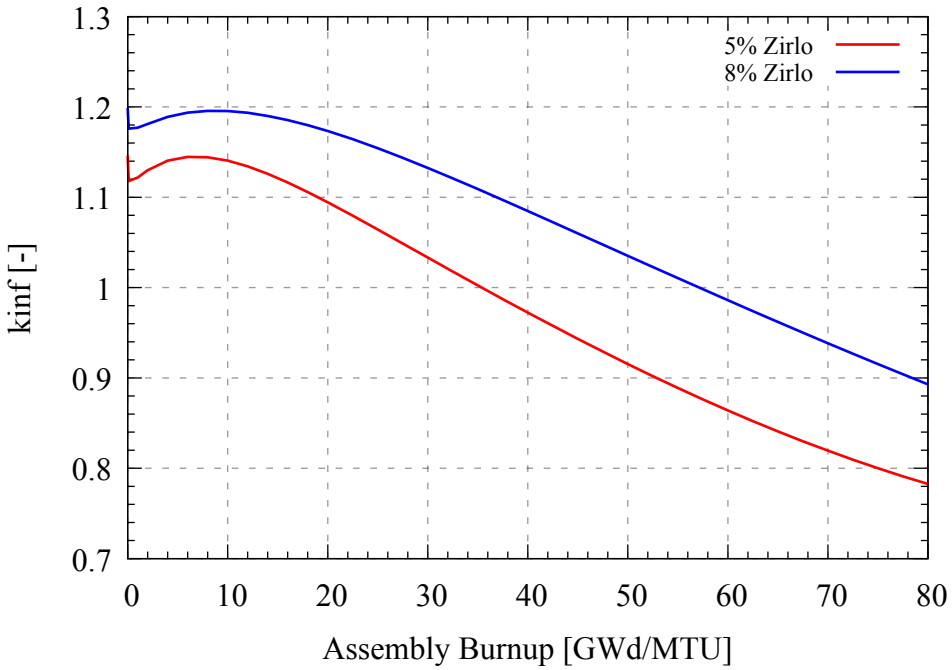

Figure 4. Multiplication factor for reference PWR lattices vs. burnup.

SCALE/Polaris depletions were performed from 0 to 80 GWd/MTU. Depletion steps to 0.1, 1, and 2 GWd/MTU were followed by 2 GWd/MTU steps to 20 GWd/MTU and 2.5 GWd/MTU steps to 80 GWd/MTU. The SCALE ENDF/B-VII.1 56-group neutron cross-section library was used for non-ATF base cases and ATF depletions.

The evaluation of BWR ATF concepts was performed using a representative GNF-2 10×10 BWR fuel lattice. This model is consistent with [Cumberland et al. 2021] and uses GE14 lattice parameters with GNF-2 vanished rod positions. The peak and average enrichments for these lattices are shown in Table 17 for the GE14 fuel assembly design. Similar to the previous analysis, the dominant region of the assembly and the vanished region were modeled because of the expected variation in neutronic behavior. Consistent with the PWR analysis, the fuel density of the doped fuel was increased by 0.5% doped UO_2. [Aborelius, Backman, Hallstadisu, et al. 2006]

Table 17. Lattice average ^{235}U enrichment.

Enrichment limit (wt % ^{235}U)	Lattice region	Average rod enrichment (% ^{235}U)
5.0	DOM	4.33%
	VAN	4.31%
10.0	DOM	7.45%
	VAN	7.47%

DOM = dominant; VAN = vanished

Figure 5 and Figure 6 show the lattice ^{235}U enrichment and gadolinia loading for both fuel assembly regions for the 5 wt % limit and 10 wt % limit lattices, respectively. [Cumberland et al. 2021] For all lattices, the nominal moderator void fraction was set to 40%. Depletion calculations were performed at up to 80 GWd/MTU for both dominant and vanished lattices. Fuel pellets in each fuel pin were modeled with six equal volume radial regions (rings) to provide information on power and burnup distribution within each pin.

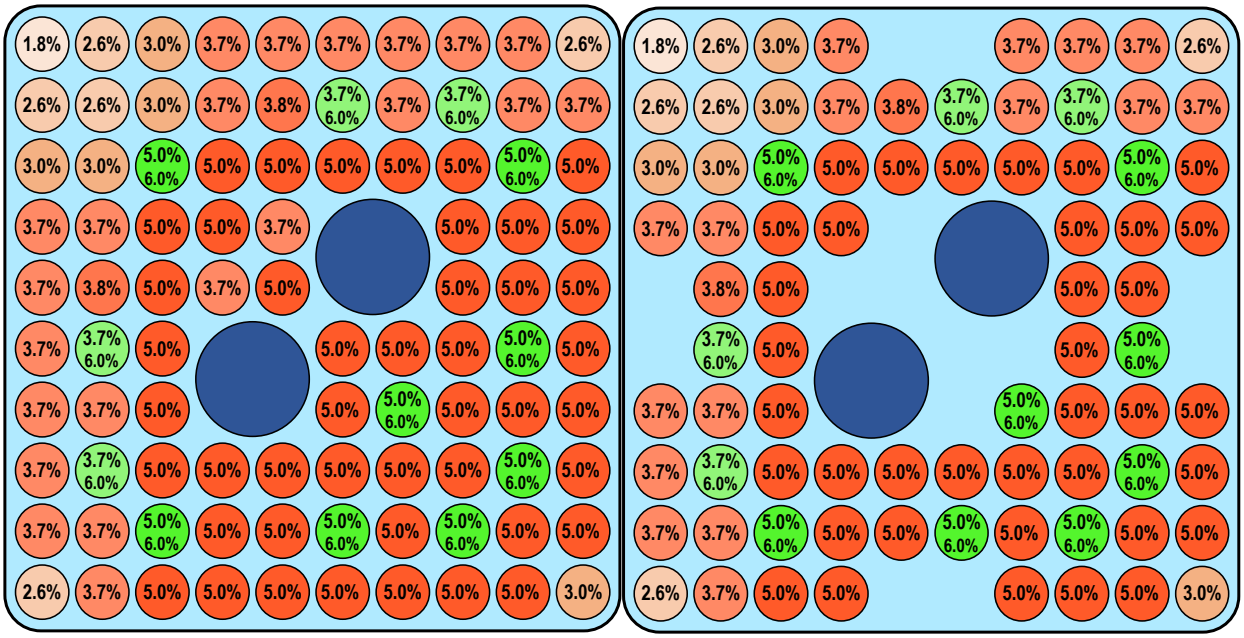

Figure 5. Layout of the reference 5% maximum enriched fuel assembly for dominant (left) and vanished (right) regions.

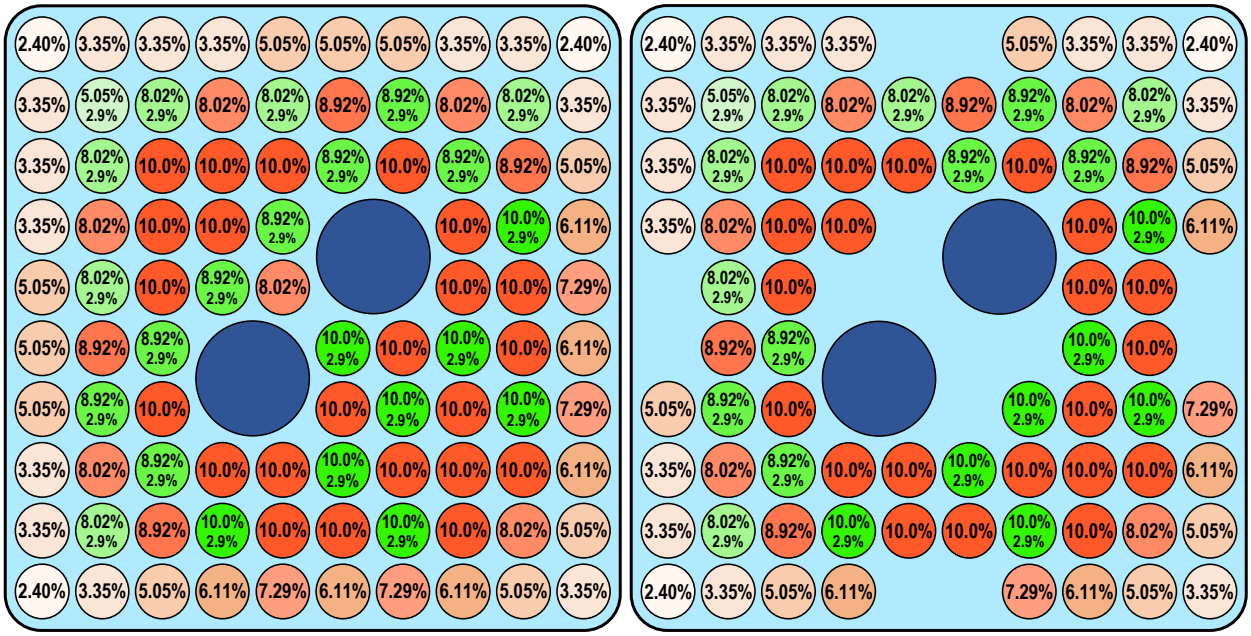

Figure 6. Layout of the 10% maximum enrichment fuel assembly for dominant (left) and vanished (right) regions.

The multiplication factor for the reference UO_2 fuel/Zircaloy-2 cladding simulations at up to 80 GWd/MTU is shown in Figure 7.

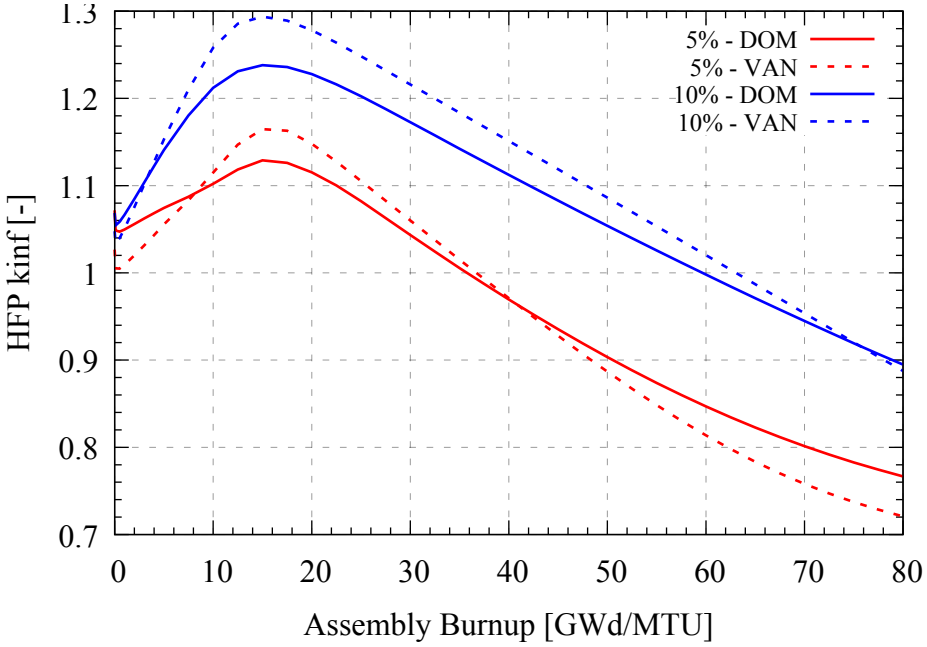

Figure 7. Multiplication factor for reference BWR lattices vs. burnup.

7. LATTICE PHYSICS RESULTS

7.1 PWR DOPANT AND COATING REACTIVITY PENALTY

Base case and ATF (doped fuel and Cr-coated clad) assembly depletions were performed for 5 and 8 wt % assemblies to assess the ATF reactivity penalty. Figure 8 shows the HFP reactivity difference of the ATF assembly relative to the base case assembly, with no soluble boron, as a function of assembly burnup. The reactivity penalty for doped pellets and Cr-coated fuel pins is roughly 350 pcm. The ATF effect is smaller for the 8 wt % depletion by about 50 pcm. There is no significant difference between the M5 and ZIRLO clad results. Reactivity differences in pcm are calculated as $10^5(1/k_1 - 1/k_2)$.

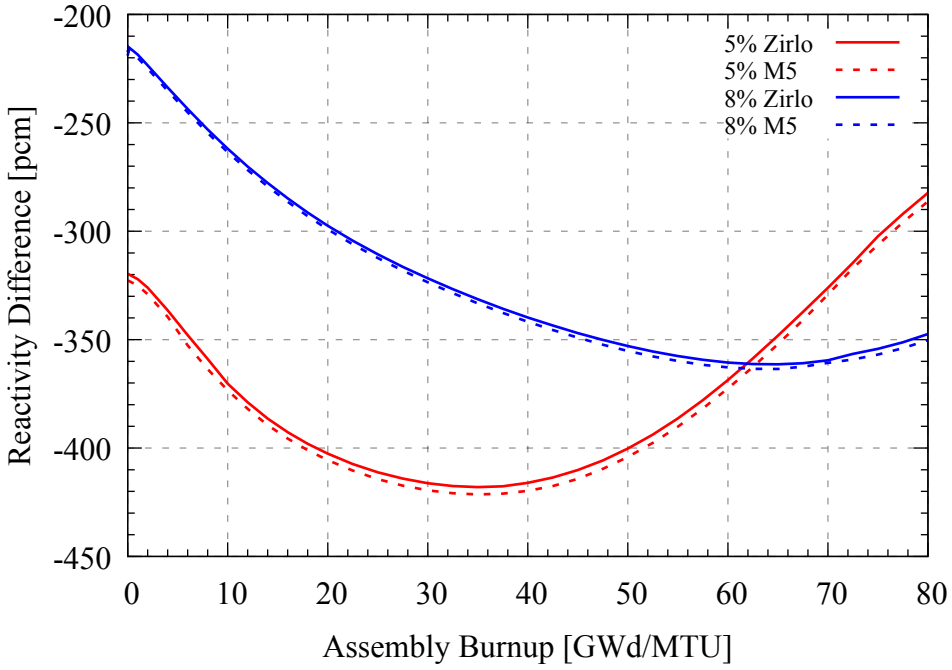

Figure 8. Reactivity penalty for doped and Cr-coated PWR ATF vs. burnup.

Some of the ATF effect shown in Figure 8 is due to the 0.5% pellet density increase, which more than offsets the 0.1% fuel displacement by dopants. The additional UO_2 means that at the same burnup, the ATF assembly will have produced 0.4% more energy. Reactivity comparisons can also be made as a function of energy produced rather than burnup. Figure 9 shows the ATF reactivity penalty as a function of assembly energy produced. Using an equal energy basis (effectively crediting the extra UO_2 made possible by the effect of the dopant on the pellet density) has the effect of reducing the ATF effect more as burnup increases. The ATF effect is reduced by 0 to about 150 pcm over the full range of burnup with 0.5% more pellet density.

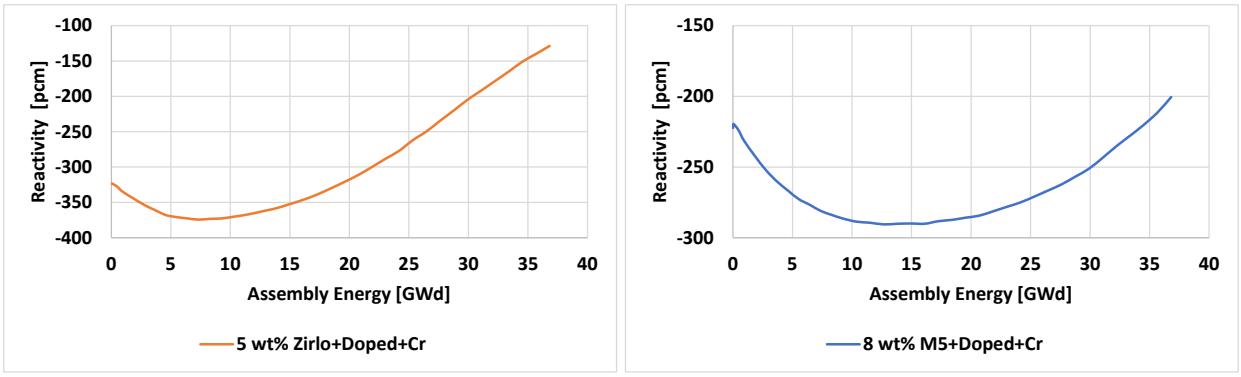

Figure 9. Reactivity penalty for doped and Cr-coated PWR ATF vs. cumulative energy release.

Two sets of additional depletions were performed to determine the enrichment required to offset the ATF penalty. The first set assumed doped fuel only, and the second set assumed doped fuel and Cr-coated clad. Depletions were performed with soluble boron; enrichment offset results were for the branch cases at HFP but with no soluble boron to represent the EOC condition. HFP reactivity differences (ATF relative to base versus burnup) in Figure 10 show that the HFP offset for dopants is negligible. On the basis of energy produced, the additional ATF UO_2 may more than offset the effect of the dopant, depending on the degree of additional pellet density achieved. With the addition of a coating, the enrichment penalty is on the order of 0.10 wt % for 5 wt % fuel and 0.15 wt % for 8 wt % fuel on an equal burnup basis. On an equal energy basis, the enrichment penalty would be reduced by ~0.02 wt % (~40 pcm / 0.01 wt %). This is shown in Figure 11.

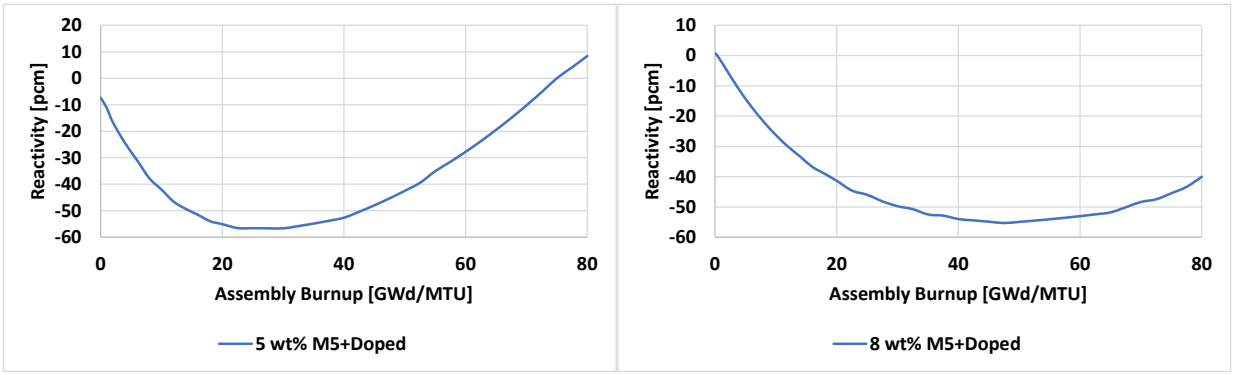

Figure 10. Reactivity penalty for doped PWR ATF.

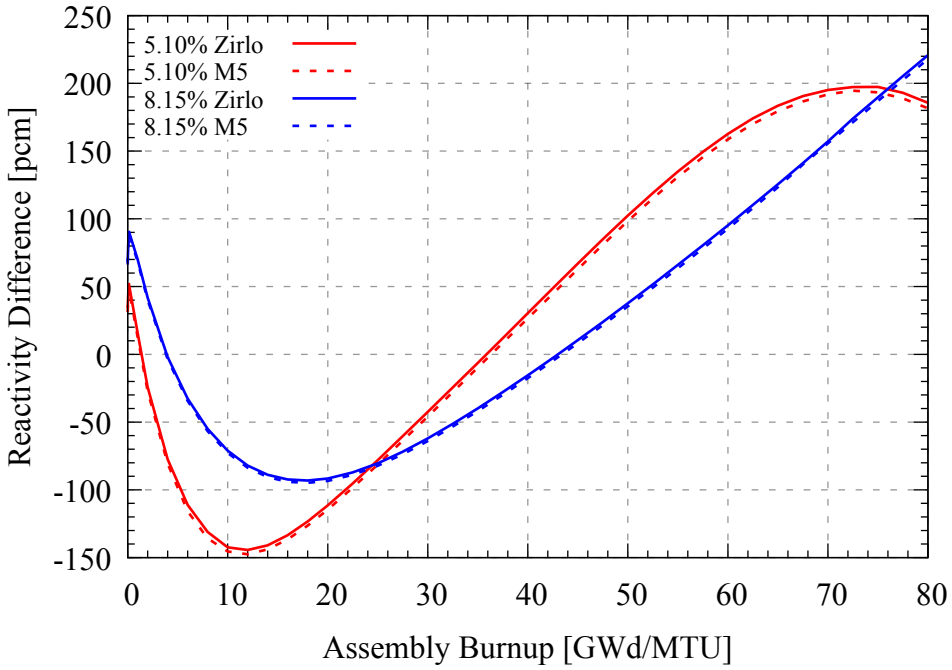

Figure 11. Reactivity penalty for doped and Cr-coated PWR ATF with enrichment offset.

7.2 PWR DOPANT AND COATING LATTICE PARAMETERS

The HFP DTC, MTC, CRW, and soluble boron worth were calculated for the PWR base cases and ATF doped and Cr-coated combinations. There was no significant effect on DTC and only a small effect on MTC, as shown in Figure 12 and Figure 13, respectively. Only the 5 wt % doped and Cr-coated case produced noticeable MTC changes, albeit still minor. MTC differences were driven by slightly less water in the lattice (more negative because of more under-moderation), slightly higher fuel density (more negative because of more under-moderation), slightly higher enrichment (more positive because of more self-shielded thermal fission cross sections), and small associated isotopic inventory changes from the slightly harder neutron spectrum. CRW and boron worth were reduced modestly by dopants and coatings as a result of a combination of slightly increased fuel enrichment and lattice water displacement (a harder spectrum) by the Cr-clad coating, as shown in Figure 14 and Figure 15, respectively. Table 18 provides β_{eff} comparisons for each ATF combination at several burnup steps with minor differences of less than 0.5%.

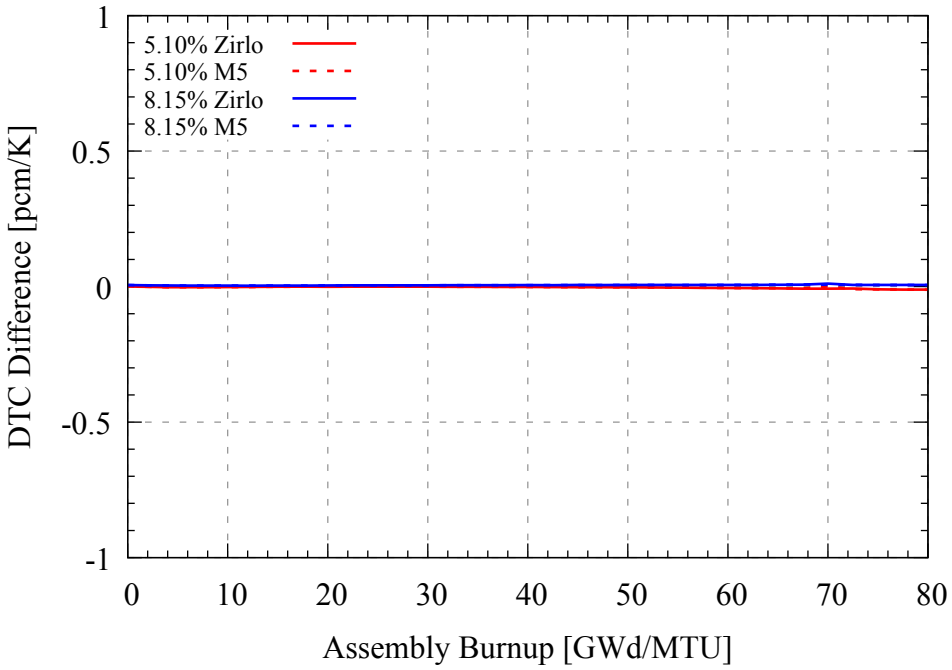

Figure 12. DTC difference for doped and Cr-coated PWR ATF.

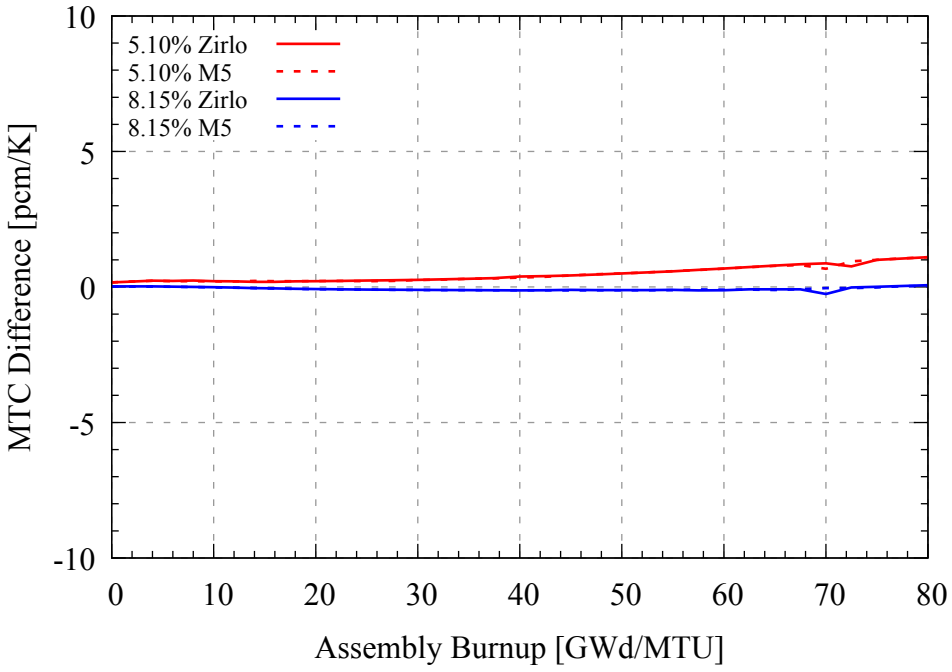

Figure 13. MTC difference for doped and Cr-coated PWR ATF.

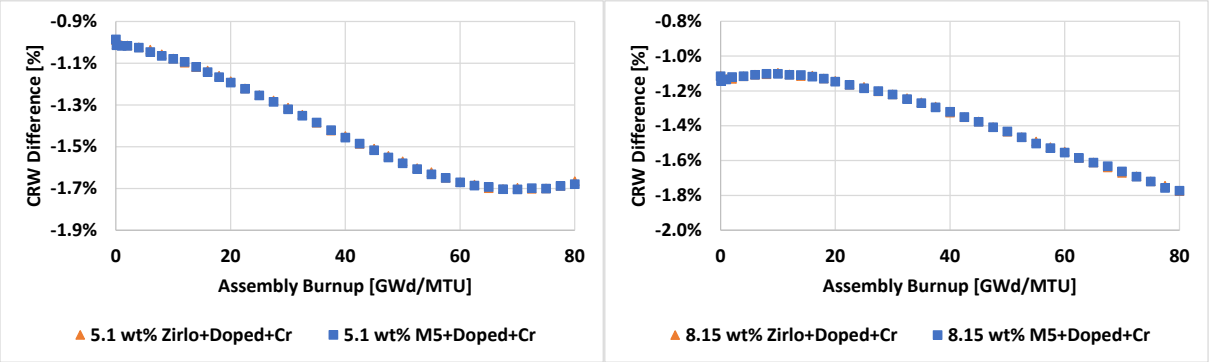

Figure 14. CRW difference for doped and Cr-Coated PWR ATF.

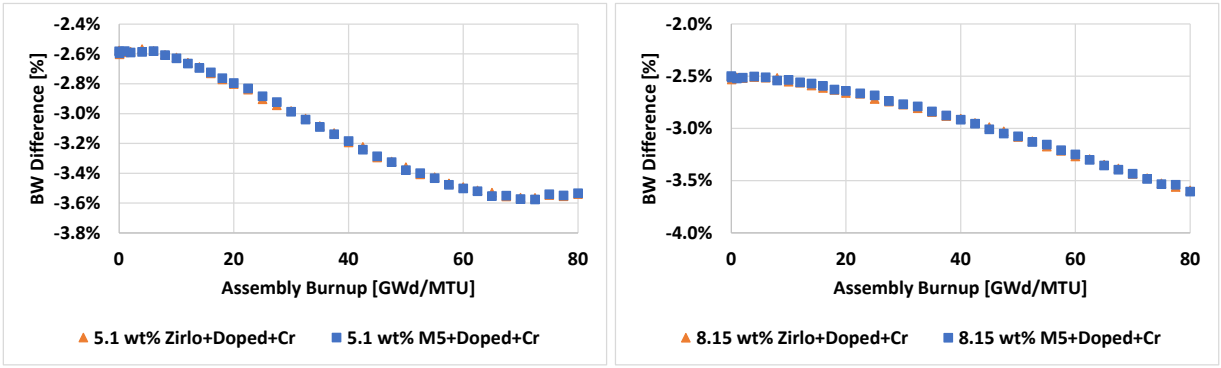

Figure 15. Boron worth difference for doped and Cr-coated PWR ATF.

Table 18. β-eff comparison for doped and Cr-coated PWR ATF.

Enrichment (wt %)	5.00	5.10	8.00	8.15
Clad	ZIRLO	ZIRLO +Cr	ZIRLO	ZIRLO +Cr
Doping	No	Yes	No	Yes
Burnup (GWd/MTU)	β_{eff}			
0	0.00686	0.00686	0.00682	0.00682
20	0.00553	0.00555	0.00594	0.00595
40	0.00490	0.00491	0.00541	0.00543
60	0.00444	0.00446	0.00499	0.00501
80	0.00411	0.00412	0.00462	0.00463

7.3 PWR FeCrAl REACTIVITY PENALTY

Although the use of FeCrAl in PWR fuel assemblies is not being actively pursued at this time, the use of FeCrAl in a PWR was evaluated to obtain insights regarding the potential effect on fuel assembly design and enrichment requirements. The clad density was assumed to be 7.2 g/cm3 and the clad thickness was assumed to be 0.0385 cm.

The base cases for evaluation of FeCrAl are the 5 wt % and 8 wt % ZIRLO clad non-doped designs discussed in Sections 7.1 and 7.2. Two FeCrAl clad dimension options were considered, one that preserved the base case clad outer diameter (OD) and pellet-clad gap but increased the fuel pellet OD

(referred to as the “large pellet option”), and one that preserved the fuel pellet OD and pellet-clad gap but reduced the clad OD (referred to as the “normal pellet option”). The primary reactivity quantity of interest was the HFP no-soluble-boron k_{inf}. Preservation of the same EOC k_{inf} was required to demonstrate that the reactivity effect of FeCrAl had been offset.

The reactivity effects of the two different types of FeCrAl (APMT and C26M) and the two different dimension options (large pellet and normal pellet) are shown in Figure 16 for a 5 wt % fuel assembly. The difference between APMT and C26M is small compared with the large reactivity penalty, so the C26M model was used for the remainder of this reactivity assessment. The trend of reactivity penalty with burnup was very different because of the different hydrogen/uranium ra (H/U) ratios for the large versus normal pellet size.

Figure 17 compares k_{inf} (HFP with no soluble boron) for the 5 wt % base case and the C26M normal pellet model with 5.6 wt % enrichment. The difference between the two curves is small across the entire burnup range, indicating the PWR FeCrAl enrichment penalty is about 0.6 wt % for the 5 wt % base case assembly, assuming no change in fuel pellet size. Further confirmation of this result is provided by a comparison of the cycle estimator EOC k_{inf} using the base case and the FeCrAl normal pellet k_{inf} data. For a typical 18-month PWR cycle (40.2 MW/MTU, 25-day outage, 99% load factor, and 36% batch fraction) the FeCrAl EOC k_{inf} was slightly lower (0.001) than the base case EOC k_{inf}. This result confirmed that a reasonable PWR FeCrAl penalty is 0.6 wt % with no change in the amount of UO_2 in the assembly. Note that the normal pellet design had a smaller clad diameter and a higher clad heat flux, which may not be within acceptable limits and will be investigated in future work.

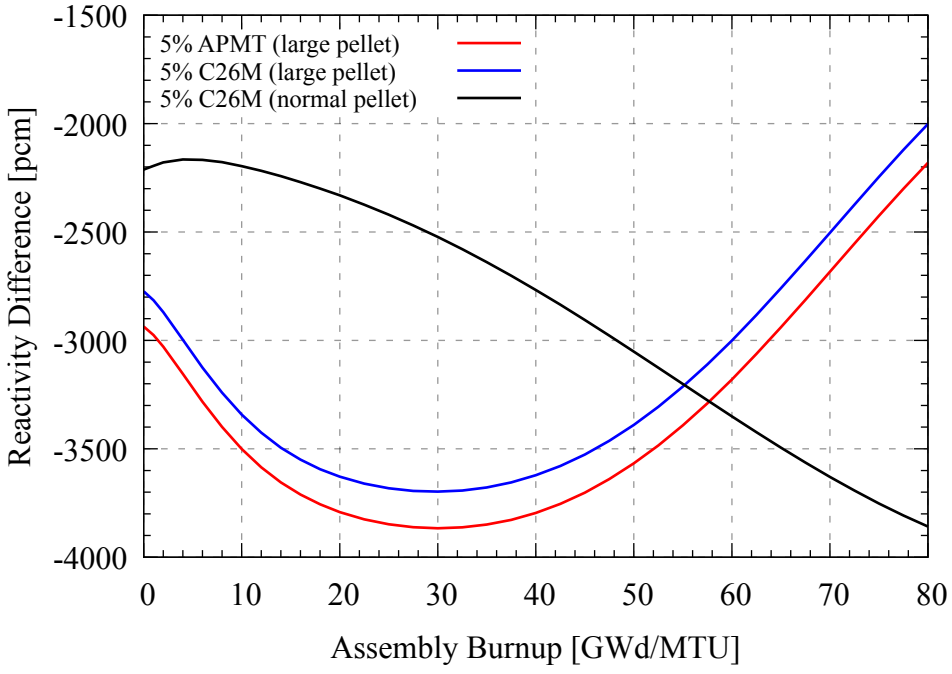

Figure 16. Reactivity penalty for PWR FeCrAl with larger pellet size.

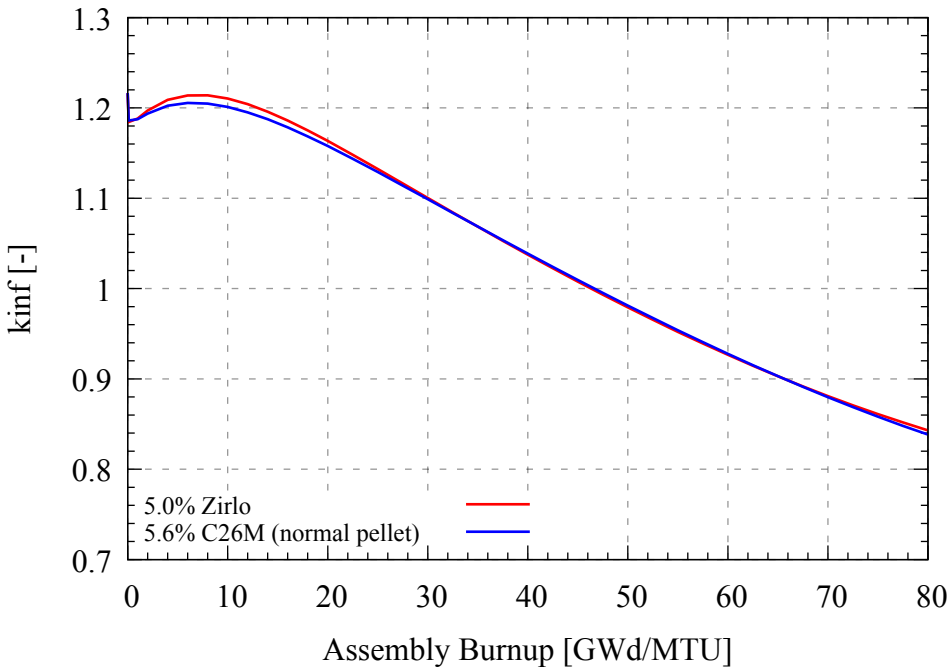

Figure 17. Multiplication factor for PWR FeCrAl (5 wt % baseline) with enrichment offset and normal pellet size.

Determining the FeCrAl enrichment offset when the base case assembly and FeCrAl assembly have different amounts of UO_2 (large pellet) is not as simple as comparing k_{inf} at multiple points along the burnup curve. With fixed maximum reactor power and heat flux, the specific power of the large pellet assembly is reduced, which leads to reduced assembly burnup for the same cycle length. A more consistent comparison for these two assemblies is the k_{inf} at the same energy produced (MWd). For the conversion from burnup to energy, burnup is simply multiplied by the heavy metal loading (MTU) of the assembly.

Figure 18 compares the k_{inf} of the base case 5 wt % depletion with that of a 5.4 wt % FeCrAl large pellet assembly depletion as a function of assembly energy produced. The FeCrAl reactivity is less than that of the base case early in the depletion and greater later in the depletion. To determine whether the large pellet FeCrAl assembly could be a reasonable replacement for the base case assembly, FeCrAl k_{inf} data were substituted for base assembly data in the cycle estimator. For an 18-month cycle (40.2 MW/MTU, 25-day outage, 99% load factor, and 36% batch fraction), the FeCrAl estimated EOC k_{inf} is only slightly lower (0.0015) than that of the base case. Therefore, with the larger pellet, a reasonable estimate of the PWR FeCrAl enrichment penalty is 0.4 wt %. Note that in addition to the cost of the 0.4 wt % increased enrichment, the large pellet FeCrAl penalty also includes the cost of more than 9% more enriched UO_2.

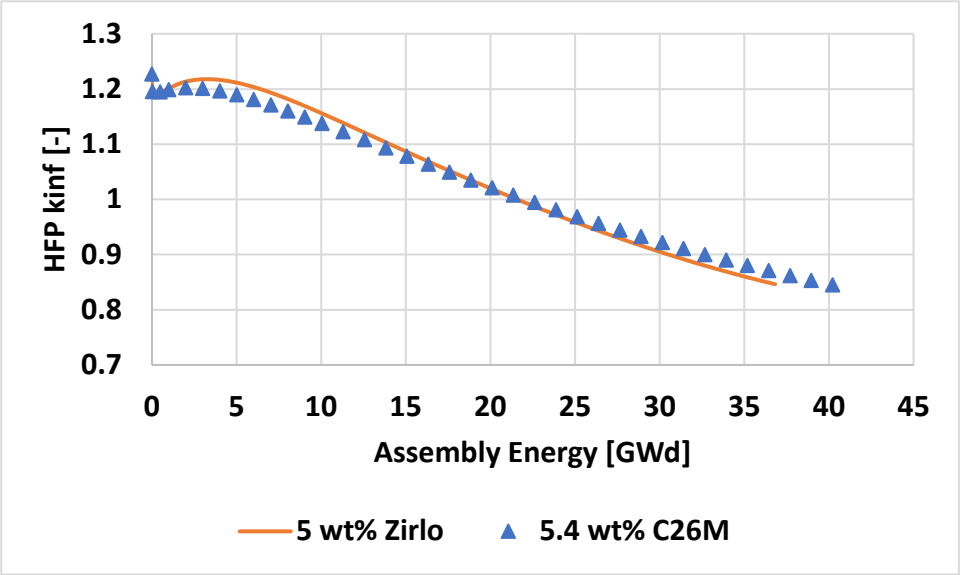

Figure 18. Multiplication factor for PWR FeCrAl (5 wt % baseline) with enrichment offset and larger pellet size.

Similar enrichment offset results were found for the 8 wt % base case enrichment. Figure 19 shows that 0.8 wt % enrichment increase offsets the FeCrAl penalty for the normal pellet option. The 8 wt % large pellet offset is about 0.6 wt % for the equivalent energy production, as shown in Figure 20.

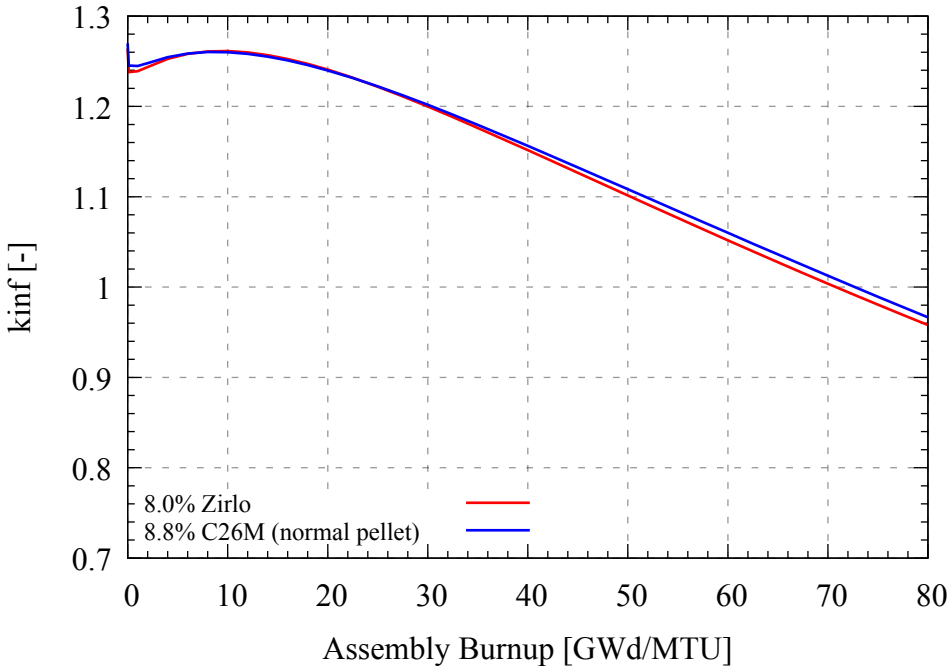

Figure 19. Multiplication factor for PWR FeCrAl (8 wt % baseline) with enrichment offset and normal pellet size.

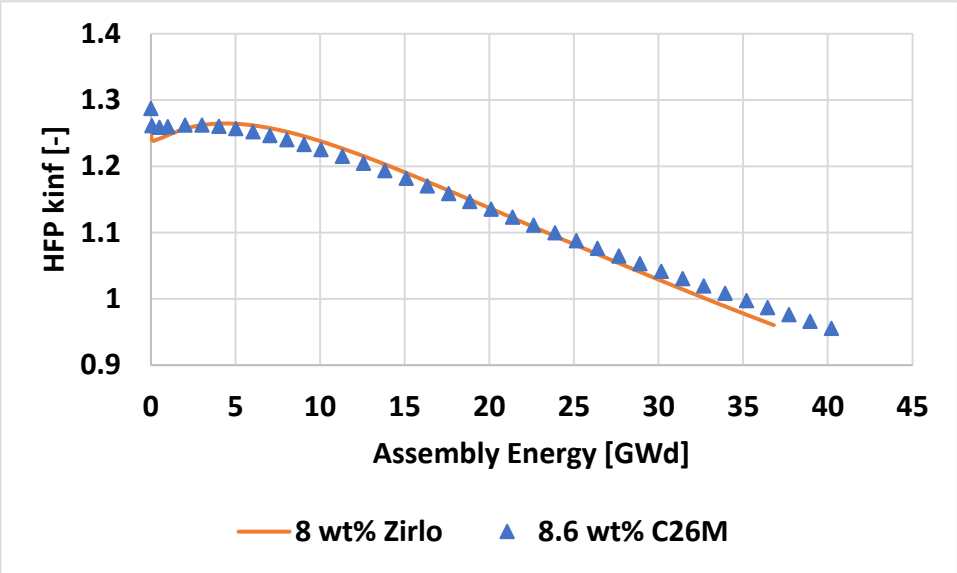

Figure 20. Multiplication factor for PWR FeCrAl (8 wt % baseline) with enrichment offset and larger pellet size.

7.4 PWR FECRAL LATTICE PARAMETERS

Polaris HFP DTC, MTC, CRW, and boron worth were calculated for the 5 wt % and 8 wt % PWR base cases and C26M FeCrAl equivalent reactivity cases (normal pellet and large pellet options). All values were HFP, and the MTC was calculated with no soluble boron with coefficients shown as differences or percentage differences from the ZIRLO base cases.

For the normal pellet FeCrAl models, DTC was slightly higher by about 0.1 pcm/K for the 5 wt % case and negligibly different from the baseline for the 8 wt % case, as shown in Figure 21 and Figure 22. MTC was slightly higher by about 5 pcm/K for both 5 wt % and 8 wt %, as shown in Figure 23 and Figure 24. The CRW was reduced by ~9% and the boron worth by ~5% for both 5 wt % and 8 wt %, as shown in Figure 25 and Figure 26.

For the large pellet FeCrAl models shown in the same figures, the DTC is unaffected, MTC is slightly more negative, CRW is reduced by 9 to 17%, and boron worth is reduced by 15 to 25%. The CRW and boron worth differences are large and may make it difficult to develop practical and efficient core designs that meet related safety analysis limits. Low boron worth could require the use of more integral poisons or combinations of different burnable absorbers in the same assembly. Reduced CRW may make meeting shutdown margin requirements difficult. The delayed neutron fraction differences shown in Table 19 are small (~0% to 3%) across all FeCrAl variants.

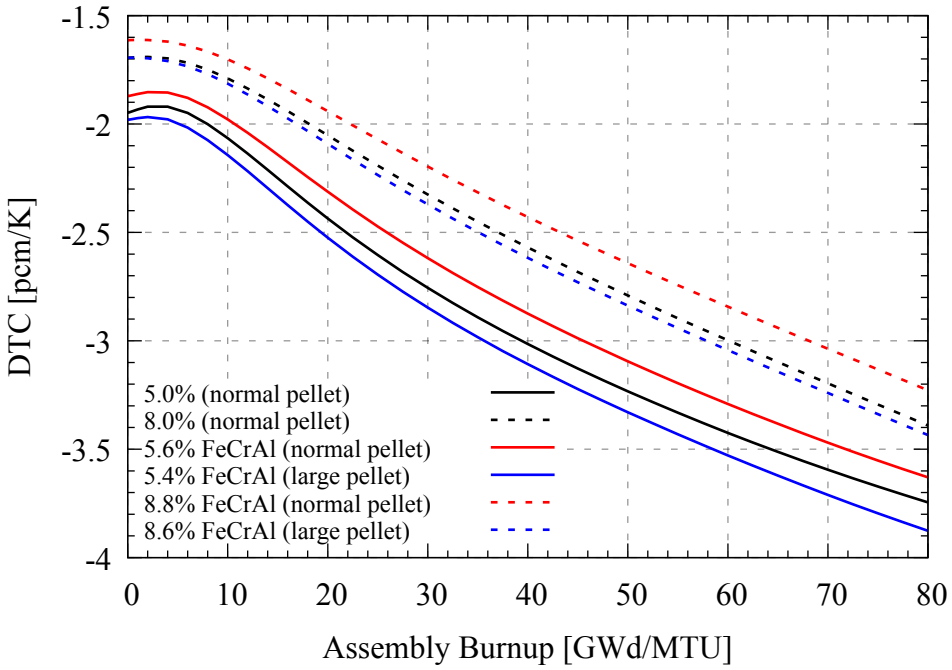

Figure 21. DTC for PWR FeCrAl.

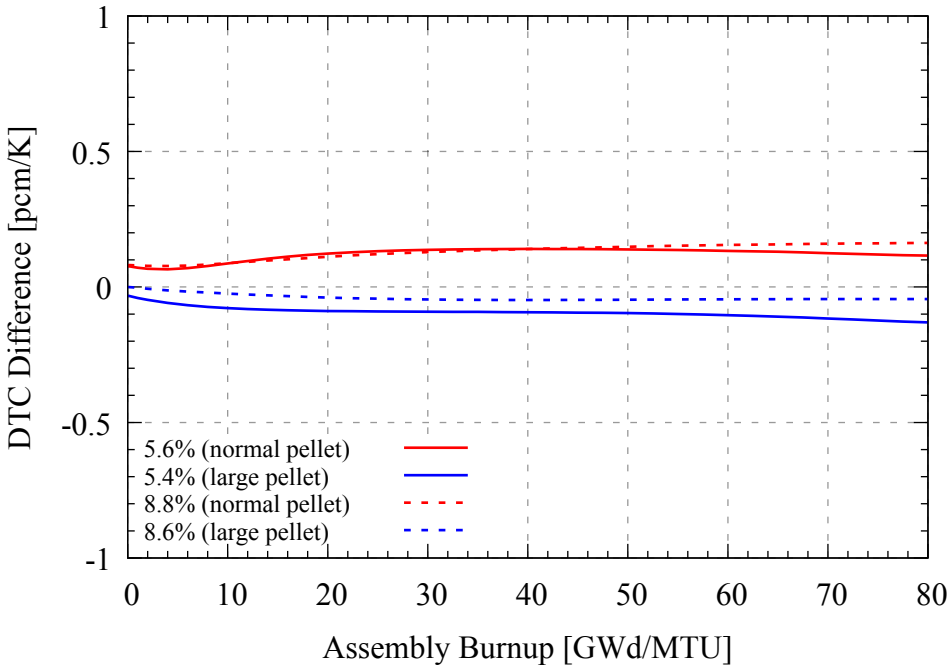

Figure 22. DTC difference for PWR FeCrAl.

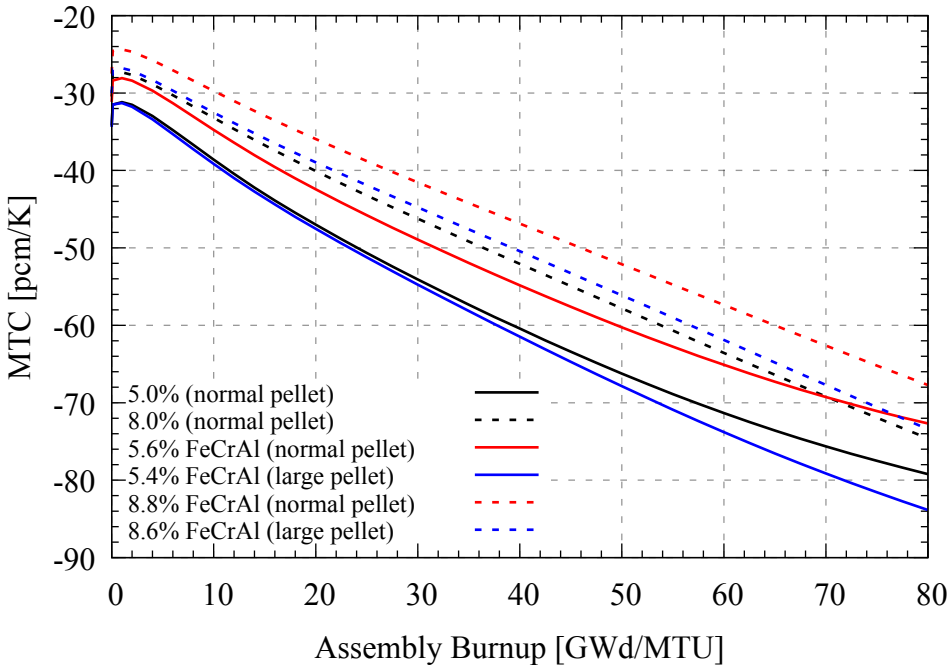

Figure 23. MTC for PWR FeCrAl.

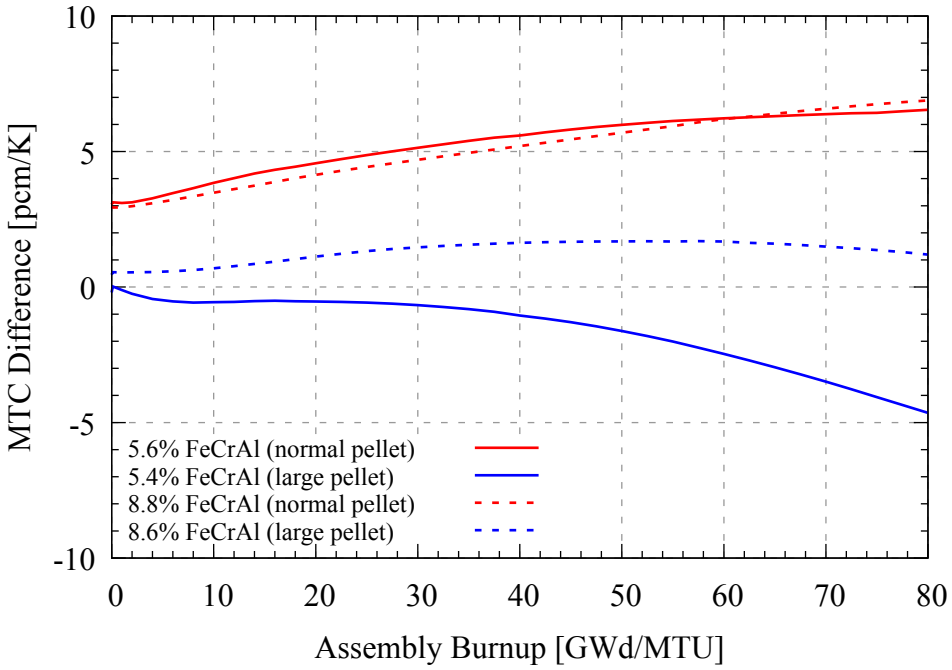

Figure 24. MTC difference for PWR FeCrAl.

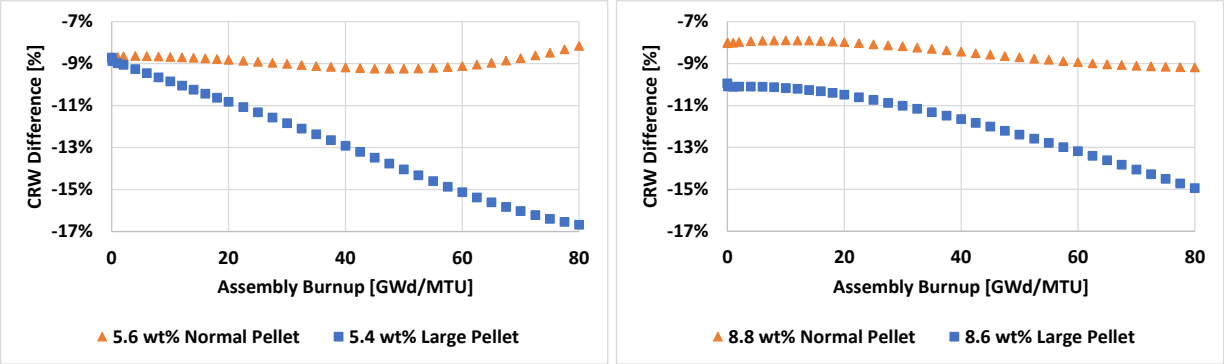

Figure 25. CRW difference for PWR FeCrAl.

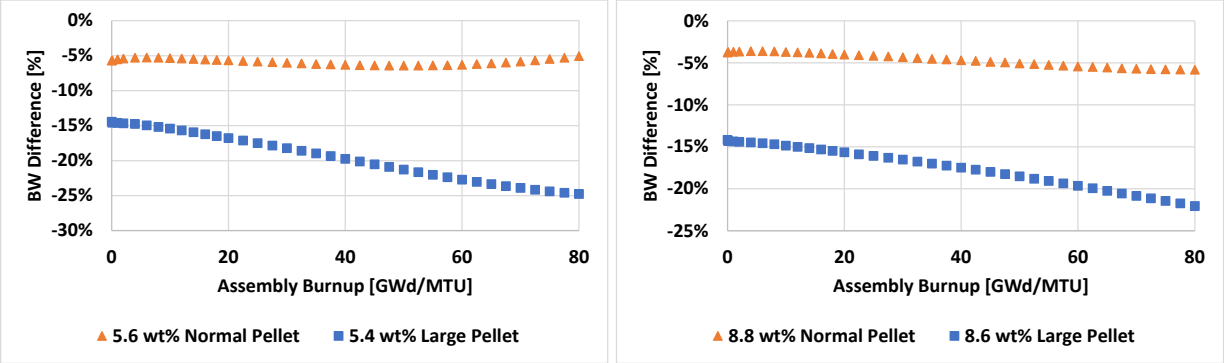

Figure 26. Boron worth difference for PWR FeCrAl.

Table 19. β-eff for PWR FeCrAl.

Enrichment (wt %)	5.0	5.4	5.6	8.0	8.6	8.8
Pellet size	Normal	Large	Normal	Normal	Large	Normal
Burnup (GWd/MTU)	β_{eff}					
0	0.00686	0.00688	0.00685	0.00682	0.00684	0.00681
20	0.00553	0.00558	0.00564	0.00594	0.00599	0.00601
40	0.00490	0.00495	0.00502	0.00541	0.00546	0.00551
60	0.00444	0.00449	0.00456	0.00499	0.00503	0.00510
80	0.00411	0.00416	0.00420	0.00462	0.00466	0.00474

7.5 PWR ATF ISOTOPIC EFFECTS

To assess the impact of ATF on used PWR fuel isotopic content, ORIGEN was used to produce isotopic inventories at decay times of 30 minutes, 5 days, 25 days, 100 days, 500 days, 5000 days, and 15000 days. That method is consistent with previous evaluations [Cumberland et al. 2021; Hall et al. 2021] but with a few additional time points primarily to represent the dry storage time frame. The focus of this evaluation is the differences between ATF and non-ATF isotopic content related to decay heat, criticality, shielding, and severe accidents. Table 20 shows the fuel design combinations evaluated. Owing to the volume of data, only major contributors in each category are shown.

Table 20. Decay heat and isotopic evaluation cases for PWR ATF.

Enrichment (wt % ^{235}U)	Clad	Pellet size	Dopant	Comment
5.00	ZIRLO	Normal	None	Base case
5.10	Cr-coated ZIRLO	Normal	Cr_2O_3 (800 ppm) + Al_2O_3 (200 ppm)	Doped and coated
5.40	C26M	Large	None	FeCrAl large pellet
5.60	C26M	Normal	None	FeCrAl normal pellet
8.00	ZIRLO	Normal	None	Base case
8.15	Cr-coated ZIRLO	Normal	Cr_2O_3 (800 ppm) + Al_2O_3 (200 ppm)	Doped and coated
8.60	C26M	Large	None	FeCrAl large pellet
8.80	C26M	Normal	None	FeCrAl normal pellet

7.5.1 PWR ATF Decay Heat

Table 21 shows the total decay heat for each fuel design over a range of decay times. For the 5–6 wt % cases, values are provided for 50 GWd/MTU assembly burnup, which is similar to the current LWR batch average discharge burnup. The 8–9 wt % cases are for 80 GWd/MTU assembly burnup, chosen based on a 10 GWd/MTU/wt % relationship selected from within the expected range of values developed in Section 3.1. All depletions were performed at 40 MW/MTU specific power.

ATF materials and fuel design variations had no significant effect on total decay heat. Short decay time decay heat was primarily a function of recent depletion power (short-lived isotopes present at shutdown). Long decay time decay heat was primarily a function of burnup (longer half-life isotopes accumulated continuously over the entire depletion).

Table 21. Total decay heat for selected fuel PWR designs.

Enrichment (wt % ^{235}U)	5.00	5.10	5.40	5.60	8.00	8.15	8.60	8.80
Clad	ZIRLO	Cr-coated ZIRLO	FeCrAl C26M	FeCrAl C26M	ZIRLO	Cr coated ZIRLO	FeCrAl C26M	FeCrAl C26M
Pellet size	Normal	Normal	Large	Normal	Normal	Normal	Large	Normal
Dopant	None	Doped*	None	None	None	Doped*	None	None
Decay time (days)	**50 GWd/MTU decay heat (W/MTU)**				**80 GWd/MTU decay heat (W/MTU)**			
0.02	665,120	662,860	666,750	663,580	673,180	670,920	674,590	671,120
5	131,850	131,290	131,950	130,810	140,830	140,200	140,830	139,410
25	66,239	66,002	66,239	65,933	73,931	73,645	73,922	73,339
100	33,526	33,371	33,505	33,168	39,618	39,418	39,568	39,041
500	10,549	10,472	10,564	10,318	14,178	14,067	14,152	13,810
5000	1,643	1,637	1,667	1,622	2,874	2,858	2,898	2,811
15000	1,008	1,006	1,036	998	1,733	1,728	1,772	1,704

*Doped indicates Cr_2O_3 (800 ppm) + Al_2O_3 (200 ppm)

Table 22 shows that dopants and the Cr coating have no significant effect on activated clad decay heat. FeCrAl clad exhibits much lower decay heat than the base case, but it is negligible compared with the total decay heat.

Table 22. Clad decay heat for selected PWR fuel designs.

Enrichment (wt % ^{235}U)	5.00	5.10	5.40	5.60	8.00	8.15	8.60	8.80
Clad	ZIRLO	Cr-coated ZIRLO	FeCrAl C26M	FeCrAl C26M	ZIRLO	Cr coated ZIRLO	FeCrAl C26M	FeCrAl C26M
Pellet size	Normal	Normal	Large	Normal	Normal	Normal	Large	Normal
Dopant	None	Doped*	None	None	None	Doped*	None	None
Decay time (days)	**50 GWd/MTU decay heat (W/MTU)**				**80 GWd/MTU decay heat (W/MTU)**			
0.02	1,584	1,587	336	334	1,569	1,569	341	340
5	412	420	158	158	408	414	158	158
25	325	328	128	127	318	322	130	130
100	168	168	91	89	163	163	96	94
500	4	4	35	34	4	4	38	37
5000	<0.5	<0.5	<0.5	<0.5	<0.5	<0.5	<0.5	<0.5
15000	<0.5	<0.5	<0.5	<0.5	<0.5	<0.5	<0.5	<0.5

*Doped indicates Cr_2O_3 (800 ppm) + Al_2O_3 (200 ppm)

7.5.2 PWR ATF Source Term

Used fuel isotopic inventory differences associated with ATF concepts were evaluated on an equivalent enrichment basis, which treated the ATF fuel assembly as a reactivity equivalent replacement for the non-ATF assembly. Differences can be explained as a result of three primary drivers—increased ^{235}U, flux level and neutron energy spectrum change associated with increased enrichment, and neutron energy spectrum changes due to changes in fuel pin geometry.

Increased ^{235}U resulted in more accumulated fissions from ^{235}U at the same burnup versus other fissile materials (e.g., ^{239}Pu and ^{241}Pu). The increase could change the fission product inventory of isotopes that have significantly different fission yields in uranium versus plutonium. Increased enrichment causes absorption hardening of the energy spectrum. Harder spectra can reduce the absorption destruction of thermal absorbing fission products and actinides. Lower total neutron flux with increased enrichment (assuming no change in fission power) results in reduced capture and activation. Because an FeCrAl clad occupies less volume than Zircaloy-based cladding, it can reduce (large pellet) or increase (smaller clad) the H/U ratio, with resulting effects on the energy spectrum. Table 23 shows the thermal flux (percentage of total flux) at 50 GWd/MTU for each of the 5 wt % equivalent and 8 wt % equivalent PWR designs evaluated. The values confirm the ATF effects on energy spectrum described.

Table 23. 50 GWd/MTU thermal flux fraction for PWR ATF fuel designs.

Enrichment (wt % ^{235}U)	5.00	5.10	5.40	5.60	8.00	8.15	8.60	8.80
Clad	ZIRLO	Cr-coated ZIRLO	FeCrAl C26M	FeCrAl C26M	ZIRLO	Cr coated ZIRLO	FeCrAl C26M	FeCrAl C26M
Pellet size	Normal	Normal	Large	Normal	Normal	Normal	Large	Normal
Dopant	None	Doped*	None	None	None	Doped*	None	None
Thermal flux fraction	10.1%	9.8%	8.1%	9.7%	7.1%	7.0%	5.9%	7.0%

*Doped indicates Cr_2O_3 (800 ppm) + Al_2O_3 (200 ppm)

Activity data (Ci/MTU) were produced using Polaris to calculate the discharge inventory; then ORIGEN was used to generate the decayed inventory at 30 minutes, 5 days, 25 days, 100 days, 500 days, 5,000 days, and 15,000 days to evaluate ATF isotopic effects over multiple time frames. The 5 wt % equivalent assembly activity data are shown in Table 24 (short times) and Table 25 (long times). Similarly, the 8 wt % equivalent assembly data are from 80 GWd/MTU depletions and are shown in Table 26. Each table lists the top 10 highest-activity isotopes for each decay time.

Isotopic changes associated with Cr-coated clad and doped pellets are very small across all decay time frames. As expected, FeCrAl designs have a larger effect, particularly in the transuranic isotopes most visible at long decay times. Differences in total activity are small for all ATF designs and across all time frames evaluated.

Table 24. Top 10 PWR ATF activity isotopes (5 wt % equivalent, short decay times).

Enrichment (wt % ^{235}U)	5.00	5.10	5.40	5.60
Clad	ZIRLO	Cr-coated ZIRLO	FeCrAl C26M	FeCrAl C26M
Pellet size	Normal	Normal	Large	Normal
Dopant	None	Doped	None	None
Isotope	**Activity at 5 days decay (Ci/MTU)**			
Np-239	5.13E+06	5.10E+06	5.14E+06	4.84E+06
Nb-95	1.78E+06	1.79E+06	1.76E+06	1.78E+06
Zr-95	1.68E+06	1.69E+06	1.66E+06	1.68E+06
Ru-103	1.64E+06	1.63E+06	1.62E+06	1.59E+06
Rh-103m	1.62E+06	1.61E+06	1.60E+06	1.57E+06
La-140	1.60E+06	1.60E+06	1.61E+06	1.62E+06
Ce-141	1.57E+06	1.58E+06	1.58E+06	1.59E+06
Pr-144	1.43E+06	1.44E+06	1.44E+06	1.46E+06
Ce-144	1.43E+06	1.44E+06	1.44E+06	1.46E+06
Ba-140	1.41E+06	1.42E+06	1.42E+06	1.43E+06
å	3.26E+07	3.26E+07	3.27E+07	3.24E+07
Isotope	**Activity at 25 days decay (Ci/MTU)**			
Nb-95	1.69E+06	1.70E+06	1.67E+06	1.69E+06
Pr-144	1.37E+06	1.37E+06	1.37E+06	1.39E+06
Ce-144	1.37E+06	1.37E+06	1.37E+06	1.39E+06
Zr-95	1.35E+06	1.36E+06	1.34E+06	1.36E+06
Ru-103	1.15E+06	1.15E+06	1.14E+06	1.12E+06
Rh-103m	1.14E+06	1.13E+06	1.13E+06	1.10E+06
Ce-141	1.03E+06	1.03E+06	1.03E+06	1.04E+06
Y-91	9.14E+05	9.20E+05	9.32E+05	9.58E+05
Sr-89	6.57E+05	6.62E+05	6.72E+05	6.94E+05
Rh-106	6.81E+05	6.74E+05	6.62E+05	6.33E+05
Total	1.57E+07	1.57E+07	1.58E+07	1.58E+07
Isotope	**Activity at 100 days decay (Ci/MTU)**			
Pr-144	1.14E+06	1.14E+06	1.14E+06	1.16E+06
Ce-144	1.14E+06	1.14E+06	1.14E+06	1.16E+06
Nb-95	1.03E+06	1.04E+06	1.02E+06	1.03E+06
Rh-106	5.92E+05	5.86E+05	5.76E+05	5.51E+05
Ru-106	5.92E+05	5.86E+05	5.76E+05	5.51E+05
Zr-95	6.01E+05	6.03E+05	5.95E+05	6.02E+05
Y-91	3.76E+05	3.78E+05	3.83E+05	3.94E+05
Ru-103	3.06E+05	3.05E+05	3.02E+05	2.97E+05
Rh-103m	3.03E+05	3.01E+05	2.99E+05	2.93E+05
Cs-134	2.45E+05	2.44E+05	2.47E+05	2.33E+05
Total	7.91E+06	7.91E+06	7.98E+06	7.96E+06

Table 25. Top 10 PWR ATF activity isotopes (5 wt % equivalent, long decay times).

Enrichment (wt % ^{235}U)	5.00	5.10	5.40	5.60
Clad	ZIRLO	Cr-coated ZIRLO	FeCrAl C26M	FeCrAl C26M
Pellet size	Normal	Normal	Large	Normal
Dopant	None	Doped	None	None
Isotope	**Activity at 500 days decay (Ci/MTU)**			
Pr-144	4.30E+05	4.31E+05	4.32E+05	4.38E+05
Ce-144	4.30E+05	4.31E+05	4.32E+05	4.38E+05
Rh-106	2.81E+05	2.78E+05	2.73E+05	2.61E+05
Ru-106	2.81E+05	2.78E+05	2.73E+05	2.61E+05
Pu-241	1.89E+05	1.90E+05	2.04E+05	1.87E+05
Cs-134	1.69E+05	1.69E+05	1.71E+05	1.62E+05
Pm-147	1.56E+05	1.56E+05	1.57E+05	1.62E+05
Cs-137	1.54E+05	1.54E+05	1.53E+05	1.54E+05
Ba-137m	1.45E+05	1.45E+05	1.45E+05	1.46E+05
Y-90	1.09E+05	1.09E+05	1.10E+05	1.12E+05
Total	2.56E+06	2.56E+06	2.61E+06	2.58E+06
Isotope	**Activity at 5000 days decay (Ci/MTU)**			
Cs-137	1.12E+05	1.12E+05	1.12E+05	1.12E+05
Ba-137m	1.06E+05	1.06E+05	1.06E+05	1.06E+05
Pu-241	8.18E+04	8.23E+04	9.19E+04	8.34E+04
Y-90	7.57E+04	7.56E+04	7.43E+04	7.54E+04
Sr-90	7.57E+04	7.56E+04	7.43E+04	7.54E+04
Pm-147	5.04E+03	5.03E+03	4.95E+03	5.02E+03
Pu-238	5.71E+03	5.74E+03	6.30E+03	5.73E+03
Kr-85	5.36E+03	5.36E+03	5.28E+03	5.35E+03
Eu-154	3.37E+03	3.39E+03	3.75E+03	3.39E+03
Cm-244	4.45E+03	4.48E+03	4.96E+03	4.42E+03
Total	4.84E+05	4.85E+05	4.95E+05	4.87E+05
Isotope	**Activity at 15,000 days decay (Ci/MTU)**			
Cs-137	6.15E+04	6.15E+04	6.15E+04	6.15E+04
Ba-137m	5.82E+04	5.82E+04	5.82E+04	5.83E+04
Y-90	4.19E+04	4.20E+04	4.22E+04	4.32E+04
Sr-90	4.18E+04	4.20E+04	4.22E+04	4.32E+04
Pu-241	2.75E+04	2.77E+04	2.98E+04	2.72E+04
Am-241	5.71E+03	5.75E+03	6.18E+03	5.65E+03
Pu-238	4.81E+03	4.82E+03	5.10E+03	4.59E+03
Cm-244	1.23E+03	1.19E+03	1.15E+03	9.59E+02
Kr-85	1.02E+03	1.02E+03	1.03E+03	1.05E+03
Pu-240	6.24E+02	6.22E+02	6.26E+02	5.95E+02
Total	2.46E+05	2.47E+05	2.50E+05	2.48E+05

Table 26. Top 10 PWR ATF activity isotopes (8 wt % equivalent, selected decay times).

Enrichment (wt % ^{235}U)	8.00	8.15	8.60	8.80
Clad	ZIRLO	Cr-coated ZIRLO	FeCrAl C26M	FeCrAl C26M
Pellet size	Normal	Normal	Large	Normal
Dopant	None	Doped	None	None
Isotope	**Activity at 5 days decay (Ci/MTU)**			
Np-239	4.74E+06	4.71E+06	4.72E+06	4.46E+06
Nb-95	1.77E+06	1.78E+06	1.75E+06	1.77E+06
Zr-95	1.67E+06	1.68E+06	1.66E+06	1.68E+06
Ru-103	1.64E+06	1.63E+06	1.62E+06	1.59E+06
Rh-103m	1.62E+06	1.61E+06	1.60E+06	1.57E+06
La-140	1.60E+06	1.60E+06	1.61E+06	1.62E+06
Ce-141	1.57E+06	1.57E+06	1.58E+06	1.59E+06
Pr-144	1.48E+06	1.48E+06	1.49E+06	1.51E+06
Ce-144	1.48E+06	1.48E+06	1.49E+06	1.51E+06
Ba-140	1.41E+06	1.41E+06	1.42E+06	1.43E+06
Total	3.37E+07	3.37E+07	3.38E+07	3.35E+07
Isotope	**Activity at 500 days decay (Ci/MTU)**			
Pr-144	4.44E+05	4.45E+05	4.47E+05	4.52E+05
Ce-144	4.44E+05	4.45E+05	4.47E+05	4.52E+05
Rh-106	3.16E+05	3.12E+05	3.05E+05	2.94E+05
Ru-106	3.16E+05	3.12E+05	3.05E+05	2.94E+05
Pu-241	2.58E+05	2.61E+05	2.80E+05	2.56E+05
Cs-134	2.95E+05	2.94E+05	2.95E+05	2.82E+05
Pm-147	1.79E+05	1.81E+05	1.82E+05	1.88E+05
Cs-137	2.40E+05	2.40E+05	2.40E+05	2.40E+05
Ba-137m	2.27E+05	2.27E+05	2.27E+05	2.27E+05
Y-90	1.73E+05	1.74E+05	1.75E+05	1.78E+05
Total	3.22E+06	3.22E+06	3.28E+06	3.24E+06
Isotope	**Activity at 15,000 days decay (Ci/MTU)**			
Cs-137	9.61E+04	9.61E+04	9.60E+04	9.62E+04
Ba-137m	9.10E+04	9.10E+04	9.09E+04	9.11E+04
Y-90	6.65E+04	6.68E+04	6.72E+04	6.85E+04
Sr-90	6.65E+04	6.68E+04	6.72E+04	6.85E+04
Pu-241	3.76E+04	3.80E+04	4.09E+04	3.73E+04
Am-241	7.91E+03	7.99E+03	8.62E+03	7.87E+03
Pu-238	1.20E+04	1.20E+04	1.26E+04	1.15E+04
Cm-244	3.16E+03	3.06E+03	2.84E+03	2.54E+03
Kr-85	1.55E+03	1.56E+03	1.57E+03	1.59E+03
Pu-240	7.79E+02	7.78E+02	7.91E+02	7.47E+02
Total	3.86E+05	3.87E+05	3.91E+05	3.88E+05

Previous evaluation of increased LWR enrichment and burnup [Hall et al. 2021] identified 6 isotopes of interest at short decay times relevant to severe accidents and 14 of interest to radiation shielding in the several years of decay time frame. Severe accident isotope activity is shown in Table 27 for the 5 wt % equivalent assembly designs and in Table 28 for 8 wt % equivalent assembly designs. FeCrAl increases ^{90}Sr and ^{85}Kr activity slightly. Shielding isotope activities for the 5 wt % and 8 wt % equivalent assembly designs are shown in Table 29 and Table 30, with no significant changes across ATF designs.

Table 27. PWR ATF accident release isotope activity (5 wt % equivalent at 50 GWd/MTU).

Enrichment (wt % ^{235}U)	5.00	5.00	5.00	5.00
Clad	Zirc-2	Cr-coated Zirc-2	FeCrAl C26M	FeCrAl C26M
Pellet size	Normal	Normal	Large	Normal
Dopant	None	Doped	None	None
Isotope	**Activity at 30 minutes decay (Ci/MTU)**			
I-133	2.19E+06	2.19E+06	2.19E+06	2.19E+06
I-135	2.01E+06	2.01E+06	2.01E+06	2.01E+06
I-131	1.10E+06	1.09E+06	1.09E+06	1.09E+06
Cs-137	1.58E+05	1.58E+05	1.58E+05	1.59E+05
Sr-90	1.13E+05	1.13E+05	1.14E+05	1.16E+05
Kr-85	1.44E+04	1.44E+04	1.45E+04	1.48E+04

Table 28. PWR ATF accident release isotope activity (8 wt % equivalent at 80 GWd/MTU).

Enrichment (wt % ^{235}U)	10.00	10.00	10.00	10.00
Clad	Zirc-2	Cr-coated Zirc-2	FeCrAl C26M	FeCrAl C26M
Pellet size	Normal	Normal	Large	Normal
Dopant	None	Doped	None	None
Isotope	**Activity at 30 minutes decay (Ci/MTU)**			
I-133	2.18E+06	2.18E+06	2.18E+06	2.18E+06
I-135	2.00E+06	2.00E+06	2.00E+06	2.01E+06
I-131	1.09E+06	1.09E+06	1.09E+06	1.08E+06
Cs-137	2.48E+05	2.48E+05	2.47E+05	2.48E+05
Sr-90	1.79E+05	1.80E+05	1.81E+05	1.84E+05
Kr-85	2.19E+04	2.20E+04	2.21E+04	2.25E+04

Table 29. PWR ATF shielding isotope activity (5 wt % equivalent at 50 GWd/MTU).

Enrichment (wt % ^{235}U)	5.00	5.00	5.00	5.00
Clad	Zirc-2	Cr-coated Zirc-2	FeCrAl C26M	FeCrAl C26M
Pellet size	Normal	Normal	Large	Normal
Dopant	None	Doped	None	None
Isotope	**Activity at 500 days decay (Ci/MTU)**			
Pu-241	1.89E+05	1.90E+05	2.04E+05	1.87E+05
Ba-137m	1.45E+05	1.45E+05	1.45E+05	1.46E+05
Y-90	1.09E+05	1.09E+05	1.10E+05	1.12E+05
Cs-134	1.69E+05	1.69E+05	1.71E+05	1.62E+05
Rh-106	2.81E+05	2.78E+05	2.73E+05	2.61E+05
Pr-144	4.30E+05	4.31E+05	4.32E+05	4.38E+05
Eu-154	1.07E+04	1.07E+04	1.15E+04	1.05E+04
Pu-238	6.53E+03	6.55E+03	6.92E+03	6.23E+03
Cm-244	5.61E+03	5.45E+03	5.23E+03	4.38E+03
Am-241	6.40E+02	6.47E+02	7.02E+02	6.41E+02
Pu-240	6.15E+02	6.13E+02	6.17E+02	5.89E+02
Pu-239	4.40E+02	4.49E+02	5.09E+02	4.57E+02
Pu-242	3.02E+00	2.95E+00	2.73E+00	2.65E+00
Cm-246	1.55E-01	1.47E-01	1.34E-01	1.02E-01
Isotope	**Activity at 5000 days decay (Ci/MTU)**			
Ba-137m	1.10E+05	1.10E+05	1.09E+05	1.10E+05
Pu-241	1.04E+05	1.05E+05	1.12E+05	1.03E+05
Y-90	8.09E+04	8.13E+04	8.17E+04	8.35E+04
Pu-238	5.97E+03	5.99E+03	6.32E+03	5.69E+03
Eu-154	3.95E+03	3.98E+03	4.28E+03	3.88E+03
Am-241	3.40E+03	3.43E+03	3.69E+03	3.37E+03
Cm-244	3.50E+03	3.40E+03	3.27E+03	2.73E+03
Cs-134	2.71E+03	2.70E+03	2.74E+03	2.59E+03
Pu-240	6.20E+02	6.18E+02	6.22E+02	5.92E+02
Pu-239	4.40E+02	4.49E+02	5.09E+02	4.56E+02
Rh-106	6.38E+01	6.31E+01	6.21E+01	5.93E+01
Pr-144	7.57E+00	7.58E+00	7.61E+00	7.70E+00
Pu-242	3.02E+00	2.95E+00	2.73E+00	2.65E+00
Cm-246	1.55E-01	1.47E-01	1.34E-01	1.02E-01

Table 30. PWR ATF shielding isotope activity (8 wt % equivalent at 80 GWd/MTU).

Enrichment (wt % ^{235}U)	10.00	10.00	10.00	10.00
Clad	Zirc-2	Cr-coated Zirc-2	FeCrAl C26M	FeCrAl C26M
Pellet size	Normal	Normal	Large	Normal
Dopant	None	Doped	None	None
Isotope	**Activity at 500 days decay (Ci/MTU)**			
Pu-241	2.76E+05	2.78E+05	3.00E+05	2.74E+05
Ba-137m	2.35E+05	2.35E+05	2.34E+05	2.35E+05
Y-90	1.86E+05	1.86E+05	1.86E+05	1.89E+05
Cs-134	4.67E+05	4.65E+05	4.68E+05	4.46E+05
Rh-106	8.02E+05	7.93E+05	7.76E+05	7.47E+05
Pr-144	1.50E+06	1.50E+06	1.51E+06	1.53E+06
Eu-154	2.13E+04	2.16E+04	2.32E+04	2.12E+04
Pu-238	1.58E+04	1.58E+04	1.65E+04	1.51E+04
Cm-244	1.52E+04	1.47E+04	1.37E+04	1.22E+04
Am-241	4.02E+02	4.11E+02	4.61E+02	4.18E+02
Pu-240	7.49E+02	7.49E+02	7.64E+02	7.23E+02
Pu-239	5.31E+02	5.43E+02	6.23E+02	5.48E+02
Pu-242	4.62E+00	4.51E+00	4.15E+00	4.13E+00
Cm-246	6.81E-01	6.43E-01	5.60E-01	4.65E-01
Isotope	**Activity at 5000 days decay (Ci/MTU)**			
Ba-137m	1.71E+05	1.71E+05	1.71E+05	1.71E+05
Pu-241	1.42E+05	1.43E+05	1.54E+05	1.41E+05
Y-90	1.29E+05	1.29E+05	1.30E+05	1.32E+05
Pu-238	1.49E+04	1.49E+04	1.56E+04	1.42E+04
Eu-154	7.08E+03	7.15E+03	7.71E+03	7.04E+03
Am-241	4.76E+03	4.81E+03	5.19E+03	4.74E+03
Cm-244	9.01E+03	8.73E+03	8.11E+03	7.24E+03
Cs-134	4.72E+03	4.70E+03	4.73E+03	4.51E+03
Pu-240	7.65E+02	7.64E+02	7.78E+02	7.36E+02
Pu-239	5.36E+02	5.48E+02	6.28E+02	5.53E+02
Rh-106	7.17E+01	7.09E+01	6.94E+01	6.69E+01
Pr-144	7.80E+00	7.82E+00	7.86E+00	7.95E+00
Pu-242	4.62E+00	4.51E+00	4.15E+00	4.13E+00
Cm-246	6.79E-01	6.41E-01	5.58E-01	4.64E-01

7.5.3 PWR ATF Transportation

Transportation of UO_2 enriched to > 5 wt % U235 has previously been investigated, but without specific consideration of ATF designs. [Hall et al. 2020] Two transportation packages reviewed are relevant to PWR ATF transportation—the Traveller (PWR pellets, rods, and fuel assemblies) and the CHT-OP-TU (PWR pellets).

The Traveller package has already been licensed for transport of fuel pellets containing dopants and fuel assemblies with doped pellets and/or Cr-coated clad. [NRC 2020a] With a few minor exceptions, ATF features reduced package k_{eff}.

Analysis of the CHT-OP-TU package showed that without a reduction in the transportation array size, UO_2 pellets enriched to as high as 16.5 wt % ^{235}U can be accommodated by using the 6-inch oxide vessel rather than larger-diameter vessels. Although the effect of dopants on UO_2 reactivity, which is predominantly negative, has not been directly evaluated for the CHT-OP-TU package, it is clear that it could be used to carry pellets of sufficient enrichment (<10 wt %) for LWR ATF fuel applications.

7.5.4 PWR ATF Used Fuel Storage Criticality

Enrichment penalty calculations have shown that Cr coating and FeCrAl reduce fuel assembly reactivity across the burnup range at in-reactor conditions. It is reasonable to assume that for the same enrichment and burnup, a penalty would also exist in conditions of wet storage. As a first-order approximation, a single region KENO rack cell case [Hall et al. 2021] was run with Cr clad coating added. Adding Cr coated clad to the 5 wt % 50 GWd/MTU rack cell reduced k_{eff} by 0.004 (400 pcm).

PWR used fuel storage typically includes burnup credit. An ATF assembly with the same enrichment and burnup as a non-ATF assembly could conservatively use a non-ATF assembly loading curve (minimum burnup versus initial enrichment). However, overcoming the ATF reactivity penalty would require a higher initial enrichment in the ATF assembly; thus, to avoid a fuel storage penalty (the additional burnup required for using a non-ATF loading curve), a separate ATF fuel burnup curve would be required. This is particularly true for FeCrAl, for which the penalty would large and perturbation to the assembly design (~10% more UO_2 or higher H/U due to the smaller clad OD) would be sufficiently significant to warrant the reanalysis of used fuel storage criticality.

7.6 BWR DOPANT AND COATING REACTIVITY PENALTY

BWR fuel assembly depletions were performed for the 5 wt % limit and 10 wt % limit lattices for both the dominant and vanished assembly regions using Cr-coated Zircaloy-2 and doped (1000 ppm Cr_2O_3) UO_2 fuel to assess the reactivity penalty, as shown in Figure 27.

The largest reactivity penalty for doped fuel and Cr-coated cladding is approximately 440 pcm for the 5 wt % limit dominant lattice, while the effect for the corresponding 10 wt % limit lattice is ~350 pcm. Both vanished regions show a similar trend to their dominant region counterparts, although the 5 wt % limit vanished lattice shows a slightly greater reactivity reduction above ~40 GWd/MTU.

Separate depletions were performed to show the individual impact of the Cr coating and Cr_2O_3 dopant against the reference case, shown in Figure 28 and Figure 29. Unlike in the PWR cases, the enrichment needed to offset the ATF concepts for the BWR lattices will be investigated in future work, owing to the necessary optimization of the enrichment zones for each lattice. Figure 28 shows a positive reactivity for some burnup ranges due to the 0.5% pellet density increase, which more than offsets the 0.1% of fuel displaced by dopants. The Cr-coated cladding has the dominant negative reactivity effect, as shown in Figure 29.

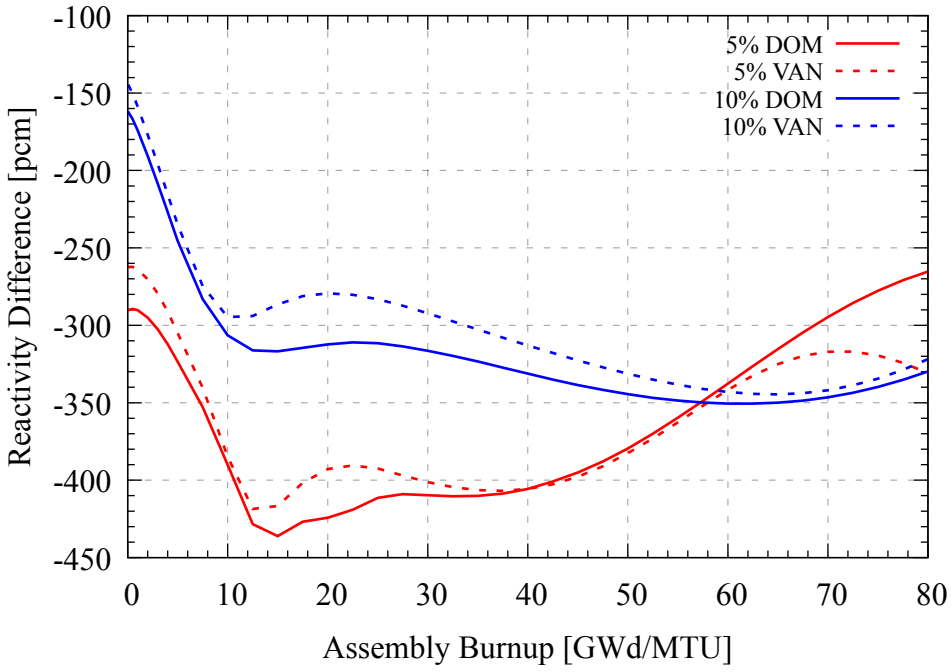

Figure 27. Reactivity penalty for doped and Cr-coated BWR ATF vs. burnup.

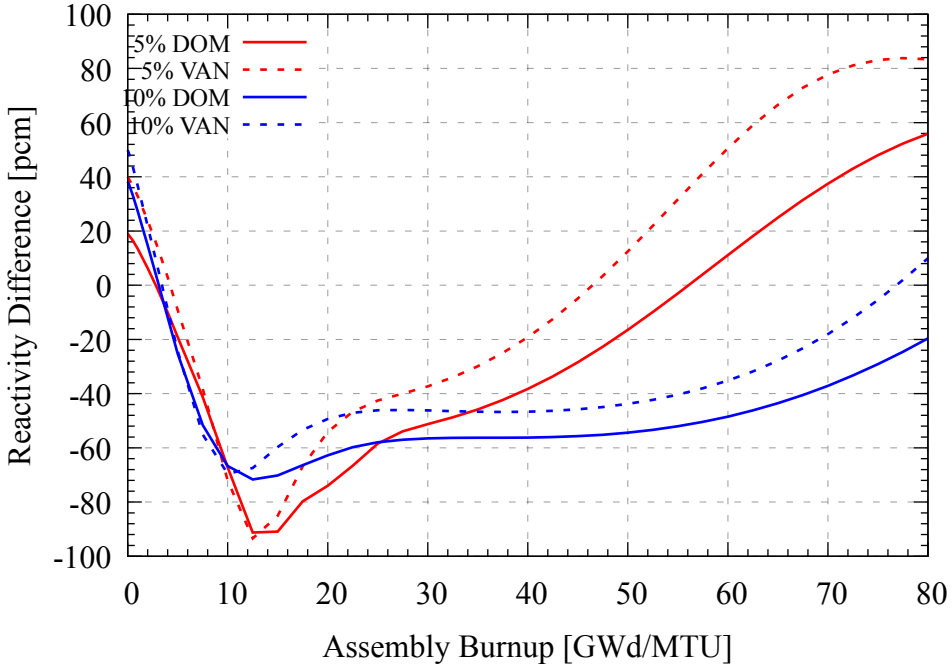

Figure 28. Reactivity difference for doped BWR ATF.

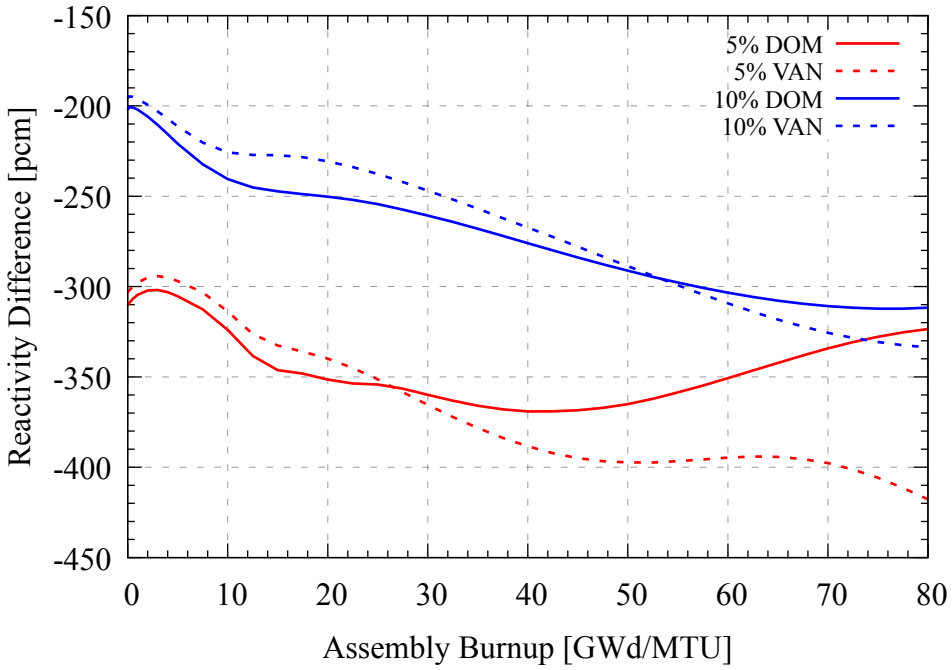

Figure 29. Reactivity difference for Cr-coated BWR ATF.

7.7 BWR DOPANT AND COATING LATTICE PARAMETERS

The DTC, moderator void coefficient (MVC), and control blade worth (CBW) were calculated for each of the BWR reference lattices and the doped fuel with Cr-coated cladding. Figure 30 shows the change in the DTC from the reference lattice and the Cr-doped fuel/Cr-coated cladding. It shows a negligible effect on the DTC due to the ATF concept. The difference in the MVC is shown in Figure 31. The difference in the MVC is noticeably higher for the vanished region and the 5 wt % limit lattices, although the maximum change is still very small (~3 pcm/void%).

The change to the CBW is shown in Figure 32, which shows an initial increase in the CBW for all Cr-doped/Cr-coated lattices followed by a monotonic decrease. The shapes of these curves track the doped fuel reactivity plots very well because of the increased density of the fuel. Table 31 and Table 32 provide the values for β_{eff} among the reference and Cr-coated/doped lattices at select burnup steps for the dominant and vanished regions respectively. Differences due to the incorporation of Cr-coated cladding and Cr-doped fuel are less than 0.25% for all lattices and enrichments.

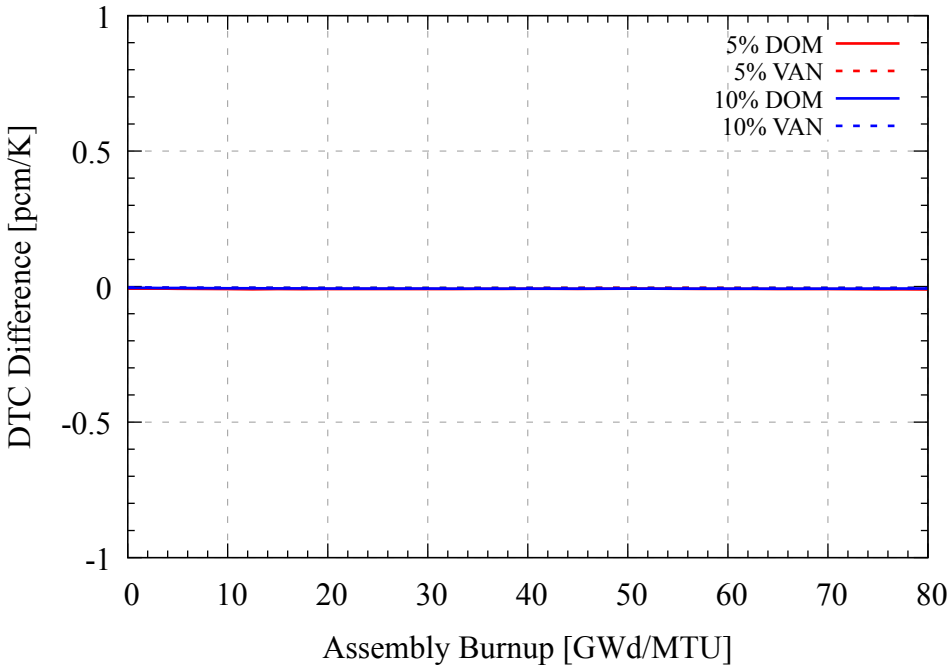

Figure 30. DTC difference for doped and Cr-coated BWR ATF.

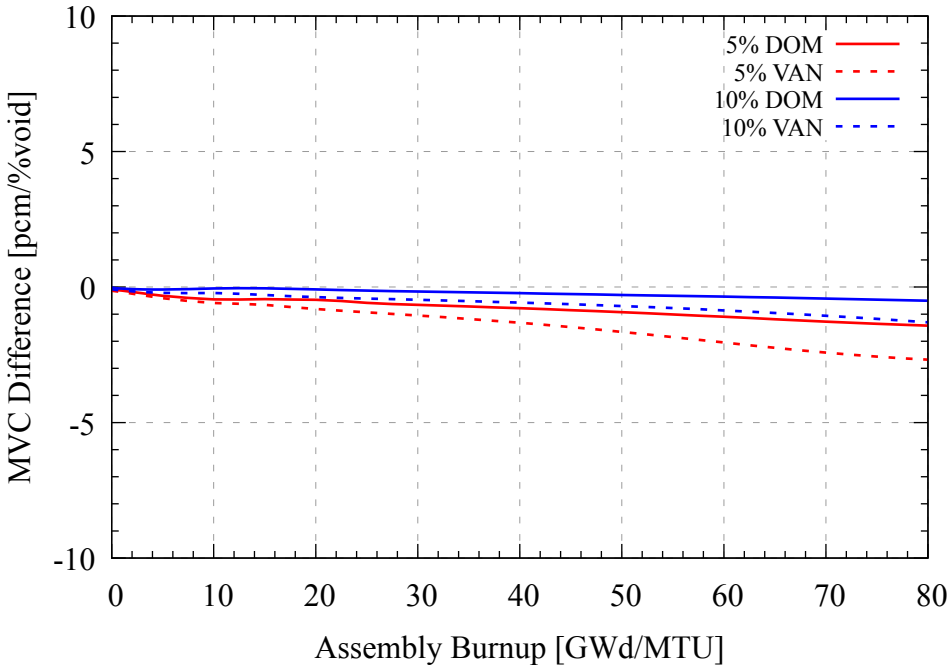

Figure 31. MVC difference for doped and Cr-coated BWR ATF.

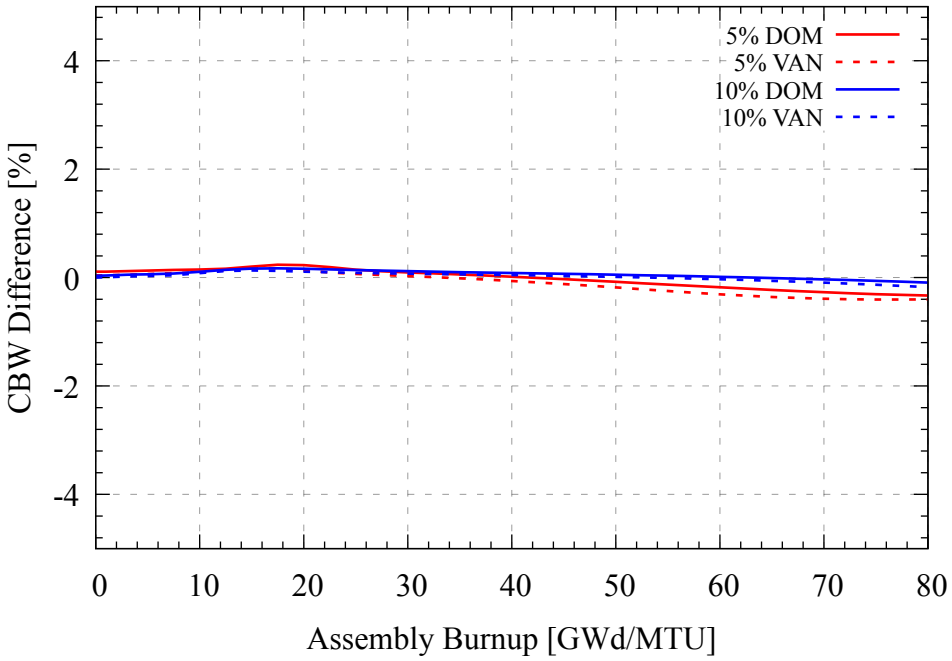

Figure 32. CBW difference for doped and Cr-coated BWR ATF.

Table 31. β-eff for doped and Cr-coated BWR ATF (dominant lattice).

Enrichment (wt %)	5.00	5.00	10.00	10.00
Clad	Zirc-2	Zirc-2+Cr	Zirc-2	Zirc-2+Cr
Doping	No	Yes	No	Yes
Burnup (GWd/MTU)	β_{eff}			
0	0.00685	0.00685	0.00681	0.00681
20	0.00544	0.00543	0.00589	0.00588
40	0.00481	0.00481	0.00539	0.00539
60	0.00435	0.00434	0.00499	0.00498
80	0.00403	0.00403	0.00462	0.00461

Table 32. β-eff for doped and Cr-coated BWR ATF (vanished lattice).

Enrichment (wt %)	5.00	5.00	10.00	10.00
Clad	Zirc-2	Zirc-2+Cr	Zirc-2	Zirc-2+Cr
Doping	No	Yes	No	Yes
Burnup (GWd/MTU)	β_{eff}			
0	0.00681	0.00681	0.00677	0.00677
20	0.00551	0.00551	0.00596	0.00596
40	0.00487	0.00487	0.00551	0.00550
60	0.00432	0.00432	0.00511	0.00510
80	0.00395	0.00395	0.00469	0.00469

7.8 BWR FeCrAl REACTIVITY PENALTY

As discussed in Section 2.1.2, GNF is currently developing several variants of FeCrAl cladding to use as replacements for Zircaloy-2 in BWRs. This work evaluates the impact of using FeCrAl cladding as a means to obtain insights regarding the potential effects on fuel assembly design and enrichment requirements. For this analysis, the FeCrAl cladding density was assumed to be 7.2 g/cm^3 and the nominal cladding thickness was 385µm. Two separate variants of FeCrAl cladding, C26M and APMT, were included in this work, as well as two different fuel rod geometries: one in which the outer cladding diameter was unchanged and the fuel pellet size increased (large pellet) and another in which the fuel pellet size was unchanged and the cladding outer diameter decreased (normal pellet).

The multiplication factor of the BWR with FeCrAl cladding is shown in Figure 33 for the 5 wt % limit and Figure 34 for the 10 wt % limit lattices. These figures show the changes due to the different geometries.

The reactivity impact of replacing Zircaloy-2 with FeCrAl is shown in Figure 35 for the 5 wt % limit and Figure 36 for the 10 wt % limit lattices. The reactivity effects of the two different types of FeCrAl (APMT and C26M) are due to the different cladding compositions (APMT has ~10% more Cr) and remain at nearly 100 pcm throughout the depletions. The C26M variant with the larger pellet was used preferentially in the lattice parameter assessment as the most likely variant of FeCrAl cladding to be deployed.

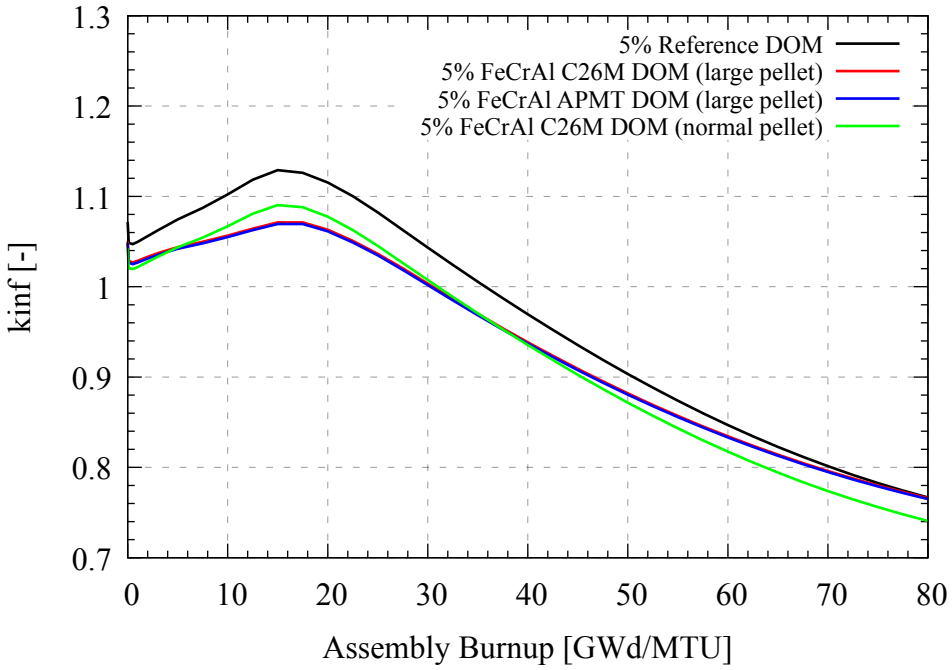

Figure 33. Multiplication factor for 5 wt % limit BWR FeCrAl (dominant lattice).

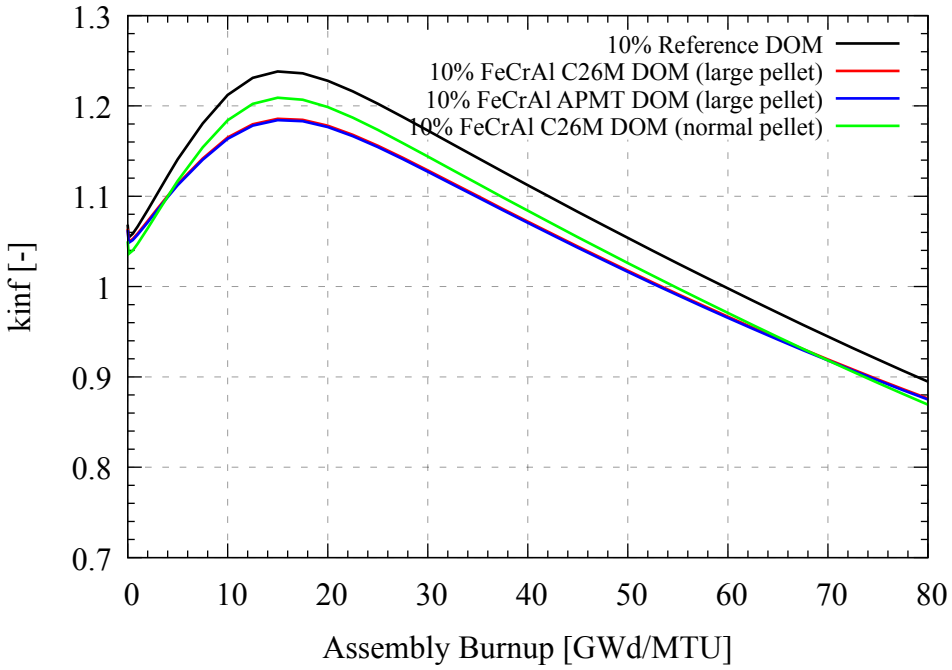

Figure 34. Multiplication factor for 10 wt % limit BWR FeCrAl (dominant lattice).

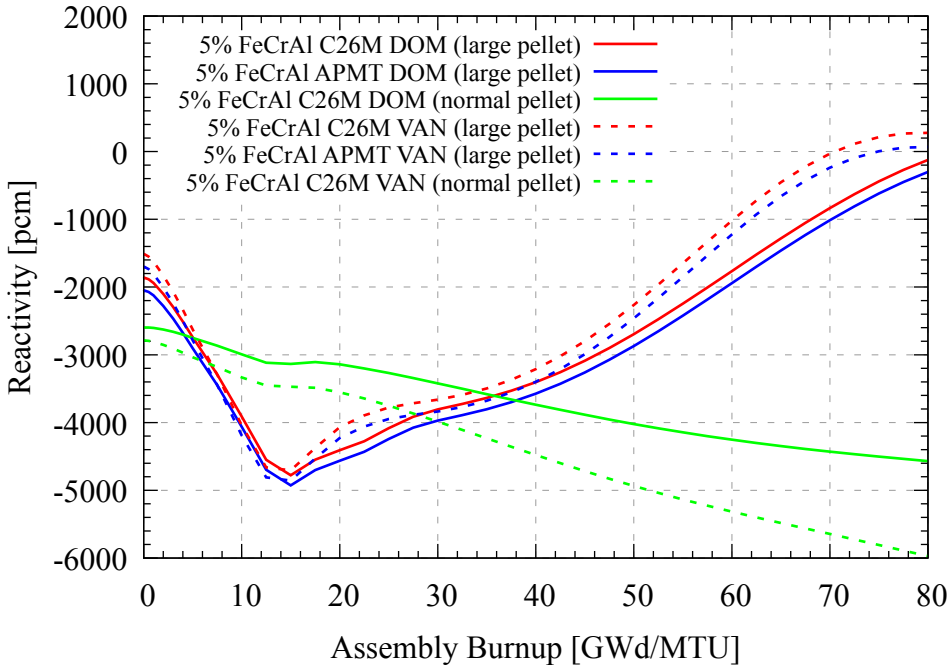

Figure 35. Reactivity difference for 5 wt % limit BWR FeCrAl.

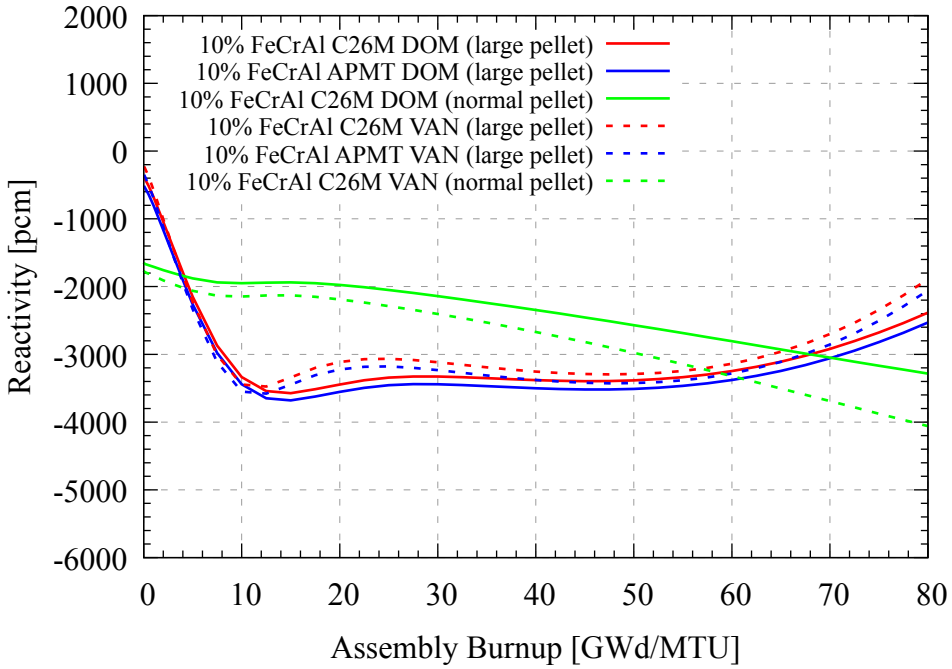

Figure 36. Reactivity difference for 10 wt % limit BWR FeCrAl.

7.9 BWR FeCrAl LATTICE PARAMETERS

The DTC, MVC, and CBW were calculated for the 5 wt % limit and 10 wt % limit lattices with FeCrAl C26M cladding and compared with the reference Zircaloy-2 cladded depletions. Coefficients are shown as differences or percentage differences from the reference cases.

The DTCs are shown in Figure 37 and Figure 38 for the 5 wt % limit and 10 wt % limit, respectively. There is a nearly negligible effect on the DTC from the FeCrAl cladding across both enrichments and lattice regions, as shown in Figure 39 and Figure 40. The C26M (normal pellet) has an identical DTC to the baseline cases. The APMT and C26M (large pellet) show a small increase in DTC, reaching ~0.2 pcm/K for the 5 wt % limit and ~0.1 pcm/K for the 10 wt % limit.

The MVCs are shown in Figure 41 and Figure 42 for the 5 wt % limit and 10 wt % limit lattices, respectively. The 5 wt % and 10 wt % differences from the reference baseline are shown in Figure 43 and Figure 44, respectively. The FeCrAl cladding geometry with the large pellet diameter shows the greatest MVC increase for the vanished (VAN) lattices. The large diameter pellet cases have larger MVC differences, whereas the normal pellet diameter geometries show very little MVC impact from FeCrAl.

The CBWs shown in Figure 45 and Figure 46 indicates significant reductions due to the FeCrAl. The 5 wt % and 10 wt % differences from the reference baseline are shown in Figure 47 and Figure 48, respectively. For the normal pellet size, the reduction is 5% or less for both lattice regions in both enrichments. For the large pellet, the CBW reduction ranges from 5% to 15% compared with the reference case. Future work will investigate whether these same reductions in CBW are observed at the core level. Although this reduction is much greater for the larger pellet option, the reduced clad surface area from the normal pellet geometry will increase the heat flux and may challenge the minimum critical power ratio limits.

Table 33 and Table 34 show the β_{eff} among the reference and FeCrAl lattices at select burnup steps for the dominant and vanished regions. Differences in the effective delayed neutron fraction due to FeCrAl cladding and modifications to the fuel diameter are less than 2.1% for all lattices and enrichments.

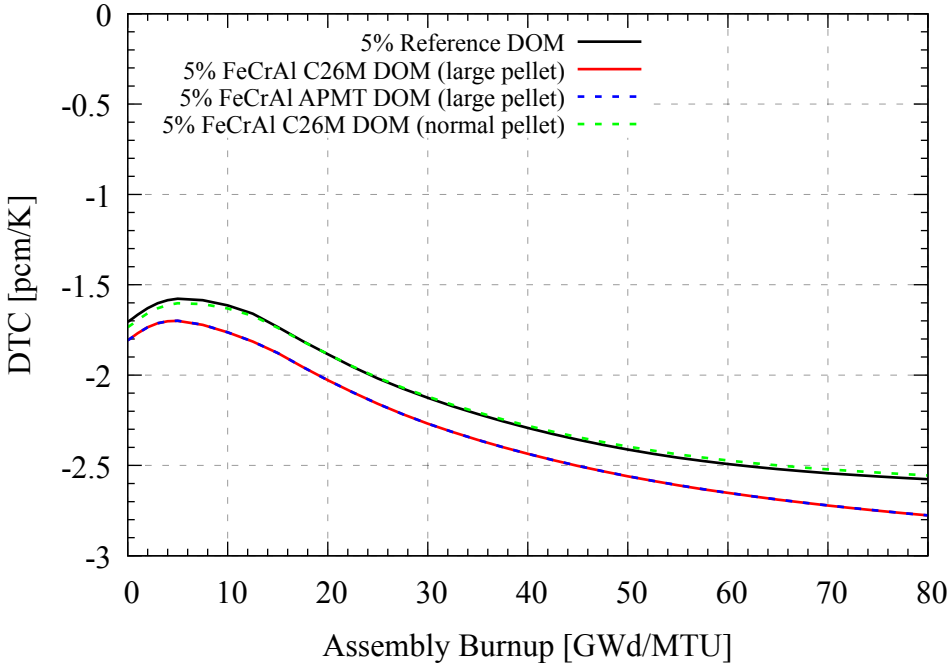

Figure 37. DTC for 5 wt % limit BWR FeCrAl.

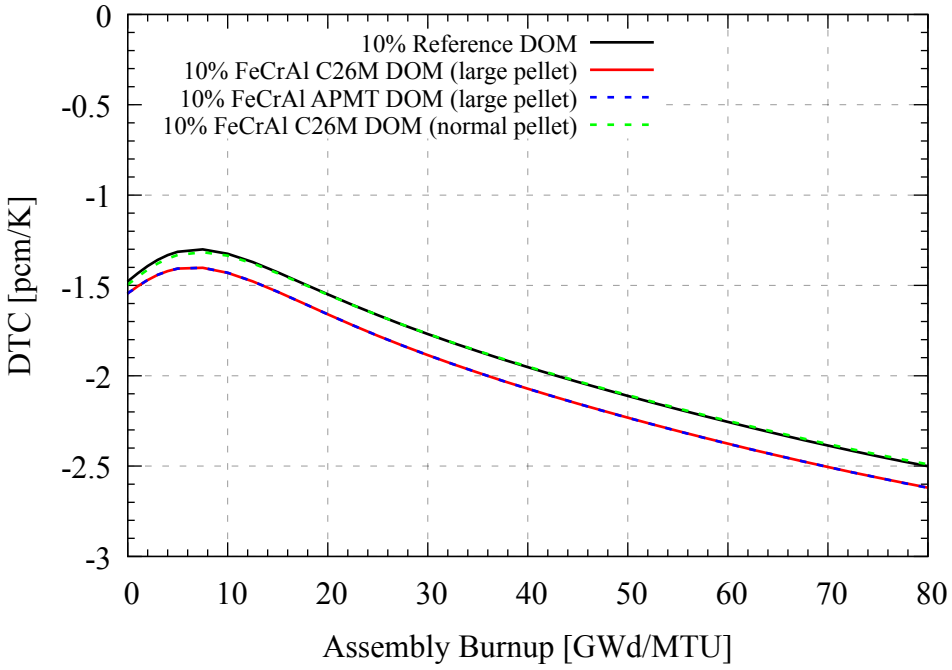

Figure 38. DTC for 10 wt % limit BWR FeCrAl.

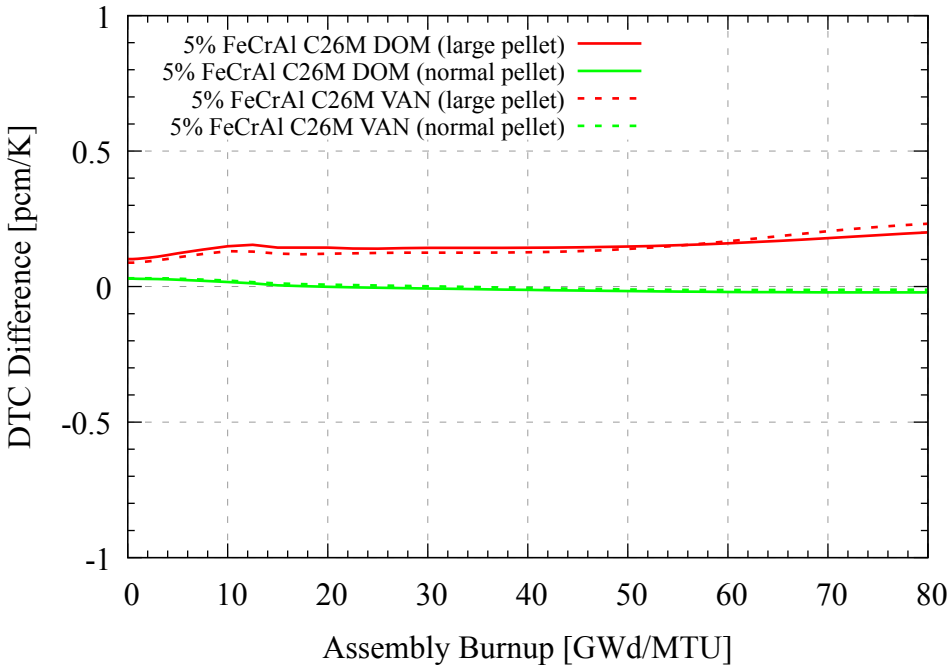

Figure 39. DTC difference for 5 wt % limit BWR FeCrAl (C26M).

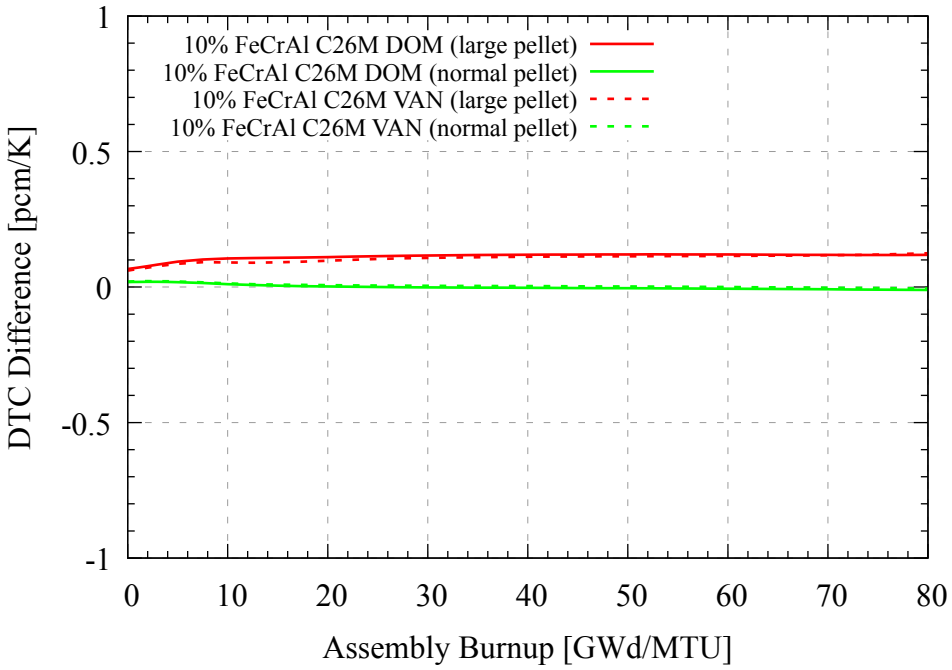

Figure 40. DTC difference for 10 wt % limit BWR FeCrAl (C26M).

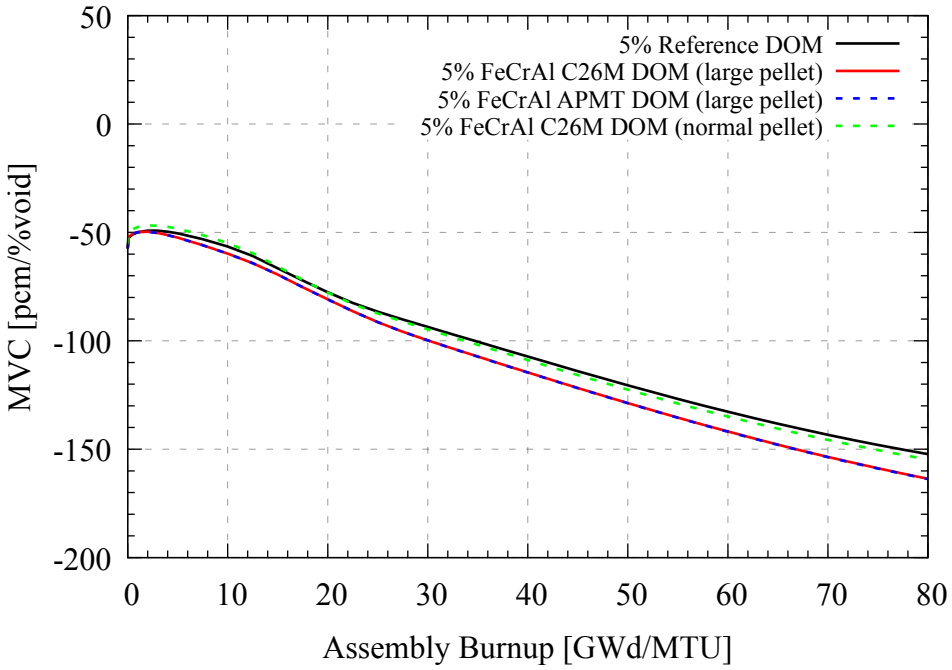

Figure 41. MVC for 5 wt % limit BWR FeCrAl.

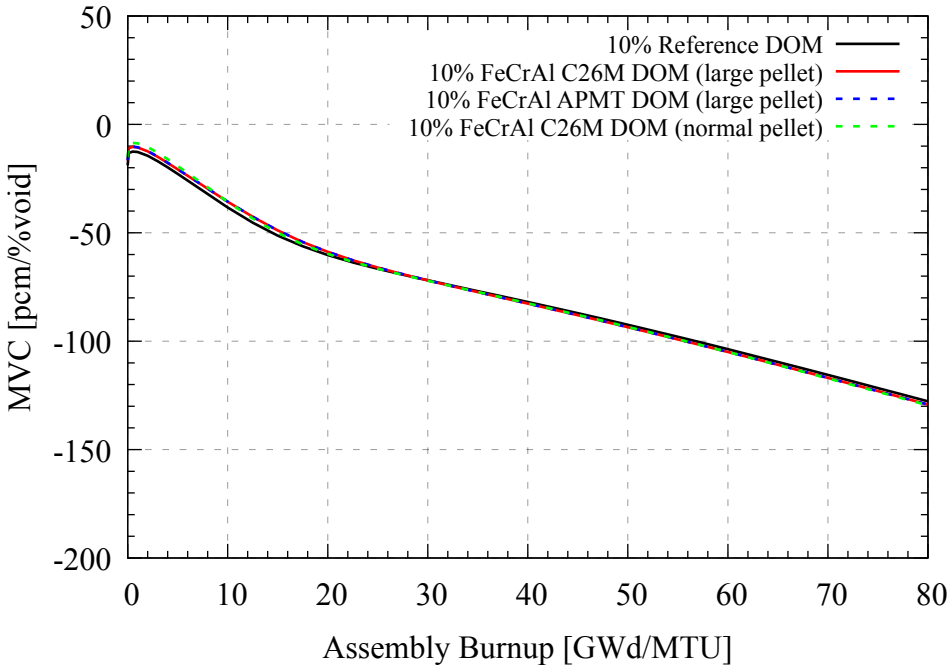

Figure 42. MVC for 10 wt % limit BWR FeCrAl.

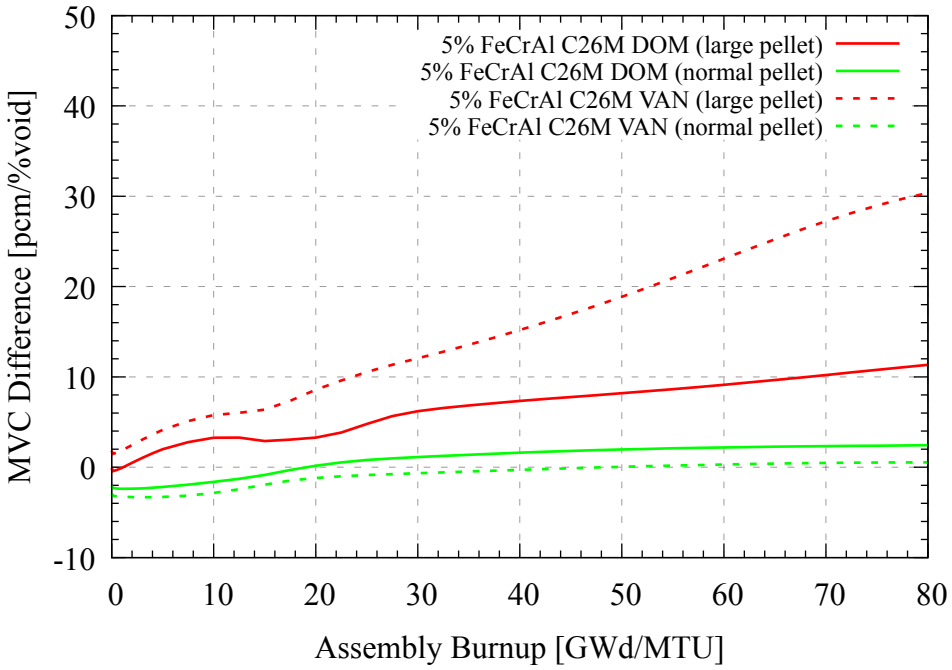

Figure 43. MVC difference for 5 wt % limit BWR FeCrAl (C26M).

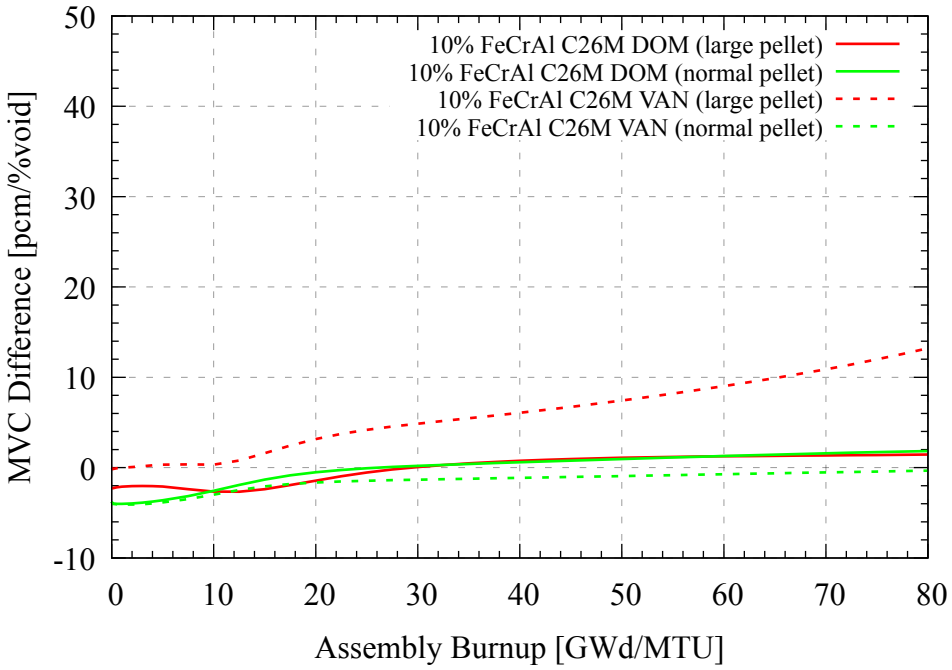

Figure 44. MVC difference for 10 wt % limit BWR FeCrAl (C26M).

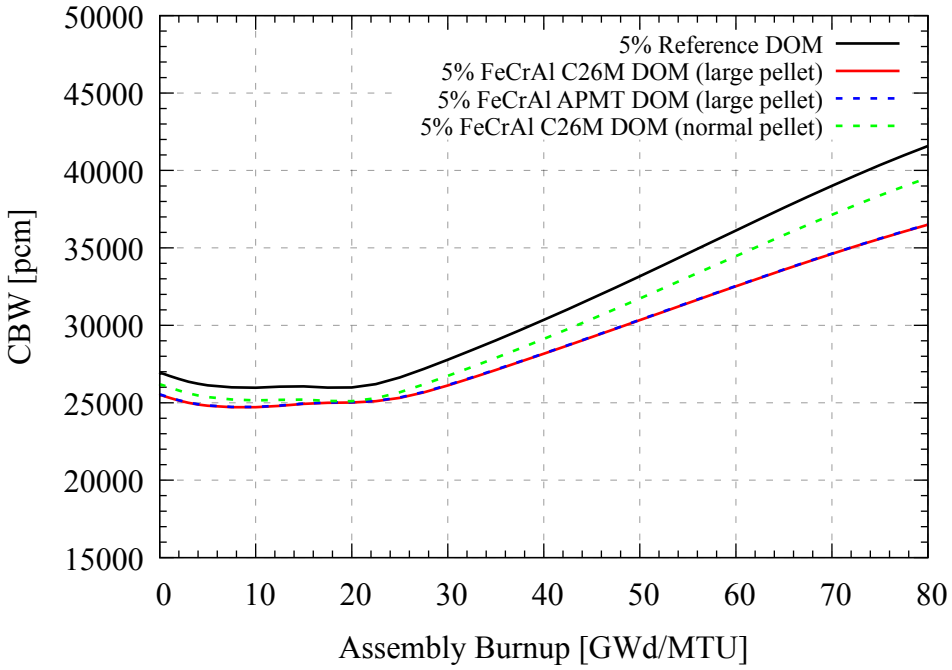

Figure 45. CBW for 5 wt % limit BWR FeCrAl.

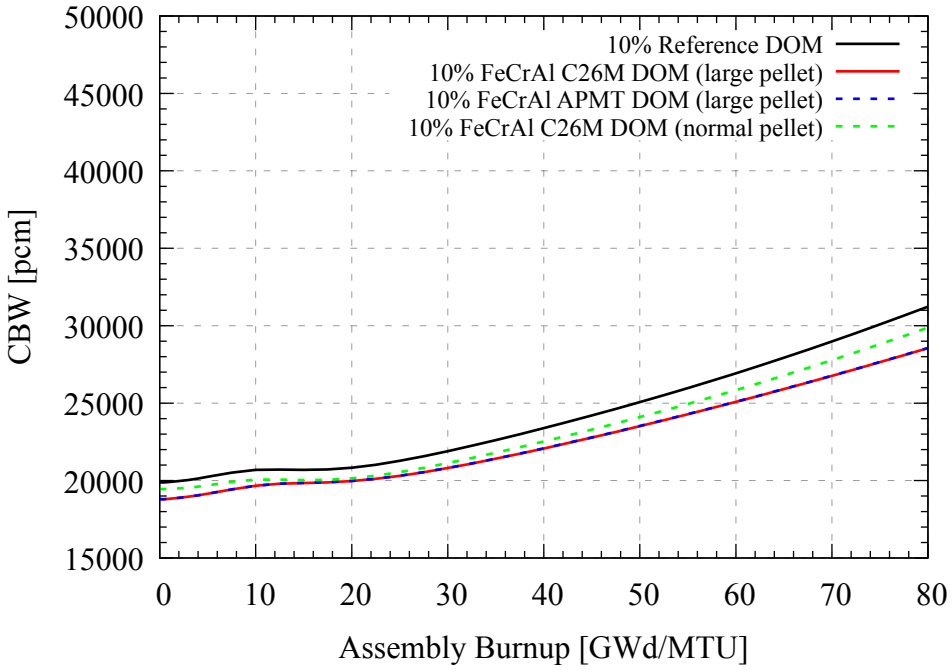

Figure 46. CBW for 10 wt % limit BWR FeCrAl.

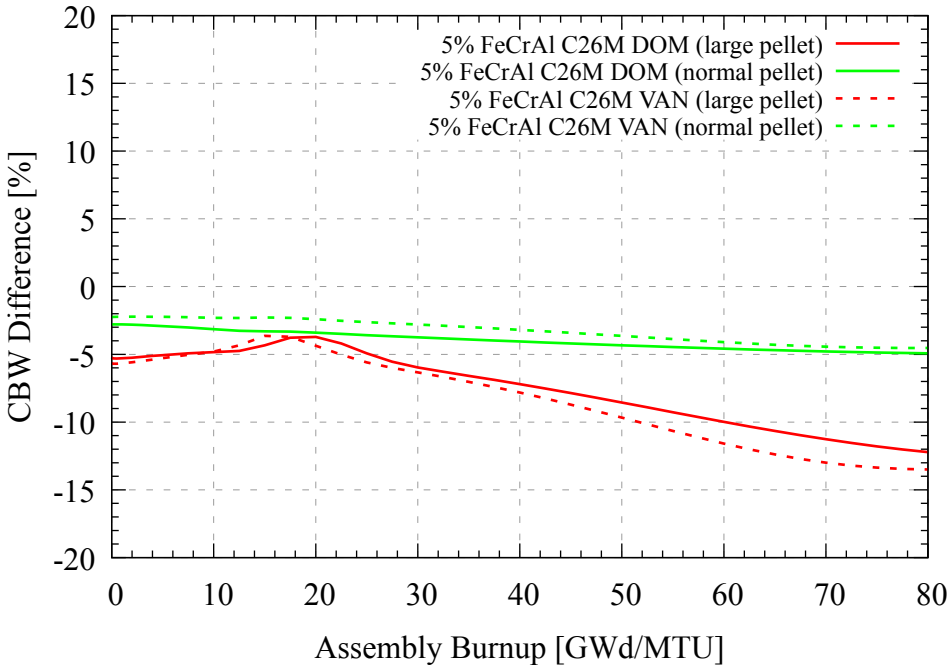

Figure 47. CBW difference for 5 wt % limit BWR FeCrAl (C26M).

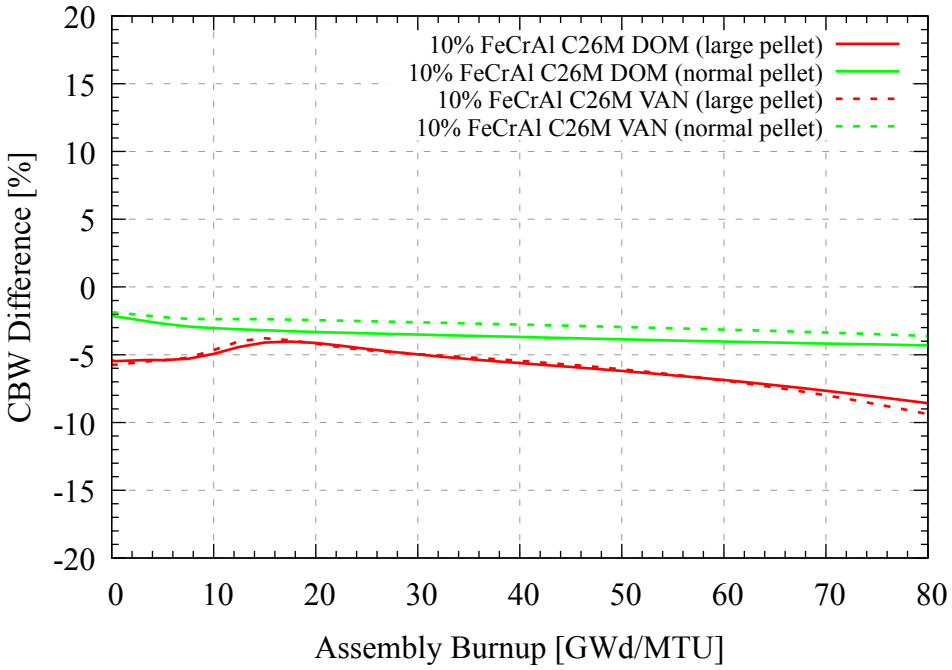

Figure 48. CBW difference for 10 wt % limit BWR FeCrAl (C26M).

Table 33. β-eff for BWR FeCrAl (dominant lattice).

Enrichment (wt %)	5.0	5.0	10.0	10.0
Pellet size	Normal	Large	Normal	Large
Burnup (GWd/MTU)	β_{eff}			
0	0.00685	0.00688	0.00680	0.00683
20	0.00543	0.00540	0.00588	0.00586
40	0.00480	0.00478	0.00538	0.00535
60	0.00434	0.00435	0.00498	0.00494
80	0.00404	0.00407	0.00461	0.00459

Table 34. β-eff for BWR FeCrAl (vanished lattice).

Enrichment (wt %)	5.0	5.0	10.0	10.0
Pellet size	Normal	Large	Normal	Large
Burnup (GWd/MTU)	β_{eff}			
0	0.00680	0.00683	0.00676	0.00679
20	0.00550	0.00548	0.00595	0.00594
40	0.00486	0.00485	0.00549	0.00546
60	0.00432	0.00436	0.00510	0.00507
80	0.00396	0.00403	0.00468	0.00468

7.10 BWR ATF ISOTOPIC EFFECTS

To assess the impact of ATF on used BWR fuel isotopic content, ORIGEN was used to produce isotopic inventories at decay times of 30 minutes, 5 days, 25 days, 100 days, 500 days, 5000 days and 15,000 days. That method is consistent with previous evaluations [Cumberland et al. 2021; Hall et al. 2021] but with a few additional time points primarily to represent the dry storage time frame. The focus of this evaluation was the differences between ATF and non-ATF isotopic content related to decay heat, criticality, shielding, and severe accidents. Table 35 shows the fuel design combinations evaluated. Owing to the volume of data, only major contributors in each category are shown and only for the dominant lattice type (DOM).

Table 35. Decay heat and isotopic evaluation cases for BWR ATF.

Enrichment limit (wt % ^{235}U)	**Clad**	**Pellet size**	**Dopant**	**Comment**
5.00	Zirc-2	Normal	None	DOM reference
5.00	Cr-coated Zirc-2	Normal	Cr_2O_3 (1000 ppm)	DOM doped and coated
5.00	C26M	Large	None	DOM FeCrAl (large pellet)
5.00	C26M	Normal	None	DOM FeCrAl (normal pellet)
10.00	Zirc-2	Normal	None	DOM reference
10.00	Cr-coated Zirc-2	Normal	Cr_2O_3 (1000 ppm)	DOM doped and coated
10.00	C26M	Large	None	DOM FeCrAl (large pellet)
10.00	C26M	Normal	None	DOM FeCrAl (normal pellet)

7.10.1 BWR ATF Decay Heat

Table 36 shows the total decay heat for each fuel design over a range of decay times. For the 5 wt % limit cases, values are provided for 50 GWd/MTU assembly burnup; for the 10 wt % limit cases, values are provided for 80 GWd/MTU. This approach allows easy comparison with the PWR results developed in Section 3.1. All depletions were performed at 25 MW/MTU specific power.

ATF materials and fuel design variations had no significant effect on decay heat. Short-decay-time decay heat is primarily a function of recent depletion power (short-lived isotopes present at shutdown). Long-decay-time decay heat is primarily a function of burnup (longer half-life isotopes accumulated continuously over the entire depletion).

Table 36. Total decay heat for selected BWR fuel designs.

Enrichment limit (wt % ^{235}U)	**5.0**				**10.0**			
Clad	Zirc-2	Cr-coated Zirc-2	FeCrAl C26M	FeCrAl C26M	Zirc-2	Cr-coated Zirc-2	FeCrAl C26M	FeCrAl C26M
Pellet size	Normal	Normal	Large	Normal	Normal	Normal	Large	Normal
Dopant	None	Doped*	None	None	None	Doped*	None	None
Decay time (days)	**50 GWd/MTU decay heat (W/MTU)**				**80 GWd/MTU decay heat (W/MTU)**			
0.02	416,680	416,710	417,090	414,780	422,220	422,260	422,930	420,560
5	85,850	85,874	86,171	85,464	91,566	91,600	92,108	91,220
25	44,611	44,626	44,747	44,377	49,788	49,811	50,105	49,579
100	23,767	23,780	23,960	23,672	27,857	27,876	28,193	27,776
500	8239	8245	8399	8245	10,845	10,855	11,081	10,853
5000	1582	1584	1628	1581	2707	2711	2788	2704
15000	946	948	984	947	1581	1584	1644	1582

*Doped indicates Cr_2O_3 (1000 ppm)

Table 37 shows that dopants and Cr coating have no significant effect on activated clad decay heat. FeCrAl clad exhibits much lower decay heat than the base case, but this difference is trivial compared with used UO_2 decay heat.

Table 37. Clad decay heat for selected BWR fuel designs.

Enrichment limit (wt % ^{235}U)	5.0				10.0			
Clad	Zirc-2	Cr-coated Zirc-2	FeCrAl C26M	FeCrAl C26M	Zirc-2	Cr-coated Zirc-2	FeCrAl C26M	FeCrAl C26M
Pellet size	Normal	Normal	Large	Normal	Normal	Normal	Large	Normal
Dopant	None	Doped*	None	None	None	Doped*	None	None
Decay time (days)	**50 GWd/MTU decay heat (W/MTU)**				**80 GWd/MTU decay heat (W/MTU)**			
0.02	990	1006	225	246	949	964	231	251
5	277	286	106	115	264	271	103	111
25	222	228	85	93	210	216	85	91
100	120	121	59	62	113	115	60	63
500	4	4	23	24	4	4	25	26
5000	<0.5	<0.5	<0.5	<0.5	<0.5	<0.5	1	1
15000	<0.5	<0.5	<0.5	<0.5	<0.5	<0.5	<0.5	<0.5

*Doped indicates Cr_2O_3 (1000 ppm)

7.10.2 BWR ATF Source Term

Similar to the PWR case, differences can be explained as a result of three primary drivers—increased ^{235}U, flux level and neutron energy spectrum change associated with increased enrichment, and neutron energy spectrum changes due to changes in geometry or composition. Table 38 shows the thermal flux (percentage of total flux) at 50 GWd/MTU for each of the 5 wt % equivalent and 10 wt % limit BWR designs that were evaluated. These results confirm the hardest spectrum for the C26M FeCrAl with a large pellet size. The normal pellet size for FeCrAl, coated clad, and doped fuel produces minimal spectral changes from the reference Zirc-2 cladding.

Table 38. 50 GWd/MTU thermal flux fraction for BWR ATF fuel designs.

Enrichment limit (wt % ^{235}U)	5.0				10.0			
Clad	Zirc-2	Cr-coated Zirc-2	FeCrAl C26M	FeCrAl C26M	Zirc-2	Cr-coated Zirc-2	FeCrAl C26M	FeCrAl C26M
Pellet size	Normal	Normal	Large	Normal	Normal	Normal	Large	Normal
Dopant	None	Doped*	None	None	None	Doped*	None	None
Thermal flux fraction (DOM)	17.04%	16.85%	14.29%	17.00%	13.22%	13.11%	11.59%	13.47%
Thermal flux fraction (VAN)	22.91%	22.68%	19.37%	22.49%	16.90%	16.78%	14.94%	17.03%

*Doped indicates Cr_2O_3 (1000 ppm)

Activity data (Ci/MTU) were produced using Polaris to calculate the discharge inventory, and then ORIGEN was used to generate the decayed inventory at 30 minutes, 5 days, 25 days, 100 days, 500 days, 5000 days, and 15000 days to evaluate ATF isotopic effects over multiple time frames. The 5 wt % equivalent assembly activity data are shown in Table 39 (short times) and Table 40 (long times). Similarly, the 8 wt % equivalent assembly data from 80 GWd/MTU depletions are shown in Table 41. Each table lists the top ten highest-activity isotopes for each decay time.

Isotopic changes associated with Cr-coated clad and doped pellets are very small across all decay time frames. As expected, FeCrAl designs have a larger effect, particularly in the transuranic isotopes most visible at long decay times. Differences in total activity are small for all ATF designs and across all time frames evaluated.

Table 39. Top 10 BWR ATF activity isotopes (5 wt % limit, short decay times).

Enrichment (wt % ^{235}U)	**5.00**			
Clad	Zirc-2	Cr-coated Zirc-2	FeCrAl C26M	FeCrAl C26M
Pellet size	Normal	Normal	Large	Normal
Dopant	None	Doped	None	None
Isotope	**Activity at 5 days decay (Ci/MTU)**			
Np-239	3.30E+06	3.30E+06	3.39E+06	3.30E+06
Nb-95	1.08E+06	1.08E+06	1.05E+06	1.05E+06
Zr-95	1.02E+06	1.02E+06	9.92E+05	9.95E+05
Ru-103	1.06E+06	1.06E+06	1.06E+06	1.05E+06
Rh-103m	1.05E+06	1.05E+06	1.05E+06	1.04E+06
La-140	9.87E+05	9.87E+05	9.83E+05	9.84E+05
Ce-141	9.71E+05	9.70E+05	9.67E+05	9.67E+05
Pr-144	8.98E+05	8.97E+05	8.90E+05	8.95E+05
Ce-144	8.98E+05	8.97E+05	8.90E+05	8.95E+05
Ba-140	8.71E+05	8.70E+05	8.67E+05	8.68E+05
Total	2.09E+07	2.09E+07	2.11E+07	2.09E+07
Isotope	**Activity at 25 days decay (Ci/MTU)**			
Nb-95	1.02E+06	1.02E+06	9.94E+05	9.97E+05
Pr-144	8.55E+05	8.55E+05	8.48E+05	8.52E+05
Ce-144	8.55E+05	8.55E+05	8.48E+05	8.52E+05
Zr-95	8.23E+05	8.23E+05	7.99E+05	8.01E+05
Ru-103	7.42E+05	7.42E+05	7.46E+05	7.40E+05
Rh-103m	7.34E+05	7.35E+05	7.38E+05	7.32E+05
Ce-141	6.34E+05	6.33E+05	6.31E+05	6.32E+05
Y-91	5.35E+05	5.34E+05	5.29E+05	5.33E+05
Sr-89	3.81E+05	3.81E+05	3.76E+05	3.79E+05
Rh-106	5.25E+05	5.25E+05	5.33E+05	5.24E+05
Total	1.03E+07	1.03E+07	1.04E+07	1.04E+07
Isotope	**Activity at 100 days decay (Ci/MTU)**			
Pr-144	7.13E+05	7.12E+05	7.06E+05	7.10E+05
Ce-144	7.12E+05	7.12E+05	7.06E+05	7.10E+05
Nb-95	6.27E+05	6.27E+05	6.08E+05	6.10E+05
Rh-106	4.56E+05	4.57E+05	4.64E+05	4.56E+05
Ru-106	4.56E+05	4.57E+05	4.64E+05	4.56E+05
Zr-95	3.66E+05	3.65E+05	3.55E+05	3.56E+05
Y-91	2.20E+05	2.20E+05	2.18E+05	2.19E+05
Ru-103	1.97E+05	1.97E+05	1.98E+05	1.97E+05
Rh-103m	1.95E+05	1.95E+05	1.96E+05	1.95E+05
Cs-134	2.02E+05	2.03E+05	2.10E+05	2.02E+05
Total	5.43E+06	5.44E+06	5.50E+06	5.47E+06

Table 40. Top 10 BWR ATF activity isotopes (5 wt % limit, long decay times).

Enrichment (wt % ^{235}U)	**5.00**			
Clad	Zirc-2	Cr-coated Zirc-2	FeCrAl C26M	FeCrAl C26M
Pellet size	Normal	Normal	Large	Normal
Dopant	None	Doped	None	None
Isotope	**Activity at 500 days decay (Ci/MTU)**			
Pr-144	2.69E+05	2.69E+05	2.67E+05	2.68E+05
Ce-144	2.69E+05	2.69E+05	2.67E+05	2.68E+05
Rh-106	2.16E+05	2.17E+05	2.20E+05	2.16E+05
Ru-106	2.16E+05	2.17E+05	2.20E+05	2.16E+05
Pu-241	1.49E+05	1.50E+05	1.67E+05	1.52E+05
Cs-134	1.40E+05	1.40E+05	1.45E+05	1.40E+05
Pm-147	1.31E+05	1.30E+05	1.28E+05	1.30E+05
Cs-137	1.49E+05	1.49E+05	1.49E+05	1.49E+05
Ba-137m	1.41E+05	1.41E+05	1.41E+05	1.41E+05
Y-90	1.02E+05	1.02E+05	9.99E+04	1.01E+05
Total	1.97E+06	1.97E+06	2.04E+06	2.02E+06
Isotope	**Activity at 5000 days decay (Ci/MTU)**			
Cs-137	1.12E+05	1.12E+05	1.12E+05	1.12E+05
Ba-137m	1.06E+05	1.06E+05	1.06E+05	1.06E+05
Pu-241	8.18E+04	8.23E+04	9.19E+04	8.34E+04
Y-90	7.57E+04	7.56E+04	7.43E+04	7.54E+04
Sr-90	7.57E+04	7.56E+04	7.43E+04	7.54E+04
Pm-147	5.04E+03	5.03E+03	4.95E+03	5.02E+03
Pu-238	5.71E+03	5.74E+03	6.30E+03	5.73E+03
Kr-85	5.36E+03	5.36E+03	5.28E+03	5.35E+03
Eu-154	3.37E+03	3.39E+03	3.75E+03	3.39E+03
Cm-244	4.45E+03	4.48E+03	4.96E+03	4.42E+03
Total	4.84E+05	4.85E+05	4.95E+05	4.87E+05
Isotope	**Activity at 15,000 days decay (Ci/MTU)**			
Cs-137	5.98E+04	5.98E+04	5.96E+04	5.96E+04
Ba-137m	5.66E+04	5.66E+04	5.65E+04	5.65E+04
Y-90	3.92E+04	3.91E+04	3.84E+04	3.90E+04
Sr-90	3.91E+04	3.91E+04	3.84E+04	3.90E+04
Pu-241	2.17E+04	2.18E+04	2.44E+04	2.21E+04
Am-241	4.57E+03	4.60E+03	5.15E+03	4.66E+03
Pu-238	4.60E+03	4.62E+03	5.07E+03	4.62E+03
Cm-244	1.56E+03	1.57E+03	1.74E+03	1.55E+03
Kr-85	9.19E+02	9.18E+02	9.04E+02	9.16E+02
Pu-240	6.48E+02	6.49E+02	6.73E+02	6.44E+02
Total	2.30E+05	2.30E+05	2.32E+05	2.30E+05

Table 41. Top 10 BWR ATF activity isotopes (10 wt % limit, selected decay times).

Enrichment (wt % ^{235}U)	**10.00**			
Clad	Zirc-2	Cr-coated Zirc-2	FeCrAl C26M	FeCrAl C26M
Pellet size	Normal	Normal	Large	Normal
Dopant	None	Doped	None	None
Isotope	**Activity at 5 days decay (Ci/MTU)**			
Np-239	2.97E+06	2.98E+06	3.07E+06	2.97E+06
Nb-95	1.09E+06	1.09E+06	1.05E+06	1.06E+06
Zr-95	1.03E+06	1.03E+06	1.00E+06	1.00E+06
Ru-103	1.04E+06	1.04E+06	1.05E+06	1.04E+06
Rh-103m	1.03E+06	1.03E+06	1.04E+06	1.03E+06
La-140	9.94E+05	9.94E+05	9.90E+05	9.92E+05
Ce-141	9.75E+05	9.75E+05	9.71E+05	9.73E+05
Pr-144	9.06E+05	9.06E+05	8.98E+05	9.04E+05
Ce-144	9.06E+05	9.06E+05	8.98E+05	9.04E+05
Ba-140	8.75E+05	8.75E+05	8.71E+05	8.73E+05
Total	2.15E+07	2.15E+07	2.17E+07	2.15E+07
Isotope	**Activity at 500 days decay (Ci/MTU)**			
Pr-144	2.72E+05	2.72E+05	2.69E+05	2.71E+05
Ce-144	2.72E+05	2.72E+05	2.69E+05	2.71E+05
Rh-106	2.22E+05	2.22E+05	2.26E+05	2.22E+05
Ru-106	2.22E+05	2.22E+05	2.26E+05	2.22E+05
Pu-241	1.89E+05	1.90E+05	2.12E+05	1.91E+05
Cs-134	2.22E+05	2.23E+05	2.29E+05	2.22E+05
Pm-147	1.49E+05	1.49E+05	1.47E+05	1.49E+05
Cs-137	2.30E+05	2.30E+05	2.30E+05	2.30E+05
Ba-137m	2.18E+05	2.18E+05	2.18E+05	2.18E+05
Y-90	1.62E+05	1.62E+05	1.59E+05	1.62E+05
Total	2.45E+06	2.45E+06	2.52E+06	2.50E+06
Isotope	**Activity at 15000 days decay (Ci/MTU)**			
Cs-137	9.23E+04	9.23E+04	9.20E+04	9.21E+04
Ba-137m	8.74E+04	8.74E+04	8.72E+04	8.72E+04
Y-90	6.24E+04	6.23E+04	6.12E+04	6.22E+04
Sr-90	6.24E+04	6.23E+04	6.12E+04	6.22E+04
Pu-241	2.75E+04	2.77E+04	3.09E+04	2.79E+04
Am-241	5.91E+03	5.95E+03	6.65E+03	5.99E+03
Pu-238	1.04E+04	1.05E+04	1.14E+04	1.04E+04
Cm-244	3.75E+03	3.76E+03	4.06E+03	3.73E+03
Kr-85	1.37E+03	1.37E+03	1.35E+03	1.36E+03
Pu-240	7.78E+02	7.79E+02	8.20E+02	7.71E+02
Total	3.56E+05	3.56E+05	3.59E+05	3.56E+05

Previous evaluation of increased LWR enrichment and burnup [Hall et al. 2021] identified 6 isotopes of interest at a short decay time relevant to a severe accident and 14 of interest to radiation shielding in the several years of decay time frame. Severe accident isotope activity is shown in Table 42 for the 5 wt % limit assembly designs and in Table 43 for 10 wt % limit assembly designs. Shielding isotope activity is shown in Table 44 and Table 45. Overall, the difference across the various time scales and BWR ATF variants is small.

Table 42. BWR ATF accident release isotope activity (5 wt % limit at 50 GWd/MTU).

Enrichment (wt % ^{235}U)	**5.00**			
Clad	Zirc-2	Cr-coated Zirc-2	FeCrAl C26M	FeCrAl C26M
Pellet size	Normal	Normal	Large	Normal
Dopant	None	Doped	None	None
Isotope	**Activity at 30 minutes decay (Ci/MTU)**			
I-133	1.36E+06	1.36E+06	1.36E+06	1.36E+06
I-135	1.25E+06	1.25E+06	1.25E+06	1.24E+06
I-131	6.85E+05	6.85E+05	6.86E+05	6.83E+05
Cs-137	1.54E+05	1.54E+05	1.54E+05	1.54E+05
Sr-90	1.05E+05	1.05E+05	1.03E+05	1.05E+05
Kr-85	1.30E+04	1.30E+04	1.28E+04	1.29E+04

Table 43. BWR ATF accident release isotope activity (10 wt % limit at 80 GWd/MTU).

Enrichment (wt % ^{235}U)	**10.00**			
Clad	Zirc-2	Cr-coated Zirc-2	FeCrAl C26M	FeCrAl C26M
Pellet size	Normal	Normal	Large	Normal
Dopant	None	Doped	None	None
Isotope	**Activity at 30 minutes decay (Ci/MTU)**			
I-133	1.36E+06	1.36E+06	1.36E+06	1.36E+06
I-135	1.25E+06	1.25E+06	1.24E+06	1.24E+06
I-131	6.79E+05	6.79E+05	6.80E+05	6.77E+05
Cs-137	2.38E+05	2.38E+05	2.37E+05	2.37E+05
Sr-90	1.68E+05	1.68E+05	1.65E+05	1.67E+05
Kr-85	1.93E+04	1.93E+04	1.90E+04	1.92E+04

Table 44. BWR ATF shielding isotope activity (5 wt % limit at 50 GWd/MTU).

Enrichment (wt % ^{235}U)	**5.00**			
Clad	Zirc-2	Cr-coated Zirc-2	FeCrAl C26M	FeCrAl C26M
Pellet size	Normal	Normal	Large	Normal
Dopant	None	Doped	None	None
Isotope	**Activity at 500 days decay (Ci/MTU)**			
Pu-241	1.49E+05	1.50E+05	1.67E+05	1.52E+05
Ba-137m	1.41E+05	1.41E+05	1.41E+05	1.41E+05
Y-90	1.02E+05	1.02E+05	9.99E+04	1.01E+05
Cs-134	1.40E+05	1.40E+05	1.45E+05	1.40E+05
Rh-106	2.16E+05	2.17E+05	2.20E+05	2.16E+05
Pr-144	2.69E+05	2.69E+05	2.67E+05	2.68E+05
Eu-154	9.10E+03	9.14E+03	1.01E+04	9.15E+03
Pu-238	6.25E+03	6.27E+03	6.88E+03	6.26E+03
Cm-244	7.13E+03	7.17E+03	7.96E+03	7.09E+03
Am-241	5.81E+02	5.84E+02	6.64E+02	5.93E+02
Pu-240	6.35E+02	6.36E+02	6.58E+02	6.31E+02
Pu-239	3.42E+02	3.44E+02	4.03E+02	3.47E+02
Pu-242	3.59E+00	3.58E+00	3.52E+00	3.59E+00
Cm-246	2.91E-01	2.93E-01	3.50E-01	2.84E-01
Isotope	**Activity at 5000 days decay (Ci/MTU)**			
Ba-137m	1.06E+05	1.06E+05	1.06E+05	1.06E+05
Pu-241	8.18E+04	8.23E+04	9.19E+04	8.34E+04
Y-90	7.57E+04	7.56E+04	7.43E+04	7.54E+04
Pu-238	5.71E+03	5.74E+03	6.30E+03	5.73E+03
Eu-154	3.37E+03	3.39E+03	3.75E+03	3.39E+03
Am-241	2.76E+03	2.77E+03	3.11E+03	2.81E+03
Cm-244	4.45E+03	4.48E+03	4.96E+03	4.42E+03
Cs-134	2.24E+03	2.24E+03	2.32E+03	2.24E+03
Pu-240	6.42E+02	6.43E+02	6.66E+02	6.38E+02
Pu-239	3.42E+02	3.44E+02	4.02E+02	3.47E+02
Rh-106	4.92E+01	4.92E+01	5.00E+01	4.91E+01
Pr-144	4.74E+00	4.74E+00	4.70E+00	4.72E+00
Pu-242	3.59E+00	3.58E+00	3.52E+00	3.59E+00
Cm-246	2.90E-01	2.93E-01	3.49E-01	2.83E-01

Table 45. PWR ATF shielding isotope activity (10 wt % limit at 80 GWd/MTU).

Enrichment (wt % ^{235}U)	**10.00**			
Clad	Zirc-2	Cr-coated Zirc-2	FeCrAl C26M	FeCrAl C26M
Pellet size	Normal	Normal	Large	Normal
Dopant	None	Doped	None	None
Isotope	**Activity at 500 days decay (Ci/MTU)**			
Pu-241	1.89E+05	1.90E+05	2.12E+05	1.91E+05
Ba-137m	2.18E+05	2.18E+05	2.18E+05	2.18E+05
Y-90	1.62E+05	1.62E+05	1.59E+05	1.62E+05
Cs-134	2.22E+05	2.23E+05	2.29E+05	2.22E+05
Rh-106	2.22E+05	2.22E+05	2.26E+05	2.22E+05
Pr-144	2.72E+05	2.72E+05	2.69E+05	2.71E+05
Eu-154	1.53E+04	1.54E+04	1.70E+04	1.54E+04
Pu-238	1.42E+04	1.42E+04	1.54E+04	1.42E+04
Cm-244	1.71E+04	1.72E+04	1.86E+04	1.70E+04
Am-241	8.52E+02	8.58E+02	9.77E+02	8.64E+02
Pu-240	7.44E+02	7.46E+02	7.83E+02	7.38E+02
Pu-239	4.04E+02	4.06E+02	4.80E+02	4.07E+02
Pu-242	5.21E+00	5.21E+00	5.13E+00	5.23E+00
Cm-246	1.22E+00	1.23E+00	1.44E+00	1.20E+00
Isotope	**Activity at 5000 days decay (Ci/MTU)**			
Ba-137m	1.64E+05	1.64E+05	1.64E+05	1.64E+05
Pu-241	1.04E+05	1.04E+05	1.17E+05	1.05E+05
Y-90	1.21E+05	1.21E+05	1.18E+05	1.20E+05
Pu-238	1.29E+04	1.30E+04	1.41E+04	1.29E+04
Eu-154	5.68E+03	5.70E+03	6.30E+03	5.69E+03
Am-241	3.61E+03	3.63E+03	4.07E+03	3.66E+03
Cm-244	1.07E+04	1.07E+04	1.16E+04	1.06E+04
Cs-134	3.56E+03	3.56E+03	3.67E+03	3.56E+03
Pu-240	7.61E+02	7.62E+02	8.01E+02	7.55E+02
Pu-239	4.03E+02	4.06E+02	4.80E+02	4.07E+02
Rh-106	5.04E+01	5.05E+01	5.13E+01	5.04E+01
Pr-144	4.78E+00	4.78E+00	4.74E+00	4.77E+00
Pu-242	5.21E+00	5.21E+00	5.13E+00	5.23E+00
Cm-246	1.22E+00	1.23E+00	1.44E+00	1.20E+00

7.10.3 BWR ATF Transportation

Transportation of UO_2 enriched to > 5 wt % ^{235}U has previously been investigated, but without specific consideration of ATF designs. [Hall et al. 2020]. Two transportation packages reviewed are relevant to BWR ATF transportation—the Framatome TN-B1 (BWR pellets, rods, and fuel assemblies) and the CHT-OP-TU (BWR pellets).

Analysis of the CHT-OP-TU package showed that without a reduction in transportation array size, UO_2 pellets enriched to as high as 16.5 wt % ^{235}U can be accommodated by using the 6-inch oxide vessel rather than larger-diameter vessels. Although the effect of dopants on UO_2 reactivity, which is predominantly negative, has not been directly evaluated for the CHT-OP-TU package, it is clear that it could be used to carry pellets of sufficient enrichment (<10 wt %) for LWR ATF fuel applications.

7.10.4 BWR ATF Used Fuel Storage Criticality

Just as for a PWR, Cr coatings and FeCrAl for BWR reduce fuel assembly reactivity across the burnup range at in-reactor conditions and all previous statements made in 7.5.4 also apply for BWRs.

8. CONCLUSIONS

Calculations were performed using the pre-release version of SCALE 6.3 Polaris and ORIGEN codes with a 56-group ENDF/B-VII.1 neutron cross-section library. The effects of EE and HBU on lattice depletion characteristics were investigated using potential near-term PWR and BWR ATF concepts that included Cr fuel dopant, Cr-clad coating, and FeCrAl cladding. The report summarizes these near-term ATF concepts, and the expected range of burnup and enrichment based on historical data was determined for the PWR and correlated to the BWR. Previous ATF studies were reviewed and Polaris models introduced. The ramifications of dopants and coatings are straightforward. However, with FeCrAl, there are additional design choices owing to the thinner clad wall and significant reactivity penalty. Pellet size, clad OD, and enrichment all became design variables for FeCrAl; and especially for the BWR, where this design space is already large. Future work will perform additional studies at the core level.

Key quantities of interest included lattice physics quantities; isotopic inventory at various decay times; and their effects on decay heat, activity and shielding applications.

1. No unexpected or anomalous trends were found that would call into question the accuracy of the Polaris code using SCALE 56-group ENDF/B-VII.1 neutron data for depletion, lattice physics, and isotopic content calculations of the analyzed ATF fuel with enrichments approaching 9 wt % average for the PWR ATF and 10 wt % limit for a single pin in the BWR.

2. Chromium fuel dopants had a negligible effect on any investigated lattice parameter for both the PWR and BWR, e.g., reactivity effects on the order of 50 pcm. The dopant increased fuel density slightly and so the heavy metal loading decreased only slightly.

3. Chromium-clad coatings had a more significant effect than dopants on lattice reactivity (~300 pcm); therefore, additional enrichment would be required for the same fuel lifetime. For the PWR, the enrichment should be increased from 5.0 wt % to 5.1 wt % for nominal burnups and from 8.0 wt % to 8.15 wt % for EE and HBU.

4. FeCrAl cladding introduced additional design decisions regarding whether to keep the normal pellet size (and thereby reduce the OD of the fuel rod), or to increase the pellet size. Decreasing the OD may have ramifications for heat flux limits. Increasing the pellet size increased the amount of fuel in the assembly. We have assumed the specific power remains the same as for the baseline (40 MW/MTU for the PWR and 25 MW/MTU for the BWR), but an assembly with increased fuel mass might run at a lower specific power and still produce the same energy as required by a fixed core power. Thus, for some comparisons, it made more sense to consider lattice behavior as a function of energy release instead of burnup. However, for the majority of this work, which followed typical lattice code usage, the main results have been interpreted as a function of burnup at this stage.

    a. Calculated fuel k_{inf}, peaking factors, and reactivity coefficients are smooth and continuous as a function of enrichment and burnup.

    b. Lattice physics trends were predictable from first principles (e.g., spectral hardening resulting from increased ^{235}U enrichment).

    c. The use of FeCrAl led to spectral hardening, which mainly impacted control element worth, reducing it by 5 to 10%.

5. Additional decay heat and activity due to ATF concepts was minimal. In all cases, including the nominal case, cladding contributed less than 0.1% to the total decay heat. FeCrAl clad had a smaller decay heat than did the baseline Zr-based cladding.

6. The results did not show significant changes when the lattice type and void fraction were changed. For the cases with the largest changes due to lattice type or void fraction changes, this assumption should be verified in the next phase.

Future work will investigate the core-level performance of ATF, using the PARCS core simulator (with Polaris cross sections) to investigate quantities such as at-power core MTC at beginning of cycle (high soluble boron) and reduced CRW. For the FeCrAl cases with a smaller fuel rod OD, a reduced clad surface area would increase the heat flux and might exacerbate crud buildup and axial offset anomalies and could challenge the departure from nucleate boiling limits.

ACKNOWLEDGMENTS

Support for this work was provided by the US NRC Offices of Nuclear Regulatory Research, Nuclear Reactor Regulation, and Nuclear Material Safety and Safeguards. The authors would also like to thank many Oak Ridge National Laboratory staff members for feedback on the contents and presentation of this report.

REFERENCES

Arborelius, J., K. Backman, L. Hallstadisu, et al. 2006. *Advanced Doped UO_2 Pellets in LWR Applications*, Journal of Nuclear Science and Technology, Volume 43, Number 9, pp 967-976.

ATI (Allegheny Technologies Incorporated) 2015. *Zirconium Alloys Technical Data Sheet*, Version 1, February.

Bischoff, J., C. Delafoy, N. Chaari, et al. 2018. *Cr-coated Cladding Development at Framatome*, Top Fuel Reactor Fuel Performance 2018 Transactions, Prague, Czech Republic, September.

Bischoff, J., C. Delafoy, C. Vauglin et al. 2018. *AREVA NP's enhanced accident-tolerant fuel developments: Focus on Cr-coated M5 cladding*, Nuclear Engineering and Technology, Volume 50, pp 223-228.

Capps, N., A. Wysocki, A. T. Godfrey, et al. 2020. *Full Core LOCA Safety Analysis for a PWR Containing High Burnup Fuel,* ORNL/TM-2020/1700.

Che, Y., G. Pastore, G., J. Hales, et al. 2018. *Modeling of Cr_2O_3-doped UO_2 as a Near-term Accident Tolerant Fuel for LWRs using the BISON Code*, INL/JOU-18-44500-Revision 0, July.

Cole, S. E. et al. 2012. AREVA Optimized Fuel Rods for LWRs, Top Fuel Reactor Fuel Performance 2012 Transactions, Manchester, United Kingdom, September 2–6, 2012.

Cooper, M.W.D., G. Pastore, Y. Che, et al. 2021. *Fission gas diffusion and release for Cr_2O_3-doped UO_2: From the atomic to the engineering scale*, Journal of Nuclear Materials 545: 152590.

Cumberland, R.M., R. T. Sweet, U. Mertyurek, R. Hall, and W. A. Wieselquist. 2021. *Isotopic and Fuel Lattice Parameter Trends in Extended Enrichment and Higher Burnup LWR Fuel Vol II: BWR Fuel,* ORNL/TM-2020/1835.

Diaz, M. 2019. DSFM Regulatory Conference, "Advanced Fuels Update on the Front End of the Fuel Cycle," https://www.nrc.gov/docs/ML1925/ML19255F598.pdf

EPRI (Electric Power Research Institute). 2018. *Accident Tolerant Fuel Technical Update*, Valuation 1.0, Gap Analysis, and Valuation 2.0, 3002012250, Technical Update, May.

GE. 2011. General Electric Systems Technology Manual, Chapter 2.2, *Fuel and Control Rods System*, Revision 0911, NRC Technical Training Center, ML11258A302.

Geelhood, K., and W. Luscher. 2019. *Degradation and Failure Phenomena of Accident Tolerant Fuel Concepts; Chromium Coated Zirconium Alloy Cladding*, PNNL-28437, January.

George, N. M., R. T. Sweet, J. J. Powers, A. Worrall, K. A. Terrani, B. D. Wirth, and G. I. Maldonado. 2019. *Full-core analysis for FeCrAl enhanced accident tolerant fuel in boiling water reactors.* Annals of Nuclear Energy, 132, 486-503.

Goodson, C., and K. Geelhood. 2020. *Degradation and Failure Phenomena of Accident Tolerant Fuel Concepts; FeCrAl Alloy Cladding*, PNNL-30445, September.

Hall, R. A., R. M. Cumberland, and W. A. Wieselquist. 2021. *Isotopic and Fuel Lattice Parameter Trends in Extended Enrichment and Higher Burnup LWR Fuel Vol I: PWR Fuel,* ORNL/TM-2020/1833.

Hall, R., W. J. Marshall, and W. A. Wieselquist. 2020. *Assessment of Existing Transportation Packages for use with HALEU,* ORNL/TM-2020/1725.

Hallman, L., Jr., et al. 2020. *Advanced Doped Pellet Technology (ADOPT™) Fuel*, WCAP-18482NP, Revision 0, May.

IAEA (International Atomic Energy Agency). 2014. *Accident Tolerant Fuel Concepts for Light Water Reactors*, Proceedings of a Technical Meeting Held at Oak Ridge National Laboratory, IAEA-TECDOC-1797, October.

Jessee, M., J. Yang, U. Mertyurek, et al. 2020. *SCALE Lattice Physics Code Assessments of Accident-Tolerant Fuel,* ORNL/TM-2019/1400.

Khatib-Rahbar, M., A. Krall, Z. Yuan, et al. 2020. *Review of Accident Tolerant Fuel Concepts with Implications to Severe Accident Progression and Radiological Releases*, ERI/NRC 20-209, Energy Research, Inc., October.

Kim, H., J.-H. Yang, W.-J. Kim, et al. 2016. *Development Status of Accident-Tolerant Fuel for Light Water Reactors in Korea*, Korea Atomic Energy Research Institute, Nuclear Engineering and Technology, Volume 48, pp 1-15, 2016.

Kim, H., H.-G. Kim, J.-H. Yang, et al. 2017. On the minimum thickness of FeCrAl cladding for accident-tolerant fuel, Korea Atomic Energy Research Institute, *ANS Nuclear Technology*, Volume 198, pp 342-346, June.

Lin, Y., R. M. Fawcett, S. S. DeSilva, et al. 2018. Path Towards Industrialization of Enhanced Accident Tolerant Fuel*,* Top Fuel Reactor Fuel Performance 2018 Transactions, Prague, Czech Republic, September 2018.

Massih, A., 2014. *Effects of Additives on Uranium Dioxide Fuel Behavior*, Swedish Radiation Safety Authority, 2014:21.

Motta, A., A. Couet, and R. J. Comstock. 2015. *Corrosion of Zirconium Alloys Used for Nuclear Fuel Cladding*, Annual Review of Materials Research, Volume 45, pp 311-343.

NEA (Nuclear Energy Agency). 2018. Organization for Economic Cooperation and Development, *State of the Art Report on Light Water Reactor Accident-Tolerant Fuels*, NEA No. 7317.

NRC (Nuclear Regulatory Commission). 2019. *Project Plan to Prepare the U.S. Nuclear Regulatory Commission for Efficient and Effective Licensing of Accident Tolerant Fuels*, Version 1.1, October (ML19301B166).

NRC (Nuclear Regulatory Commission. 2020. Letter: Revision No. 12 of Certificate of Compliance no. 9297 for the Model Nos. Traveller STD, Traveller XL, and Traveller VVER Packages, ADAMS ML20255A297.

NRC (Nuclear Regulatory Commission). 2020. *Supplemental Guidance Regarding the Chromium-Coated Zirconium Alloy Fuel Cladding Accident Tolerant Fuel Concept*, Interim Staff Guidance, ATF-ISG-2020-01, January (ML19343A121).

ORNL (Oak Ridge National Laboratory) 2015. *Technical Basis for Peak Reactivity Burnup Credit for BWR Spent Nuclear Fuel in Storage and Transportation Systems,* NUREG/CR-7194.

ORNL (Oak Ridge National Laboratory) 2016. *US Commercial Spent Nuclear Fuel Assembly Characteristics: 1968-2013,* NUREG/CR-7227.

Parisi, C., Z. Ma, D. Mandelli, et al. 2020. *Risk-Informed Safety Analysis for Accident Tolerant Fuels*, Nuclear Science and Engineering, Volume 194, pp. 748-770, August–September.

Pastore, G., K. A. Gamble, and J. D. Hales 2017. *Modeling Benchmark for FeCrAl Cladding in the IAEA CRP ACTOF*, *FeCrAl-C35M Material Models and Benchmark Cases Specifications*, INL/EXT-17-43695, October 2017.

Pimental, F. 2019. “The Economic Benefits and Challenges with Utilizing Increased Enrichment and Fuel Burnup for Light-Water Reactors,” Nuclear Energy Institute.

Pint, B., K. A. Terrani, Y. Yamamoto, et al. 2015. *Material Selection for Accident Tolerant Fuel Cladding,* Metallurgical and Materials Transactions, Volume 2E, pp 190-196, September.

Rebak, R. 2018. *Versatile Oxide Films Protect FeCrAl Alloys Under Normal Operation and Accident Conditions in Light Water Power Reactors*, JOM Volume 70, No. 2, pp 176-185.

Richardson, K., H. Medema, S. Hayes, 2019. *Advanced Fuels Campaign 2019 Accomplishments*, INL/EXT 19-56259.

Sanders, C. E., and J. C. Wagner. 2001. *Study of the Effect of Integral Burnable Absorbers for PWR Burnup Credit*, NUREG/CR-6760.

Shah, H., 2006. *Optimized ZIRLO™*, WCAP-14342-A & CENPD-404-NP-A, Addendum 1-A, July.

Shah, H., J. Romero, P. Xu, et al. 2018. *Westinghouse Exelon EnCore® Fuel Lead Test Rod (LTR) Program including Coated cladding Development and Advanced Pellets*, Top Fuel Reactor Fuel Performance 2018 Transactions, Prague, Czech Republic, September.

Singh, G., J. Gorton, D. Schappel, N. R. Brown, Y. Katoh, B. D. Wirth, and K. A. Terrani. 2019. *Deformation analysis of SiC-SiC channel box for BWR applications*. Journal of Nuclear Materials, 513, 71-85.

Singh, G., R. Sweet, N. Brown, B. Wirth, Y. Katoh, and K. Terrani. 2018. *Parametric evaluation of SiC/SiC composite cladding with UO_2 fuel for LWR applications: fuel rod interactions and impact of nonuniform power profile in fuel rod*. Journal of Nuclear Materials, 499, 155-167.

Sweet, R. T., Y. Yang, K. A. Terrani, B. D. Wirth, and A. T. Nelson. 2020. *Performance of U_3Si_2 in an LWR following a cladding breach during normal operation*. Journal of Nuclear Materials, 539, 152263

Wagner, J. C. and M. D. DeHart. 1999. *Review of Axial Burnup Distribution Considerations for Burnup Credit Calculations,* ORNL/TM-1999/246.

WEC (Westinghouse Electric Company). 2020. *Westinghouse Advanced Doped Pellet Technology (ADOPT™) Fuel*, WCAP-18482-NP, Revision 0, May.

Wieselquist, W. A., R. A. Lefebvre, and M. A. Jessee, Eds. 2020. *SCALE Code System*, ORNL/TM-2005/39, Version 6.2.4, Oak Ridge National Laboratory, Oak Ridge, TN.

Zhang, H., C. Blakely, J. Yu, et. al. 2019. *Fuel Rod Burst Potential Evaluation under LOCA Conditions for an Existing Plant with Extended Burnup Exceeding the Current Limit by 20%,* INL/EXT-19-55888.

APPENDIX A. PWR CYCLE ESTIMATOR

The PWR cycle estimator is a spreadsheet tool that uses the Polaris 17×17 PWR assembly k_{inf} as a function of burnup and initial enrichment to estimate the fuel batch relative power and burnup and equilibrium cycle core average kinf. Data from Polaris are for hot full power, equilibrium xenon with no soluble boron to replicate end of reactivity core conditions. Given a target critical core k_{inf} and input describing the core—including fuel uranium mass, core power, core size, cycle length, and batch size—the user can estimate the equilibrium cycle batch average discharge burnup by iterating on the batch average enrichment. The spreadsheet (Discharge_burnup_estimator_spline_Rev2.xlsx) "Calculator" sheet contains the input and performs the calculations.

INPUT

Polaris depletions and no soluble boron branch cases were performed to obtain k_{inf} data up to 110 GWd/MTU for the following enrichment/IFBA/cycle average soluble boron combinations:

- 4.0 wt % ^{235}U / 104 IFBA / 750 ppm
- 5.0 wt % ^{235}U / 104 IFBA / 900 ppm
- 6.5 wt % ^{235}U / 128 IFBA / 1125 ppm
- 8.0 wt % ^{235}U / 148 IFBA / 1370 ppm

User-supplied input is provided in yellow cells, as shown in this screenshot from the "Calculator" sheet:

Input variables		
FA in core	157	
Rated power	2900	MW
MTU/assembly	0.503	MTU
Batch size	56.0	
Enrichment	5	wt%
Cycle length	18	months
Outage + maintenance	25	days
Cycle load factor	99	percent
Last cycle power penalty (20% of FA in core)	0.5	
Effective full power days	517.6	
Specific power at 100%	36.7	

The enrichment is a batch average (including axial blankets). The cycle load factor is the percentage of maximum possible energy produced between startup and shutdown for refueling (it excludes the outage and maintenance days). The last cycle power penalty assumes a low-leakage loading strategy in which the lowest reactivity batch is preferentially loaded on the core periphery where high neutron leakage reduces assembly relative power. The value provided is the fraction of the relative power that 20% of the highest-burnup assemblies would have if they were placed in an "average" core location.

CALCULATIONS

A spline interpolation routine (SPLINE.XLA) is used to create kinf versus burnup data for the user-supplied enrichment (partial view for 5.5 wt % in blue shaded column):

HFP, 0 soluble boron brnach case k-infinity vs burnup					
	4	5	6.5	8	Enr. Interp
0	1.15721	1.22009	1.24023	1.27719	1.233
0.05	1.12782	1.19013	1.21376	1.25287	1.204
0.1	1.1257	1.18743	1.2109	1.24972	1.201
0.5	1.12794	1.18787	1.21122	1.24921	1.201
1	1.1361	1.19123	1.21394	1.2503	1.204
2	1.15161	1.20104	1.22133	1.25457	1.212
3	1.16318	1.20848	1.22813	1.25911	1.219
4	1.17153	1.2138	1.23356	1.26295	1.224
5	1.17724	1.21734	1.23768	1.26594	1.228
6	1.18075	1.21938	1.24065	1.26813	1.230
7	1.18241	1.22015	1.24263	1.2696	1.231
8	1.1825	1.21984	1.24372	1.27044	1.231

The batch power and core average kinf calculation is performed iteratively over three estimates. The first, shown below for a 193-assembly core, assumes a batch relative power of 1.0 that is adjusted by the last cycle power penalty and renormalized so that the core average relative power is 1.0. In the case below, 20% of the core is ~39 assemblies; there are 32 in the highest-burnup batch (power multiplier = 0.5), and ~7 in Batch 2 (power multiplier = 0.96). Renormalized batch powers are shown in the "Batch power est" column. EOC batch burnup added for a cycle is cycle burnup × batch relative power, with burnup for each older batch adding to the prior batch EOC burnup. SPLINE is used to determine the EOC k_{inf} for each batch. Batch k_{inf} values are batch fraction (batch assemblies / core assemblies) and batch power weighted to determine the core average k_{inf}.

		1st estimate			
		Location power mult	Batch power est	Batch burnup	EOC k-inf
Batches	3				
Avg Specific power	34.7			0	
Batch 1	80.5	1	1.111	28200	1.139
Batch 2	80.5	0.96	1.066	55244	0.978
Batch 3	32.0	0.50	0.556	69344	0.907
Batch 4	0.0	0.50	0.556	83444	0.850
Batch 5	0.0	0.50	0.556	97545	0.807
Core avg		0.900	1.000		**1.046**

A second estimate is performed similarly, but rather than assume a batch power of 1.0, the batch power estimate is set equal to the mid-cycle SPLINE interpolated k_{inf} for each batch.

2nd estimate			
Mid-depl power est	Batch power est	Batch burnup	EOC k-inf
		0	
1.216	1.207	30634	1.124
1.012	1.005	56137	0.973
0.471	0.467	67992	0.913
0.438	0.435	79035	0.866
0.413	0.410	89449	0.830
1.007	1.000		**1.044**

A third estimate is obtained in the same way:

3rd estimate			
Mid-depl power est	Batch power est	Batch burnup	EOC k-inf
		0	
1.211	1.209	30688	1.123
1.003	1.001	56103	0.973
0.471	0.470	68044	0.913
0.444	0.444	79306	0.865
0.423	0.423	90039	0.828
1.001	1.000		**1.0443**

The number of assemblies discharged in each batch (starting from the highest-burnup batch) and the batch burnup estimates are used to determine the batch average burnup. Other quantities calculated include core average burnup (batch burnup weighted by batch fraction) and power-weighted burnup (batch burnup weighted by batch power and batch fraction).

Discharge burnup	**60849**	Core average burnup	47482	Power weighted burnup	44217

The cycle estimator cannot account for numerous variables, such as different neutronic efficiency of different fuel designs, non–low-leakage loading patterns, different leakage fractions for different core sizes, nonequilibrium fuel cycles, residual poison effects (removable burnable poison rods and residual gadolinia), and uncertainties in the benchmark data. Regardless, the estimator is useful for quick estimates and for understanding the effects of different fuel management strategies (e.g., using increased enrichment to reduce batch size versus increasing the cycle length).